

Lincoln University Digital Thesis

Copyright Statement

The digital copy of this thesis is protected by the Copyright Act 1994 (New Zealand).

This thesis may be consulted by you, provided you comply with the provisions of the Act and the following conditions of use:

- you will use the copy only for the purposes of research or private study
- you will recognise the author's right to be identified as the author of the thesis and due acknowledgement will be made to the author where appropriate
- you will obtain the author's permission before publishing any material from the thesis.

**Adaptation of biofuel cell technology for electricity generation
from wastewater and lactose measurement**

A thesis
submitted in partial fulfilment
of the requirements for the Degree of
Doctor of Philosophy

at
Lincoln University
by
Mimi Hani Abu Bakar

Lincoln University

2015

Abstract of a thesis submitted in partial fulfilment of the
requirements for the Degree of Doctor of Philosophy.

Adaptation of biofuel cell technology for electricity generation
from wastewater and lactose measurement

by

Mimi Hani Abu Bakar

Biofuel cell (BFC) is an emerging renewable technology that can perform high direct energy conversion efficiency to electricity. BFC system uses low energy density sources, such as organics in wastewater and converts them into electricity. The system is based on biological catalysts such as microorganisms and enzymes, which are capable of consuming the organics in the sewage for metabolism. In the process, the BFC system will convert the organics in the wastewater and reduce the biological oxygen demand of the sewage to a safe level before it is released to the environment. Nevertheless, commercialisation of BFC applications are still a long way to go due to many weaknesses that have to be overcome. Culturing exoelectrogenic bacteria and applying new materials to enhance catalytic process in microbial fuel cell (MFC) are some of the options to improve MFC operation. The aims of this study are two-fold: To develop (i) a MFC for electricity generation from wastewater by bacteria isolated from a trickling filter, and (ii) an enzymatic fuel cell (EFC) for continuous measurement of lactose concentration in dairy wastewater as well as electricity generation. This thesis shows that the multi-cultured bacteria could generate electricity after 30 days exposure to oxygen at a concentration of 7.5 ppm and that the fabricated graphite-epoxy composite anodes possess the desired characteristics of a good electrode. Such fabricated electrodes can be prepared within a very short time-span compared to commercial electrodes. These electrodes are cheap and flexible for surface modification. However, due to inherent high resistance of the graphite-epoxy composite, it was unable to generate as much current intensity as commercial material electrodes. This study has highlighted several areas that can be further explored such as reducing inherent resistance in graphite composite electrode and the potential use of combined multi-walled carbon nanotube (MWCNT)-diazonium salt within graphite matrix as a reusable high performance electrode.

Keywords: biofuel cell, microbial fuel cell, enzymatic fuel cell, aerobic, composite, *cellobiose dehydrogenase*, aryl diazonium.

Acknowledgements

IN THE NAME OF ALLAH, THE MOST GRACIOUS, THE MOST MERCIFUL,

All praise and thanks to Allah for giving me the strength and patience of pursuing my studies until this level. It is only with the will of Allah SWT that I have managed to complete writing of this thesis.

I would like to thank Ministry of Higher Education (MOHE), Malaysia as my sponsor and the National University of Malaysia (UKM) as my employer for believing in me and giving me the opportunity to do my research in this field. Throughout this journey, I am indebted to Prof. Dato' Ir. Dr. Hj. Wan Ramli bin Wan Daud, Prof. Dr. Abu Bakar Muhamad, Prof. Dr. Siti Kartom Kamarudin, Dr. Manal Ismail and Dr Khuzaimah Arifin for showing me the path and the many academics and researchers in Fuel Cell Institute, UKM that have helped me along the way. A special mention to Pn. Norly Ishak and Pn. Sakinah for always readily assisting me in administrative duty.

The highest gratitude and thanks to Assoc. Prof. Dr. Ravi Gooneratne for always advising and guiding me throughout my studies. It is a great honour that I had the pleasure of being supervised by the late Dr Neil F Pasco. I will always remember him as an attentive supervisor, always with a smile and willing to help. I like to thank LINCOLN AGRITECH^{LTD} team, especially Drs Richard Weld and Joanna Hay, Simon Lee, Nick, Claire and Roger for helping me in the laboratory. I would also like to thank Dr Venkata Chelikani for his help during the last four weeks of thesis writing.

This acknowledgement will not be completed without mentioning Distinguished Prof Kim Byung Hong for assisting me in finalizing my thesis.

Finally, I would not have come through this journey without the support and love of my husband (Ahmad Amryl Abd Malek), my son (Iman), my parents, relatives and all my friends at Lincoln University and University of Canterbury batch 2011/ 2015 (you know who you are ;-)

Thank You.

Table of Contents

Abstract	1
Acknowledgements	2
Table of Contents	3
List of Tables	6
List of Figures	7
Chapter 1 Introduction	8
1.1 Background	8
1.2 Aims	8
1.4 Thesis format	9
Chapter 2 Literature Review	10
2.1 Energy conversion	10
2.2 Bioenergy conversion	10
2.3 Fuel Cell as clean alternative energy	11
2.4 Types of biofuel cells (BFCs).....	12
2.4.1 Microbial fuel cell (MFC)	13
2.4.2 Enzymatic fuel cell (EFC)	15
2.5 Electron transfer pathways.....	16
2.5.1 Mediated electron transfer (MET)	16
2.5.2 Direct electron transfer (DET)	16
2.6 Modification of anode	19
2.6.1 Carbon-epoxy composite electrode.....	20
2.6.2 Carbon nanotube (CNT)	21
2.7 BFC applications.....	21
2.7.1 Bioremediation	21
2.7.2 Wastewater treatment for power generation	22
2.7.3 Control process	23
2.8 BFC improvement	25
Chapter 3	27
3.1 Abstract.....	28
3.2 Introduction	29
3.3 Methods.....	30
3.3.1 Chemicals	30
3.3.2 Inoculum, buffers, reagents and media	30
3.3.3 MFC air-cathode construction	31
3.3.4 Operation	31
3.3.5 Analytical methods and calculation	32
3.4 Results and discussion	32
3.5 Conclusions	40
Chapter 4	41
4.1 Abstract.....	42

4.2	Introduction	43
4.3	Methods	44
4.3.1	Inoculation	44
4.3.2	Anode construction.....	45
4.3.3	Electrografting with 9,10- Anthraquinone-2,6-disulfonic acid disodium salt (AQDS)/ polypyrrole (PPy).....	45
4.3.4	Single chamber air-cathode MFC.....	46
4.3.5	Operation	47
4.3.6	Analyses	47
4.4	Results and discussion	47
4.4.1	Fabrication of graphite-epoxy composite anodes	47
4.4.2	Power generation.....	52
4.5	Conclusion.....	56
Chapter 5		57
5.1	Abstract.....	58
5.2	Introduction	59
5.3	Methods	63
5.3.1	Chemicals	63
5.3.2	Enzyme strain.....	64
5.3.3	Preparation of working electrodes	64
5.3.4	Enzymatic fuel cell air-cathode system construction	65
5.3.5	Electrochemical measurements.....	66
5.4	Results and discussion	66
5.4.1	Sensitivity in lactose detection	66
5.4.2	Prepared electrodes provide continuous current signal	71
5.5	Conclusion.....	72
Chapter 6 General discussion, Conclusions and Future Research.....		73
Appendix A Effect of long time oxygen exposure on power generation of enriched multi-cultured microbial fuel cell (MFC).....		78
A.1	Enrichment of anaerobic MFCs of batch feed modes.	78
Appendix B 9,10-Anthraquinone-2,6-disulfonic acid disodium salt / epoxy graphite composite for anode in microbial fuel cell (MFC).....		79
B.1	Electrode-epoxy mould from modified polyethylene PCR tube	79
B.2	Cyclic voltammograms (CV) of unmodified graphite composite anodes at 20 mV/ s.	79
B.3	Cyclic voltammograms (CV) of graphite composite anodes at multiple scan rates.	80
B.4	Cyclic voltammograms (CV) of non-soluble mediators embedded in graphite composite of 730 mg graphite matrix at 20 mV/ s.	81
B.5	Cyclic voltammograms (CV) on different method applying 9,10-Anthraquinone-2,6-disulfonic acid disodium salt (AQDS) on surface of MWCNT modified 730 mg graphite composite anodes at scan rate 20 mV/s.	82
B.6	Synthesis of polypyrrole (PPy) and molecular structure of 9,10-Anthraquinone-2,6-disulfonic acid disodium salt (AQDS).....	82
Appendix C.....		84

Cellobiose dehydrogenase/ epoxy-graphite composite with aryl diazonium reduction for lactose detection.....	84
C.1 Lactose detection capability in different lactose concentrations via batch mode for electrodes made from commercial graphite rod materials (a) and combined commercial material electrodes (b).....	84
C.2 Lactose detection capability in different lactose concentrations via continuous intermittent flushing for commercial material electrodes with MWCNT added into the system.	85
C.3 Stability test for commercial graphite material anodes modified surface with CDH-gelled at 5 mM lactose.	86
References	87

List of Tables

Table 2.1	Analysis of energy carriers' outlet from glucose	11
Table 2.2	Redox potentials of various couples at T: 303 K (based on Standard Hydrogen Electrode, SHE) and pH 7 (unless stated otherwise).	14
Table 2.3	Types of anode modifications	19
Table 3.1	Daily average current calculated after gas swapping (\pm standard error of mean) (n=2).	34
Table 3.2	Details obtained from MFC electrochemical characterizations.	39
Table 4.1	Inherent resistance measured for graphite-epoxy composite anodes	48
Table 5.1	Some publications on interaction between lactose and CDH-modified electrodes for biosensor and EFC applications.....	60
Table 5.2	Anode reproducibility test at several lactose concentrations.....	69

List of Figures

Figure 2.1	Chemical fuel cell (a), Microbial fuel cell (MFC) (b) and Enzymatic fuel cell (EFC) (c).	12
Figure 2.2	Half reactions in an MFC when glucose and acetate is used separately as substrate in anode compartment.	13
Figure 2.3	Glimpse at bacterial cell and respiration mechanism	14
Figure 2.4	Half reaction in an EFC when ethanol is used as substrate in anode compartment.	15
Figure 2.5	CDH 1: An illustration of CDH enzyme oxidizing lactose for a substrate	17
Figure 2.6	Half reaction of lactose oxidation by CDH at external electron acceptor	18
Figure 2.7	Epoxy resin cross-linking with primary amines	20
Figure 2.8	Schematic diagram of lab-scale bioremediation	22
Figure 2.9	The major component of bovine milk in % (w/w)	24
Figure 3.1	MFC used in this study	31
Figure 3.2	Biocatalytic current generation compared between aerobic and anaerobic environment.	33
Figure 3.3	Effect of gas swapping (↓) between the aerobic and anaerobic MFCs.	34
Figure 3.4	Polarization (a) and power density (b) curves recorded.	37
Figure 3.5	Oxygen concentration within biofilm	38
Figure 4.1	Cyclone shape MFC (a) and the fabricated graphite-epoxy electrodes (b) used in this study	46
Figure 4.2	Cyclic voltammograms between different MWCNT loadings in graphite-epoxy composite anodes at scan rate 20 mV/ s and in 50 mM ferricyanide/ferrocyanide electrolyte at room temperature (n=3)	50
Figure 4.3	Cyclic voltammograms of AQDS/ PPY surface modified on 78% graphite samples (a) without and (b) with 0.04% (w/w) MWCNT loading embedded in the surface of composite matrix before (—) and after 24 h rinsing (- - -) in 0.1 M PB electrolyte at room temperature. Scan rate used was 20 mV/ s.	53
Figure 4.4	Power generation for MFCs operated with (MFC _{Cym} , $y= 1, 2$) and without (MFC _y , $y= 1, 2$) the AQDS/ PPY surface modified anodes on plan graphite-epoxy anodes and on anodes with embedded MWCNT (MFC _{2x} , $x= m, 0$) and without the embedded MWCNT (MFC _{1x} , $x= m, 0$). (a) Anode and cathode polarization curves when using plain graphite as base, (b) when using graphite-epoxy composite embedded with MWCNT as base, and (c) power density curves of four MFCs. Data presented in this figure are representative of at least three independent experiments.	55
Figure 5.1	The in-house EFC made in this study equipped with self-drained system.	66
Figure 5.2	Lactose detection capability in different lactose concentrations via batch mode (a) and continuous mode (b). The (△) represents the modified electrodes without embedded MWCNT, while (▲) represents modified electrodes with embedded MWCNT. Data were obtained using DCPA analysis with working electrode poised at +100 mV/s. The electrolyte was 200 mM lactose diluted in 0.1 M CB to make into different lactose concentrations. Error bars represent standard error of the mean (n=3).	67
Figure 5.3	Molecular representation of safranin (a), the formed diazonium ion getting ready to make bonding (b) and the attachment of the aryl diazonium salt through covalent bond onto a surface (c).	71
Figure 5.4	Stability test done in an air-cathode EFC for fabricated graphite-epoxy anodes with CDH on aryl diazonium surface modification. (▣) represents anodes with embedded MWCNT while (□) represents anodes without embedded MWCNT. Data were obtained using DCPA analysis with working electrode poised at +100 mV/s. The electrolyte was 5 mM lactose in 0.1 M CB at 0.5 mL/ min (n=3).	72

Chapter 1

Introduction

1.1 Background

Our world is dependent on energy for growth and development. At present, the world is facing an energy crisis since the consumption of fossil fuels is projected to last only for another 120 years (Eriksson, 2010). To address the problem, clean alternative energy based on renewable sustainable energy is favoured to ensure a stable supply and clean sustainable environment for strong nation development. Among the wide range of emerging renewable technologies, a biofuel cell (BFC) system stands out because it can perform high direct energy conversion efficiency to electricity, up to 81% (Rabaey et al., 2004). This high-energy conversion efficiency to electricity is far superior to the combustion method, which seldom achieve 40%. A further advantage of the BFC system is its capability to simultaneously extract energy and treat wastewater to a state acceptable for the aquatic ecosystem. Some of these attributes are made possible through utilizing the free and well diverse microorganisms and fabricated electrodes. There are two types of BFCs, one is microbial fuel cell (MFC) that uses microbes and the other is the enzymatic fuel cell (EFC), which uses isolated enzyme(s) mainly from these microbes.

1.2 Aims

The main aims of this PhD project are:

- i. To understand the role of long term oxygen exposure on enriched multi-cultured bacteria in MFC system
- ii. Fabricate graphite-epoxy composite electrodes with more than 70% of graphite using simple procedure(s) and apply them in MFC system with enriched multi-cultured bacteria
- iii. Lactose detection and electricity generation using the above mentioned fabricated electrodes immobilized with cellobiose dehydrogenase (CDH) in EFC system

1.3 Objectives and hypotheses

1. To analyse the effect of long term oxygen exposure on enriched multi-cultured bacteria of anode in MFC system.

Emphasis will be on characterising the MFC performance by plotting power (P) vs current density (I) over varying load ranges using enriched multi-cultured bacteria exposed to oxygen for an extended time period.

Hypothesis: Selected exoelectrogenic bacteria will tolerate both aerobic and anaerobic conditions.

2. To investigate the capability of MFC system when operated with graphite-epoxy composite electrode fabricated with more than 70% of graphite using simple procedure(s) and within 24 h.

Emphasis will be to:

- Operate MFCs using the exoelectrogenic bacteria selected from a tricking filter (see Objective 1) on fabricated graphite based anodes.
- Comparison of fabricated carbon anode and fabricated carbon anode embedded with multi-walled carbon nanotube (MWCNT) for electron transfer improvement in MFC.

Hypotheses:

- i. The fabricated graphite-epoxy composite with more than 70% graphite shows electrochemical response almost similar to the conductive commercial graphite rod.
 - ii. 9,10-antraquinone-2,6-disulfonic acid disodium salt/ polypyrrole-modified fabricated anode improves the electron transfer in MFC.
3. To investigate the performance of immobilised CDH for lactose detection and its stability using aryl on graphite-epoxy electrodes developed from objective 2 with and without MWCNT.

Emphasis will be to use the anode immobilised with CDH (from fungus, *Phanerochaete sordida*) and lactose as a substrate.

Hypotheses:

- i) The current measured by the prepared electrodes will be proportional to the lactose concentration.
- ii) Graphite-epoxy composite anode in EFC will help to produce a continuous current signal for up to 25 days.

1.4 Thesis format

This thesis acknowledges the contribution from other researchers with the term 'they' and 'their' while referring to the original results observed by myself with the term 'this study'. Some chapters (3, 4, and 5) in this thesis are organized as stand-alone scientific publications. This has led to some overlap in the materials and methods section (particularly between chapters 3, 4, and 5). Some material has been intentionally left out of the general introduction and literature review to avoid repetition in the introductions to data chapters. The specific discussions in each data chapter (chapters 3 to 5) contain most of the discussion material, while a more concise general conclusion at the end is aimed to raise synergies between the different chapters and to show the coherence of different chapters to the overall purpose of the research. That too has been intentionally kept short to avoid repetition.

Chapter 2

Literature Review

2.1 Energy conversion

In reality, it is not possible to convert energy at 100% efficiency. Factors such as type of fuel and instrument to convert the energy to work hinder the possibility of higher efficiency (the second law of thermodynamics). For instance, gasoline's energy density is 45 MJ/ kg (Golnik, 2003). The conventional pathway for harnessing the free energy from this non-renewable fossil fuel using an internal combustion engine can only give 35% of work efficiency (Lewis, 2008) while most of the internal energy is lost into the surrounding as heat. Although this pathway gives poor energy conversion, the combustion is still popular due to its simplicity and available infrastructure. Unfortunately, non-renewable fossil fuel will eventually come to an end. Alternative fuels that are renewable, sustainable and non-pollutant need to be available and functional before the world runs out of fossil fuel to ensure continuity in energy supply. This creates opportunity for renewable energy technologies that come either direct from sunlight or manifested from sunlight, in the form of biomass, wind and water. These choices of renewable technology, except biomass, are very costly and highly dependent on geographic aspects. Renewable biomass is diverse, ranging from living organisms, dead organisms to biodegradable waste (Nag, 2008) and can be converted to energy through various means.

2.2 Bioenergy conversion

Biomass can be converted to different energy carriers, such as methane, ethanol, hydrogen and electricity (Rittmann, 2006) (Table 2.1). In the bioenergy conversion pathways, the first step involves biocatalytic activity. The normal biology conversion pathways will be through fermentation reaction that requires anaerobic environment. Different fermentation will dictate the type of energy carriers. For instance, when yeast ferments glucose through glycolysis pathway, ethanol will be produced. In this pathway, 91% energy from the glucose, which is -15.96 MJ/ kg will be retained in ethanol (The Japan Institute of Energy, 2008). Alternatively, the methanogenesis pathway will produce methane from fermentation of glucose. In order to tap the methane to produce electricity, a combustion process is needed. This further reduces the net energy output to only 33% of electrical-energy conversion efficiency. Unlike methane and ethanol, hydrogen and electricity do not require combustion to liberate the electrons. These two energy carriers can go through an isothermal direct redox process via the fuel cell that boosts the electrical-energy conversion efficiency to more than 50%.

Table 2.1 Analysis of energy carriers' outlet from glucose

Energy carrier	Gibbs free energy (kJ/ mol C ₆ H ₁₂ O ₆)	Electrical energy-conversion efficiency (%)	Net yield (kJ/ mol C ₆ H ₁₂ O ₆)
C₂H₅OH	-2,630		-870
C ₆ H ₁₂ O ₆ → 2C ₂ H ₅ OH + 2CO ₂ ... (fermentation)			
C ₂ H ₅ OH + 3O ₂ → 2CO ₂ + 3H ₂ O ... (combustion)		~33	
CH₄	-2,450		-730
C ₆ H ₁₂ O ₆ → 3CH ₄ + 3CO ₂ ... (biomethanation)			
CH ₄ + 2O ₂ → CO ₂ + 2H ₂ O ... (combustion)		~33	
H₂ + CH₄	-2,590		-1,090
C ₆ H ₁₂ O ₆ + 2H ₂ O → 2CH ₃ COOH + 4H ₂ + 2CO ₂ ... (fermentation)			
2CH ₃ COOH → 2CH ₄ + 2CO ₂ ... (biomethanation)			
2H ₂ + O ₂ → 2H ₂ O ... (chemical fuel cell)		~55	
CH ₄ + 2O ₂ → CO ₂ + 2H ₂ O ... (combustion)		~33	
Electricity	-2,870		-1,870
C ₆ H ₁₂ O ₆ + 6H ₂ O → 24H ⁺ + 24e ⁻ + 6CO ₂ ... (bacterial catabolism)			
4H ⁺ + 4e ⁻ + O ₂ → 2H ₂ O ... (microbial fuel cell)		~65	

Source: (Logan, 2004; Rittmann, 2006; The Japan Institute of Energy, 2008)

2.3 Fuel Cell as clean alternative energy

Fuel cell technology is a form of renewable energy source that is being actively engaged through research. Although bound by the second law of thermodynamics, fuel cell has higher energy efficiency as compared to a Carnot heat engine. A fuel cell converts chemical energy directly to electrical energy as work (Hassanzadeh & Mansouri, 2005) without any need for combustion. This is an advantage with regards to the environment and work conversion efficiency. The principle of fuel cell was first published in 1838 by Christian Friedrich Schönbein and after languishing for more than a century, a resurgence of research in this technology is beginning to show improvement in power output.

A basic single fuel cell (Figure 2.1a) is constructed with two compartments of anode and cathode separated by a selective permeability membrane. These compartments are connected together with a conductor forming an external circuit. During a fuel cell operation, the substrate, which acts as fuel will be oxidized in the anode compartment. This releases electrons and hydrogen ions with the assistance from the catalyst at the anode. Due to the selective permeability membrane, only hydrogen ions are able to flow to the cathode. The potential difference between the anode and cathode drives electrons to move through the external circuit to reach the cathode. Electrons that reached the cathode will reduce an electron acceptor, usually oxygen in air and will combine with hydrogen ions to produce water.

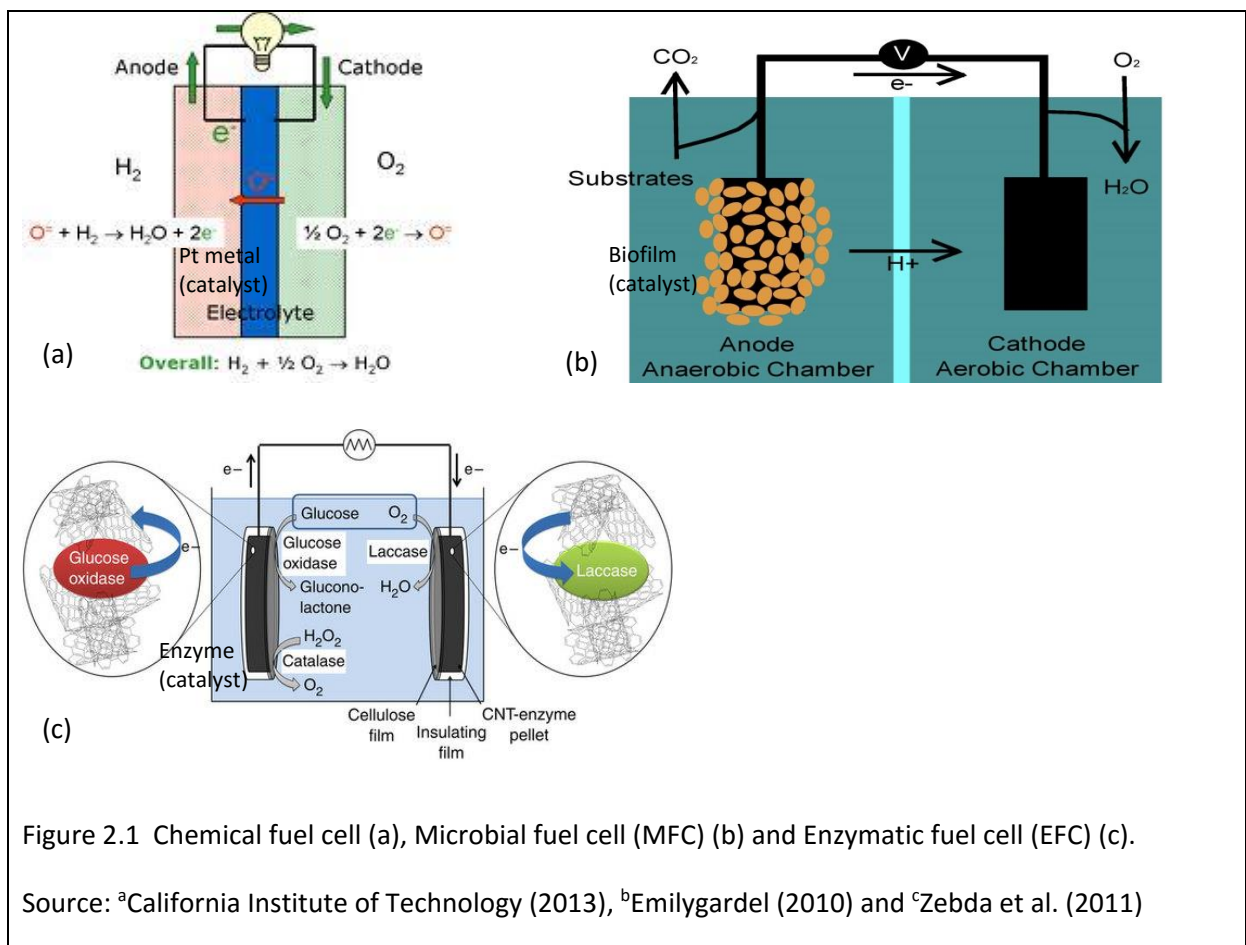


Figure 2.1 Chemical fuel cell (a), Microbial fuel cell (MFC) (b) and Enzymatic fuel cell (EFC) (c).

Source: ^aCalifornia Institute of Technology (2013), ^bEmilygardel (2010) and ^cZebda et al. (2011)

2.4 Types of biofuel cells (BFCs)

In comparison with chemical fuel cells, a BFC has the advantage to work at ambient temperatures that requires less external energy source. BFCs are categorized into two groups based on the biocatalyst used, the microbial fuel cell (MFC) (Figure 2.1b) that uses the microbes and the enzymatic fuel cell (EFC)(Figure 2.1c) that uses isolated and purified enzymes. Though the catalysts are different, the working mechanisms of these biofuel cells are similar, which is extracting electrons

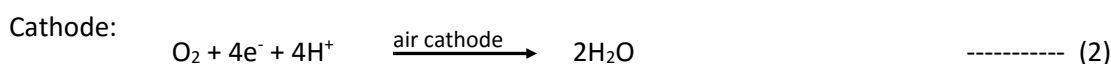
through favoured substrate oxidation and passing them to an anode electrode. The electron then travels to the cathode via an outer circuit.

2.4.1 Microbial fuel cell (MFC)

Advantages of bacteria (prokaryote) and yeast (eukaryote) are that they are abundant in nature, easy to self-replicate, able to consume various biodegradable organics for carbon source (Chae et al., 2009) and have flexible low operating temperature between the range of 15 to 60°C (Logan, 2008). The carbon source, which is also called as substrate, is the energy source and contains nutrients for microorganism.

The common electrochemical reactions in an MFC are as shown in equations (1) – (4).

Glucose as substrate:



Acetate as substrate:



Figure 2.2 Half reactions in an MFC when glucose and acetate is used separately as substrate in anode compartment.

Organic compounds; such as acetate, butyrate, propionate and glucose that serves as electron donor (Chae et al., 2009) will be broken down to simple molecular unit, to go through process of glycolysis and citric acid cycle (Figure 2.3). Series of oxidation processes will take place with the assistance of the coenzymes NAD^+ and FAD and other electron carriers between the cytoplasm and the cell membrane. At the cell membrane, the electron transfer chain (ETC) takes place through redox sites bound in the membrane and finally to a soluble terminal electron acceptor, such as oxygen or some inorganic compounds, such as nitrate, sulphate, carbon dioxide (Cutright 2002; Osman et al., 2010).

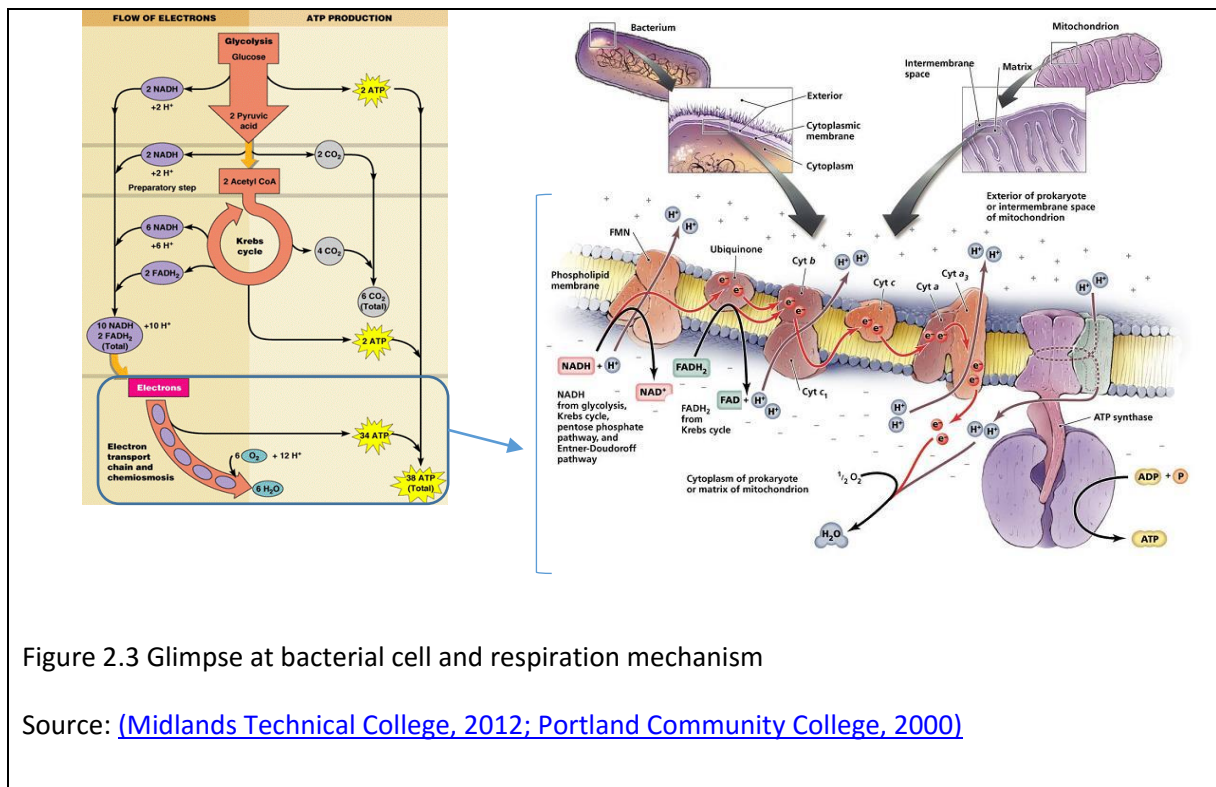


Figure 2.3 Glimpse at bacterial cell and respiration mechanism

Source: [\(Midlands Technical College, 2012; Portland Community College, 2000\)](#)

Oxygen and nitrate are preferred terminal electron acceptors over the solid anode in BFCs due to their high redox potentials (Table 2.2) and their excessive presence inhibited the electricity generation. However, this is not crucial because any oxygen left in the anode compartment will soon get exhausted through bacterial respiration. Commonly, the bacteria at the anode compartment will usually be in an anaerobic environment (Table 2.1b). To gain energy, bacteria needs to perform anaerobic respiration. Since this is an oxidation-reduction reaction process, it could only happen when the electron acceptor is more electronegative than the electron donor.

Table 2.2 Redox potentials of various couples at T: 303 K (based on Standard Hydrogen Electrode, SHE) and pH 7 (unless stated otherwise).

Couple	Potential (V)	Couple	Potential (V)
^a CO ₂ / C ₆ H ₁₂ O ₆ , 24 e ⁻	-0.43	^b Methylene blue _{ox/red} , 1e ⁻	0.01
^a 2H ⁺ / H ₂ , 2e ⁻	-0.42	^a S ₄ O ₆ ²⁻ / S ₂ O ₃ ²⁻ , 2e ⁻	0.02
^a CO ₂ / CH ₃ OH, 6e ⁻	-0.38	^a Fumarate, succinate, 2e ⁻	0.03
^a NAD ⁺ / NADH, 2e ⁻	-0.32	^a Cytochrome b _{ox/red} , 1e ⁻	0.04
^a CO ₂ / acetate, 8e ⁻	-0.28	^a Ubiquinone _{ox/red} , 2e ⁻	0.11
^a S ⁰ / H ₂ S, 2e ⁻	-0.28	^c Ferrocene/ferrocenium, 1e ⁻	0.17
^a SO ₄ ²⁻ / H ₂ S, 8e ⁻	-0.22	^a Fe ³⁺ / Fe ²⁺ , 1e ⁻ (pH=7)	0.20
^a Pyruvate/ lactate, 2e ⁻	-0.19	^a Cytochrome c _{ox/red} , 1e ⁻	0.25
^b 2,6-AQDS/ 2,6-AHQDS, 2e ⁻	-0.19	^a Cytochrome a _{ox/red} , 1e ⁻	0.39
^b FAD/ FADH ₂ , 2e ⁻	-0.18	^a NO ₃ ⁻ / NO ₂ ⁻ , 2e ⁻	0.42

^b Menaquinone _{ox/red} , 2e ⁻	-0.08	^a NO ³⁻ / ½ N ₂ , 5e ⁻	0.74
^b Pyocyanin _{ox/red} , 2e ⁻	-0.03	^a Fe ³⁺ / Fe ²⁺ , 1e ⁻ (pH=2)	0.76
		^a ½ O ₂ / H ₂ O, 2e ⁻	0.82

Source: ^aLogan (2008), ^bDu et al. (2007) and ^cMailley et al. (2003)

When oxygen is supplied to the cathode that has been separated from the anode by a membrane, it attracts the bacteria in the anode compartment, which is anaerobic to transfer their electrons to the anode. This happens because oxygen has a very high electronegativity (Table 2.2) and will draw the electrons from the bacteria, creating a flow of electrons through the external circuit from anode to cathode. The bacteria that are capable of performing anodic respiration without help from soluble exogenous mediators are called exoelectrogens (Schaetzle et al., 2008).

2.4.2 Enzymatic fuel cell (EFC)

In contrast to MFC, an EFC utilizes enzymes as biocatalyst and has specific action, which is confined to a single compound or a family of compounds. Unlike MFC that utilizes the whole microorganisms, an EFC uses the enzyme instead (Figure 2.1c). The inability of an enzyme to regenerate itself as microorganism could, causes an EFC to have a much shorter operational life in comparison to an MFC. Each enzyme has specific activity and highly selective in choices of substrates. This is unlike bacteria that are able to consume a variety of substrates as fuel in MFC. The substrate specific limitation leads to the application of several enzymes for complete oxidation of only one substrate. For instance, in the process to oxidize ethanol to acetate at an EFC anode compartment, two types of enzymes and a coenzyme are required. The first enzyme, alcohol dehydrogenase, oxidizes the ethanol to acetaldehyde with the help of coenzyme NAD⁺ (Equation 5). The second enzyme, aldehyde dehydrogenase, then oxidizes the acetaldehyde to acetate with the help of coenzyme NAD⁺ (Equation 6). These oxidation processes produce four electrons which when transferred to the cathode, reduce oxygen to water (Topcagic & Minteer, 2006) (Equation 7).

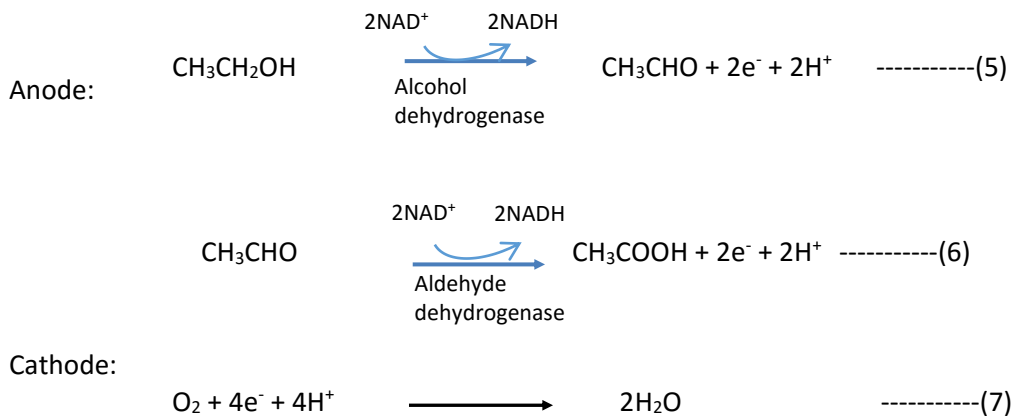


Figure 2.4 Half reaction in an EFC when ethanol is used as substrate in anode compartment.

In addition to that, only a small current signal is detected from the EFC in comparison to an MFC. Although the latter seems like a disadvantage towards the EFC, it actually proves that an EFC system could become a control system on specific substrate.

2.5 Electron transfer pathways

Electron transfer pathways across interfaces are very important to all living systems and involve molecules both large, such as redox proteins and redox enzymes and small, such as NADH, quinones, ions and redox mediators. Only few of these biocatalysts that could perform direct electron transfer (DET) to an electrode while many others are still onto mediated electron transfer (MET).

2.5.1 Mediated electron transfer (MET)

For the DET incompetent biocatalysts, assistance from artificial redox mediator is required to overcome the energy barrier caused by activation polarization (Du et al., 2007) and proceeds at much faster rates (Schaetzle et al., 2008). During the early mediator application in BFC, soluble mediator type was chosen such as neutral red (NR) (Daniel et al., 2009; Ieropoulos et al., 2005), methylene blue (MB) (Daniel et al., 2009; Ieropoulos et al., 2005; Rahimnejad et al., 2011b), thionine (Ieropoulos et al., 2005; Tanaka et al., 1983), meldola's blue (MelB)(Ieropoulos et al., 2005), 2-hydroxy-1,4-naphthoquinone (HNQ)(Ieropoulos et al., 2005) and Fe(III) EDT (Vega & Fernandez, 1987). When in oxidized state, the soluble mediator penetrates the outer membrane and cytoplasmic membrane of the cell. The electrons produced by the bacterial cell, which are carried by electron carriers such as NADH and FADH₂ during the substrate oxidation process will be passed on to these mediators. The reduced mediators will then diffuse out of the cell and transfer the electrons to the anode surface (Du et al., 2007; Wang et al., 2006). Although adding soluble mediators into the BFC system is simple, the problem occurs when the system is in continuous flow mode, hence requires the expensive mediators to be continually replenished (Park & Zeikus, 2002). In addition to that, these mediators are toxic and should be removed before wastewater is discharged to the environment (Prasad et al., 2007).

2.5.2 Direct electron transfer (DET)

Microbial cells gain energy from pumping of protons across the inner membrane to form a proton gradient, which drives the formation of ATP from ADP through ATPase (Franks & Nevin, 2010). Extracellular electron transfer acts to move the electrons to the anode surface. The microorganism that are able to perform DET are known as exoelectrogens. Studies on electron transfer between bacteria and an anode has led to the findings that bacteria such as *Pseudomonas aeruginosa* (Logan & Regan, 2006) and *Shewanella oneidensis* (Lanthier et al., 2008) are able to reduce an external electron acceptor at a distance, without the addition of exogenous mediators using self-produce

mediator and pili respectively. Some bacteria such as *Geobacter sulfurreducens* (Bond & Lovley, 2003) and *Geothrix fermentans* (Bond & Lovley, 2005) lack the nanowires, however are capable to perform DET when their active centre of the membrane enzymes are in direct contact with electrodes (Schaetzle et al., 2008). This goes the same with *Shewanella putrefaciens* strain, where DET through direct physical contact between the cells and the electrode are achievable in anaerobic environment (Kim et al., 2002). In addition, there are number of studies analysing microbial activity in view of the electrode in assisting electricity production (Peng et al., 2010; Xu et al., 2009; Zou et al., 2008). Rosenbaum et al. (2007) shows through anode modification with tungsten carbide, common fermentation products, such as hydrogen, formate and lactate generated by the microbes, could be oxidized in MFCs to generate electricity (Rosenbaum et al., 2007). As for yeast cells, though the cell walls are reported to be thick (100- 200 nm) with building block from polysaccharides and proteins, *Saccharomyces cerevisiae* (Rawson et al., 2012) and *Arxula adenivorans* (Haslett et al., 2011) are capable to perform DET through exported soluble redox species and directly from the external surface of the cell wall.

In the context of redox active enzymes, the DET is when electrons are tunnelled directly from the active site fixed in the enzyme to the electrode (Bullen et al., 2006). The normal enzymes involved in redox activities are from the classes of oxidases and dehydrogenases. While some have diffused redox centres, such as NADH/ NAD⁺, some have redox centres near or at the periphery of the protein shell of the enzyme (Bullen et al., 2006). These inherent physical structures help the enzyme to perform DET naturally. For the purpose of objective 3 in this study, the enzyme of interest is the cellobiose dehydrogenase (CDH) enzyme because of the simplicity of using a single enzyme and its high specificity for lactose oxidation.

Cellobiose dehydrogenase (CDH) enzyme

CDH enzyme contains two domains, a dehydrogenase (represented by FAD) and a cytochrome (represented by heme) in close proximity to allow internal electron transfers between the domains (Figure 2.5). These two domains are responsible for the electrons transfer from substrate oxidation reaction to electron acceptors (Glithero et al., 2013; Harreither, 2010; Tasca et al., 2009).

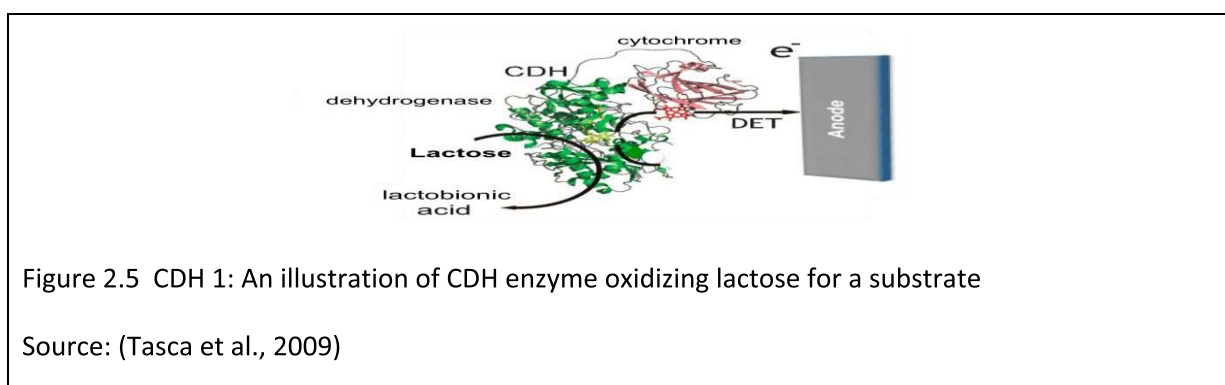


Figure 2.5 CDH 1: An illustration of CDH enzyme oxidizing lactose for a substrate

Source: (Tasca et al., 2009)

Enzyme kinetics of CDH enzyme

During lactose oxidation, the FAD domain, which performs the catalysis in the CDH enzyme, will accept two electrons from the substrate (Figure 2.6). This will oxidize the lactose into lactobionic acid and eventually reduce FAD to FADH₂ (Equation 8 – 9). The electrons will be passed one at a time to the heme domain (Fe³⁺/ Fe²⁺), which lies about 15 Å from the FAD domain via a flexible linker. Upon being reduced, the heme will release a proton to the solution and flavin semiquinone is formed (Equation 10). The reduced heme will then be reoxidized by transferring the electrons to an external electron acceptor provided there are no dissolved electron acceptor in the solution (Equation 11). Process of fully oxidizing FAD will continue in Equation 12 - 13 to enable the CDH to catalyze oxidation of another substrate molecule (Larsson et al., 2000; Ludwig et al., 2010).

Substrate oxidation at FAD domain:



ET from FAD to heme and DET from heme to external electron acceptor:



Figure 2.6 Half reaction of lactose oxidation by CDH at external electron acceptor

In nature, CDH enzyme is produced by white rot fungi from the phyla of Basidiomycota (*Phanerochaete sordida*, *Phanerochaete chrysosporium* and *Trametes villosa*) and Ascomycota (*Myriococcum thermophilum*). Between these two phyla, basidiomycete CDHs show substrate specificity towards β-1,4- linked substrates, such as cellobiose, lactose and a distinct discrimination over glucose and maltose (Tasca et al., 2009). These features make the CDH enzyme an efficient oxidizing agent and a preferred enzyme in shuttling the electrons from the substrate, especially lactose to the electrode (Canevascini et al., 1982; Henriksson et al., 2000). In addition, the CDH because of its robust characteristic is able to extend the lifespan of EFC (Tasca et al., 2009).

2.6 Modification of anode

The ability for DET requires fulfilment of at least one of the following (Kumar et al., 2013; Tasca et al., 2011a):

- i) Close proximity of the active site of the redox enzyme to the protein surface, or
- ii) Connection with the protein surface/ microorganism by a built in electron transfer pathway constructed by a chain of redox active cofactors/ electric wire, or
- iii) Strength of adhesion between protein surface/ microorganism and the electrode surface

Unfortunately, the above prerequisites are not enough to ensure high electron transfer rates since it is dependent on correct orientation of the active site and vicinity to the electrode surface. This has initiated the researchers to experiment on various ways to get the desired effect through anode modifications (Table 2.3).

Table 2.3 Types of anode modifications

Types	Aim
Surface treatment	
<i>Ammonia</i>	Increase adhesion of microorganisms onto the anode interface by enhancing the positive charge of the electrode surface (microorganisms are negatively charged)
<i>Acid</i>	
<i>Heat</i>	Facilitate adhesion and inoculation of microorganism on the electrode surface by increasing surface area of anode materials.
<i>Electrochemical oxidation</i>	Generates new native functional groups such as carboxyl to create strong hydrogen bonds between microorganisms and anode.
Nanostructured materials	Enhance surface area of the electrodes
Conductive polymers and composites	Enhance electronic conductivity of anode materials
Polymer nanocomposites	Enhance both electronic conductivity and surface area, hence decreased the electron and mass transfer resistance and increased contact between electrode and microorganisms.

Source: Kumar et al. (2013) and Li et al. (2014)

2.6.1 Carbon-epoxy composite electrode

Carbon in many aspects conforms to most of the criteria of a good biosensor (Chaplin, 2004; Logoglu et al., 2006), such as: 1) Highly specific in its operation and maintain stability when in storage, 2) Operation should be independent of physical parameters used in the measurement, such as stirring, pH and temperature. This is related to electrode surface coating with catalyst, which should be hydrophilic and have good mechanical properties and stable over the temperature and pH ranges used, 3) Output has to be accurate, precise, reproducible and linear over the analytical range and free from noise, 4) Resistant to fouling or proteolysis (breakdown of proteins or peptides into amino acids by the action of enzymes), 5) System should be cheap, portable and simple, and 6) System should be marketable, thus making it a popular material for electrode fabrication. A carbon-epoxy composite consists of cheap construction material with an output exhibiting rigid feature. This happens when the epoxy resin that contains the epoxide groups cross-linked (cured) with polyfunctional hardeners that contains amine to form thermosetting polymer, often possess strong mechanical properties with good resistance to high temperature and chemical (Bhatnagar, 1996; Karayannidou et al., 2006). These resins contain hydroxyl groups (OH), which created hydrogen bonding throughout the backbone and able to perform other cross-linking reactions (Figure 2.7).

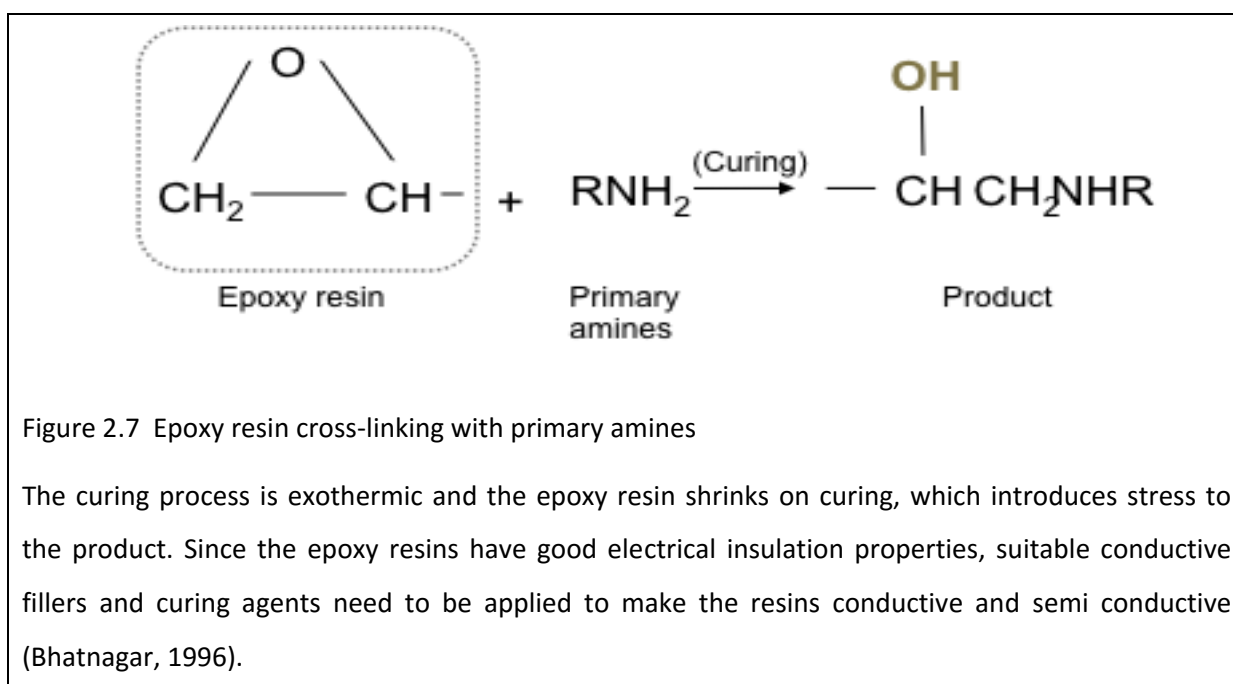


Figure 2.7 Epoxy resin cross-linking with primary amines

The curing process is exothermic and the epoxy resin shrinks on curing, which introduces stress to the product. Since the epoxy resins have good electrical insulation properties, suitable conductive fillers and curing agents need to be applied to make the resins conductive and semi conductive (Bhatnagar, 1996).

The OH will take in hydrogen from carbon black that mixed with the epoxy resin polymer and left the surface of carbon black high in electron density (Martin et al., 2005). Since graphite is a conducting material with regards to its delocalized electrons, the combination between the graphite as filler and the epoxy resin provide versatility in fabricating custom made electrodes, i.e. having various sizes

and shapes, and easy adaptation to wide electrode configurations (Kirgoz et al., 2006). Apart from that, it is also simple to make and have reusable surface through polishing.

However, the graphite-epoxy composites was known to have significant ohmic resistance and large capacitance, which in turn produces a response delay (O'Hare et al., 2002). Based on Ma et al. (2010) and Martin et al. (2005), application of nanotubes could improve conduction pathway in the epoxy matrix and increase its conductivity when made as filler at a low carbon nanotube (CNT) loading, as low as 0.5 wt.% (Ma et al., 2010; Martin et al., 2005).

2.6.2 Carbon nanotube (CNT)

There are two subclasses of CNT; the single walled CNT (SWCNT), consist of single hallow tube with diameter between 0.4 – 2 nm and multiwalled CNT (MWCNT), consist of multiple concentric nanotubes with diameter between 2 – 100 nm. For SWCNT, the diameter and chirality defined its characteristic either metallic or semi-conductors while MWCNT is regarded as metallic conductors. Treatment with mineral acids, such as nitric (HNO₃) and sulphuric acid (H₂SO₄) will cause the capped ends of the CNT to be removed and reveal the open ended tubes. These open ended tubes contain dangling bonds of sp² carbon. The sp² is CNT bonding structure and responsible for CNT's extremely high mechanical properties. These sp² will become active when in organic solvents by involving further in chemical reaction or produced other oxygenated functional groups. Creation of specific functional groups can increase the rate of electron transfer that is surface independent (Gooding, 2005)

2.7 BFC applications

Based on the reported BFC studies, there are many of its attractive features, such as operating at moderate temperature, wide choices of fuel, low fuel concentration and fuel selective ability that show opportunities for broad applications. Some of the practical applications of the BFC identified by Bullen et al. (2006) are in the bioremediation, power generation sectors and control processes (Bullen et al., 2006).

2.7.1 Bioremediation

Human activities often cause adverse impact on environment, such as crude oil spill, untreated sewage effluent, uncontrolled chemigation, gasoline spill/ dumping and chlorinated solvents. Since the world can be seen as a closed system, the consequences of these contaminations will eventually be thrown back at us. This happens when permeable soil or an aquifer loaded with contaminants leaches into the ground water system, which we then later used in our everyday life. To lessen the

impact, the application of bioremediation shows great potential for this purpose (U.S Geological Survey, 1997).

Bioremediation removes organic and inorganic matter by using microorganism's natural ability in consuming wide range of substrates. The microorganism, under environmental conditions suitable for microbial growth, will consume the contaminant through oxidation. When this happens, carbon dioxide will be released while the soil and sediment becomes free from contamination. The carbon dioxide released will then return to the carbon cycle (Vidali, 2001).

The discovery of several metal-reducing bacteria, such as *Geobacter spp.*, *Shewanella spp.*, *Rhodoferrax ferrireducens*, *Aeromonas hydrophila*, *Pseudomonas aeruginosa*, *Clostridium butyricum* and *Enterococcus gallinarum*, as laid out by Jung (2007), has increased the opportunity of cleaning soil pollutions on aquatic sediments and aquifers from heavy metal contamination, such as arsenic. One of the studies done in the field of remediation was by Hong et al. (2009) (Hong et al., 2009). They used MFC with graphite electrodes on sediment organic matter (SOM) from three different freshwater lakes. The anode was buried in the sediment to create anoxic environment for the bacteria while the cathode was laid at surface of the sediment (Figure 2.8). From this, they were able to demonstrate that the MFC could self-sustain while remediating the SOM from contaminants until 30% under closed-circuit condition.

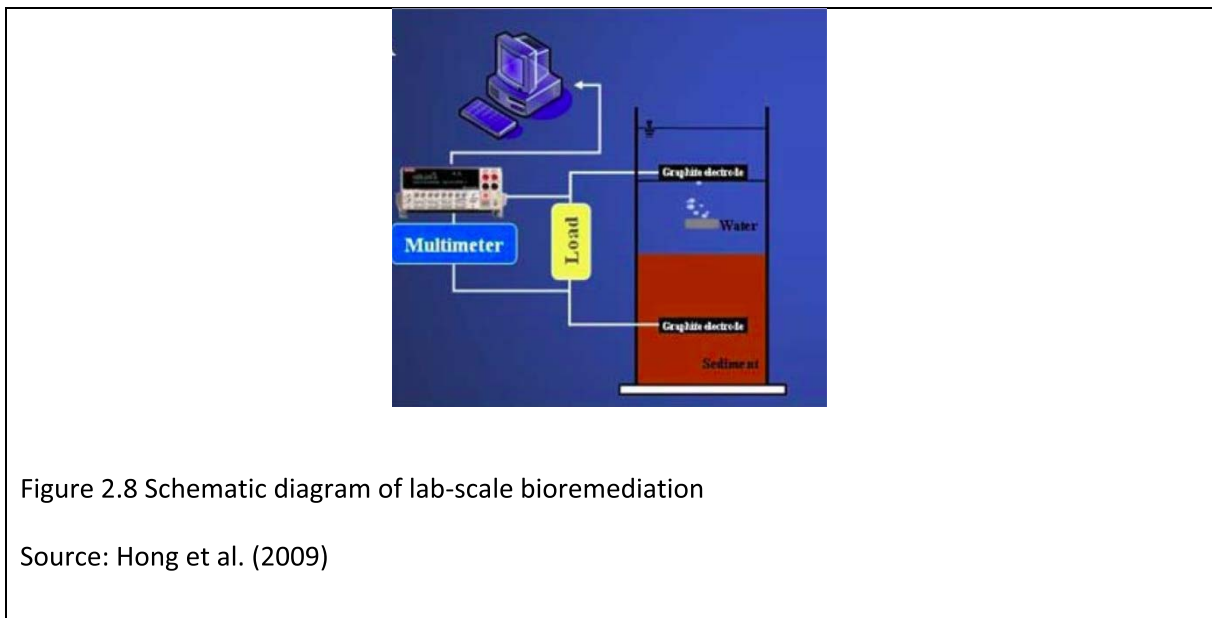


Figure 2.8 Schematic diagram of lab-scale bioremediation

Source: Hong et al. (2009)

2.7.2 Wastewater treatment for power generation

A continuity of the bioremediation technology will be the utilization of electrons produce by the bacteria for power generation (Daniel et al., 2009; Kiely et al., 2010; Lu et al., 2009; Min et al., 2005;

Scott et al., 2007). In this context, wastewater from a wastewater treatment plant is a suitable choice (Antonopoulou et al., 2010). Wastewater contains a wide range of highly diluted contaminants, such as organic waste, metals, chemicals, microorganisms and solvents (Ferguson et al., 2003), which have yet to be biodegraded, manifested as the biological oxygen demand (BOD) value. A typical influent of wastewater to a wastewater treatment plant has a BOD value of 300 mg/ L (Bitton, 2005), and need to be lowered to ≤ 20 mg/ L to avoid environmental water pollution (Rich, 2003). By applying the MFC treatment to the present infrastructure of the wastewater treatment system, the effluent from a wastewater treatment system will not just have a compliant BOD value, but also a reduction in sludge and a self-sustaining treatment process (Venkata Mohan et al., 2014). Based on prior research, MFC can reduce almost 100% of the chemical oxygen demand (COD) in various types of wastewaters (Kiely et al., 2010; Lu et al., 2009; Min et al., 2005) while concurrently generating power density until 260 mW/ m² (Min et al., 2005). In a different study done on performance durability and stability of MFC, Moon et al. (2006) made artificial wastewater from glucose and glutamic acid to closely resemble the actual wastewater as substrate (Moon et al., 2006). The use of artificial wastewater was to reduce unknown variables in the study with regards to their two chambers MFC. The biocatalyst used in the MFC was an enriched mix consortia originating from activated sludge of the wastewater treatment plant. They reported that a maximum power density of 560 mW/ m² was achievable for a 20 mL anode by fixing its feeding rate at 0.53 mL/ min and maintained the temperature at 35°C.

Conventional wastewater treatment system

The conventional wastewater treatment plant requires wastewater to undergo four different consecutive treatments, which are preliminary, primary, secondary and tertiary treatment. The preliminary and the primary treatment perform physical process of removing large objects and sedimentation of suspended solid respectively. This removes up to 35% of organic material and 65% of suspended solids. The secondary treatment performs aerobic biological method, which utilizes microorganisms to further remove biodegradable dissolved organic matter until less than 30 mg/ L. Most of the dissolved organic matters are removed in the secondary treatment stage. The final stage is the tertiary treatment where further removal of organic solid until 15 mg/ L takes place. The remainder, such as raw sludge and biological solids, which are the by-products of the four main treatments, are then directed to digesters. These by-products with BOD more than 2,000 mg/ L will be further consumed by anaerobic bacteria that inhabit the digester (Chan et al., 2009).

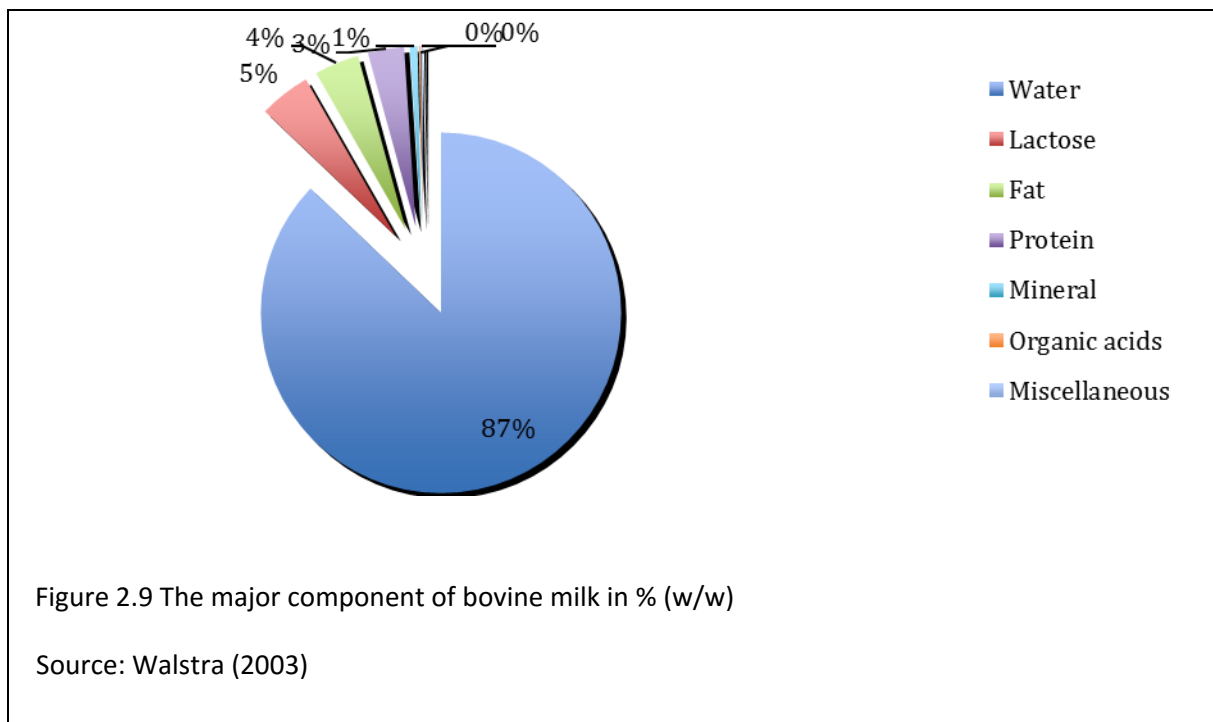
2.7.3 Control process

Another important application that has the potential for BFC would be in the context of control process. This is a process to rectify situation based on comparing actual performance monitored

against a standard (Farlex 2012), such as in BOD sensors and biomedical sector. The common industrial practise to quantify the degree of organic contamination in natural waters as well in wastewater monitoring process is through BOD₅, which is time consuming and demand for skilled operator (Abrevaya et al., 2015). The use of MFC in this area seems appropriate because the Coulomb generated in the MFC is proportional to the concentration of the fuel consumed by the exoelectrogen bacteria, provided there is inhibition of other unwanted electron acceptors other than the exoelectrogen in the anodic compartment (Chang et al., 2005; Lorenzo et al., 2009).

In biomedical sector, many researches are focusing on implantable biomedical devices. This is crucial to closely monitor blood glucose concentration to reduce the risk of diabetes complication (Jiang et al., 2008). Hence, importance are placed on design requirement, small, low power source system (BarriÈre et al., 2006), low concentration sensitivity and longer stability performance. For this purpose, enzyme is preferred rather than a whole microorganism cell because of its high substrate selectivity and action specificity. Recently, a research team from Joseph Fourier University in Grenoble, France implanted an improved design of glucose blood monitoring devise into two rats. The device showed maximum power of 6.5 mW, which is 3.5 mW less than power requirement of a pacemaker and could last for three months (Weaver, 2010).

Apart from research in medical area, some of the studies in this field has also focuses on application in dairy products, such as lactose (Conzuelo et al., 2010; Eshkenazi et al., 2000; Goktug et al., 2005; Glce et al., 2002; Jenkins & Delwiche, 2003; Rajendran & Irudayaraj, 2002; Stoica et al., 2009; Tasca et al., 2009), which is also the interest in this study.



Lactose from dairy plantation

Lactose is a disaccharide in milk synthesized from two simple sugars: galactose and glucose. In terms of taste, lactose is 16% less sweet than ordinary table sugar, which makes it unqualified as sweetening agent. Lactose composition varies from species, for instance human's milk has 7% of lactose composition while bovine milk has 4.6 % (Figure 2.9).

In dairy industry, whey was previously treated as waste, and released into the environment through land irrigation and sewer causing environmental pollution (Fox, 2009). The uncontrolled disposal of whey has caused lactose to pollute the environment by inducing the growth of microorganism, which in turns increase the BOD value of water. To reduce this problem, lactose is recovered from whey to become raw material for food and pharmaceutical industries, such as in production of infant milk formula and filler/ binder in tablets and capsules respectively. The pure lactose is obtained from whey, which has gone through series of process involving evaporation to induce lactose crystallization and washing to remove impurities. This process however did not manage to recover 100% of the lactose, contributing to traces of lactose in the wastewater stream (Kellam, 1998).

At present, techniques to detect lactose in milk products include chromatography and mass spectrometry which offer high sensitivity and good reliability results. However, such analytical techniques are expensive, require skilled personnel and are time consuming (Yakovleva et al., 2012).

Some of the requirements for an efficient biosensor is low cost and to be able to give a fast analytical response. Safina et al. (2010) improved lactose detection sensitivity by using CDH as a biocatalyst (Safina et al., 2010). The lactose linear detection limit they obtained was 0.0005 to 0.1 mM. The minimum detection limit is lower than when using common enzymes such as β -galactosidase and glucose oxidase or β -galactosidase separately with reported detection limit range of 0.1 to 3,500 mM (Göktug et al., 2005) and 0.2 to 5 mM (Jenkins & Delwiche, 2003) respectively. Conzuelo et al. (2010) examined the performance of trienzyme electrodes: β -galactosidase, glucose oxidase and peroxidase for lactose detection. They were able to detect lactose at concentration between 0.0015 to 0.12 mM with an operational lifetime of 28 days (Conzuelo et al., 2010).

2.8 BFC improvement

Commercialising BFC applications are still in infancy and many weaknesses have to be overcome. Improvement in power density and energy efficiency, suitability of electrode materials used, cell design, performance durability, enzyme / mediator immobilization technique are some that need to be addressed (Nandy et al., 2015; Osman et al., 2011; Osman et al., 2010) to significantly increase MFC power generation, and durability together with improvement in the detection limit for EFC.

Therefore, in this research, areas of study will focus on the durability of the power performance of anaerobic MFCs and suitability of electrode materials to increase electricity generation and operational lifetime for application in both MFCs and EFCs.

Chapter 3

Effect of long time oxygen exposure on power generation of enriched multi-cultured microbial fuel cell[#]

Mimi Hani Abu Bakar^{a,b,c,*}, Neil F Pasco^b, Ravi Gooneratne^c, Kim Byung Hong^a

^a Fuel cell Institute, Universiti Kebangsaan Malaysia (UKM), 43000 Bangi, Selangor, Malaysia

^b Lincoln Ventures Ltd, PO Box 133, Lincoln, Christchurch 7640, New Zealand

^c Lincoln University, PO Box 84, Lincoln, 7647, New Zealand

[#] For submission to the Malaysian Journal of Analytical Sciences

*Corresponding author: Mimi Hani Abu Bakar, email: mimihani@ukm.edu.my

3.1 Abstract

A microbial fuel cell (MFC) system is a bioenergy converter that utilizes bacteria to generate electricity through bacterial metabolic pathway. A typical MFC consists of two electrodes: the anode and the cathode, two compartments for anolyte and catholyte separated using a selective permeability membrane and a conductor to link the electrodes together. In an MFC, bacteria are in an oxygen-free anolyte compartment together with a suitable carbon source. The high electronegativity at the cathode relative to the anode attracts the bacteria in the anode compartment to transfer electrons outside their cell to the anode, which acts as electron acceptor. Many authors have reported of the harmful effect of dissolved oxygen in anolyte that will reduce the capability of the bacteria to transfer electrons to external anode, and in some cases it can result in a complete loss of electrochemical activity of bacteria within three hours of exposure to air. In this work, enriched multi-cultured anaerobic inoculum was obtained from effluent of MFC operated for a long duration. This inoculum was used for both aerobic and anaerobic MFCs. After allowing 30 days for the bacteria to acclimatize in their new environment, the condition of these systems were changed by swapping the aerobic into anaerobic and anaerobic into aerobic for 11 days. This was done to study the effect of long time exposure of the MFCs in oxygen on the electrochemical performance. Results proved that prolonged exposure of enriched multi-cultured anaerobic bacteria culture from effluent to oxygen at 7.5 ppm had lowered the power generation in MFCs. The situation however was reversible once the anaerobic environment was introduced into the system, showing improvements up to 100% in P_{max} and I_{max} and a reduction in R_{int} up to 53%. Future studies would be conducted to develop a more in-depth understanding of electrochemical performance of MFCs before and after gas swapping, and understanding its effect on microbial community in the biofilm and half-wave redox potential ($E_{1/2}$). Studies can also be carried out using electrode polarization and further investigation is required to understand the effect of different oxygen concentration on MFC performance.

Keywords: *microbial fuel cell, aerobic, oxygen exposure, wastewater*

3.2 Introduction

A microbial fuel cell (MFC) system is a bioenergy converter that utilizes bacteria to generate electricity through bacterial metabolic pathway (Rittmann, 2006). A typical MFC consists of two electrodes: the anode and the cathode, two compartments for anolyte and catholyte separated using a selective permeability membrane and a conductor to link the electrodes together. MFC behaves as an electrochemical cell, using oxidation/ reduction activity in its operation. In an MFC, bacteria are put in an oxygen- free anolyte compartment together with suitable carbon source, while the catholyte acts as electron sink. The high electronegativity at the cathode in relative to the anode attracts the bacteria in the anode compartment to transfer electrons outside their cell and pass it to anode electrode, which acts as electron acceptor. These bacteria are known as exoelectrogens and could transfer electrons to anode electrode via direct electron transfer (DET): nanowires, surface blebs, self-produced/ endogenous chemical mediators, and via mediated electron transfer (MET): self-produced hydrogen for interspecies hydrogen transfer and intermediate metabolites (Logan, 2008). When oxygen and other anaerobic electron acceptors: nitrate (NO_3^-), sulphate (SO_4^{2-}), sulphur (S) or fumarate, existed in the anolyte, electricity generation in the MFCs will be impacted. Tests on the impact of oxygen in air on anaerobic MFCs had been done on both single cell culture, such as from the genus *Shewanella* (Kim et al., 2002; Li et al., 2010), *Escherichia coli* (*E.coli*) (Wang et al., 2006) and multi-cultured bacteria from anaerobic wastewater treatment streams (Kim et al., 2004; Liu et al., 2005). Most of them discovered that the dissolved oxygen in anolyte will reduce the capability of the bacteria to transfer electrons to external anode. Kim et al. (1999) in their research on biosensor, found that *Shewanella Putrefaciens* completely loss its electrochemical activity within three hours of exposure to air (Kim et al., 1999). Wang et al. (2006) discovered that *E.coli* had about 61- 68% decreased in capability to reduce external mediator, hexacyanidoferrate (III) $[\text{Fe}(\text{CN})_6]^{3-}$ in anaerobic MFC when oxygen is presence (Wang et al., 2006). In the case of multi-cultured bacteria, Liu et al. (2005) found that the diffusion of oxygen to the anolyte from the cathode site would lead to 21- 50% loss of substrate to aerobic oxidation by bacteria (Liu et al., 2005), which translates as the loss of generated electricity through the MFC. A more detail work was done by Li et al. (2010) on the response of *Shewanella decolorationis* with oxygen (Li et al., 2010). Within about six days, they had changed the flowing of gas into the MFCs about five times between argon gas and air to create alternate condition of aerobic (0.4 day)-anaerobic (0.6 day) –aerobic (1.1 days) – anaerobic (2 days)-aerobic (2.2 days). They discovered that when in contact with oxygen, *S. decolorationis* was able to produce a lot of nicotinamide adenine dinucleotide (NADH), which in turns increase in charge production. However, the oxygen dissolved in the anolyte will influenced the bacteria for aerobic respiration and biomass production that leads to current reduction in MFCs. Though other available findings pointed out the adverse effect of oxygen on generation of current by bacteria in MFCs, to our knowledge there are no reports that show long term oxygen exposure on anolyte in MFC. In this

work, effluent from a long duration operated enriched multi-cultured anaerobic air-cathode MFC was made as inocula for aerobic and anaerobic MFCs. After allowing 30 days for the bacteria to acclimatize in their new environment, the conditions of the system were changed by swapping between the nitrogen and air. This turned the aerobic into anaerobic and anaerobic into aerobic and were let to acclimatize in their new condition for 11 days. The electrochemical performance of the MFCs before and after the gas swapping were compared in view of maximum power density (P_{max}), current density (I_{max}) at P_{max} and internal resistance (R_{int}) accomplished within the systems.

This study was conducted to analyse the effect of oxygen long time exposure on enriched multi-cultured bacteria of anode in acetate fed air-cathode MFC system. The consequence of alternate presence and absence of oxygen in air were characterised through polarization and power curves. From the results obtained, prolonged exposure towards oxygen at 7.5 ppm had lowered the power generation from MFCs, when using effluent from enriched multi-cultured anaerobic bacteria culture as inocula. The situation however was reversible once anaerobic environment was introduced into the system, showing improvement up to 100% in P_{max} and I_{max} and a reduction in R_{int} up to 53%.

3.3 Methods

3.3.1 Chemicals

Chemicals were of analytical grade. Peptone from casein was purchased from Merck (Darmstadt, Germany). Yeast extract was purchased from Scharlau (Barcelona, Spain). Ammonium chloride (NH_4Cl) and sodium acetate anhydrous (CH_3COONa) was purchased from AnalaR®, BDH Laboratory Supplies (Poole, England). Di-sodium hydrogen orthophosphate anhydrous (Na_2HPO_4) and potassium chloride (KCl) were purchased from Fisher Scientific UK Ltd. (Leicestershire, UK). Sodium dihydrogen orthophosphate ($\text{NaH}_2\text{PO}_4\cdot\text{H}_2\text{O}$) was purchased from LabServ™, Biolab (Aust) Ltd. (Victoria, Australia).

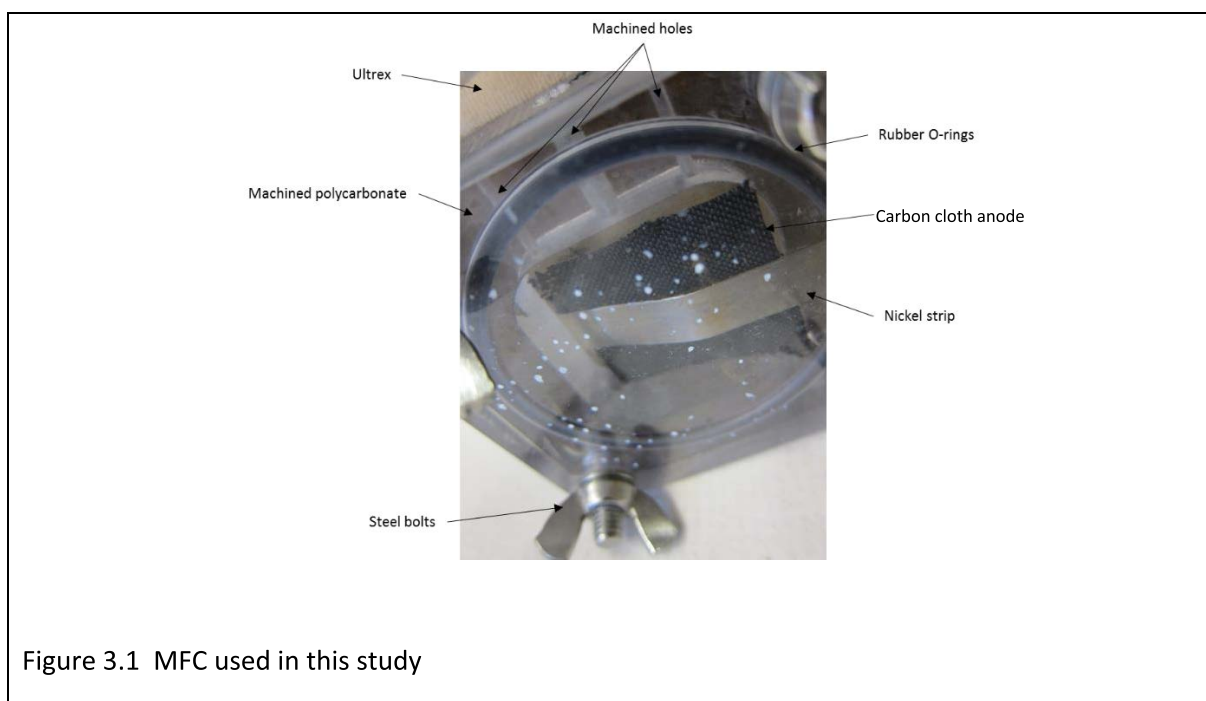
All analytical solution was made using distilled water unless otherwise stated.

3.3.2 Inoculum, buffers, reagents and media

The inoculum was originated from sludge collected from plastic media of aerobic trickling filter in Bromley wastewater treatment plant. It was enriched in acetate fed air-cathode MFCs (Appendix A) for about eight months when the anolyte was used as inoculate in this study. Working buffer was a 50 mM phosphate buffer solution (PBS) (0.31 g/L NH_4Cl , 3.12 g/L $\text{NaH}_2\text{PO}_4\cdot 2\text{H}_2\text{O}$, 4.58 g/L Na_2HPO_4 , and 0.13 g/L KCl) at pH 7 (Kim et al., 2005; Rader & Logan, 2010), used for preparing acetate media and for analysis. Basal media of 7 mM acetate (1 g/ L CH_3COONa , 1 g/ L peptone of casein and 2 g/ L yeast extract) was dissolved in PBS prior to use (Atlas, 2005). The media was autoclaved at 121 °C for 15 min prior to use.

3.3.3 MFC air-cathode construction

The study utilized single chambered air-cathode MFCs as described in Weld & Singh (2011)(Weld & Singh, 2011). Each of the MFCs had internal volume of 19.2 mL and were constructed from three machined polycarbonate, joint with rubber O-rings and assembled with steel bolts (Figure 3.1). The middle polycarbonate had its top equipped with three holes: two big holes of ϕ 1.8 cm for batch mode feeding / reference electrode / anode port and one small hole of ϕ 0.4 cm for gas inlet. The anode chamber was separated from an air cathode by using cation exchange membrane (Ultrax) from BASF Fuel Cell Inc. (Somerset, NJ. USA). The air-cathode was a 4 cm x 4 cm of 10% Pt-carbon cloth (Fuel Cell Earth LLC, Stoneham, MA) covered with a layer of 4 cm x 4 cm plain carbon cloth (Fuel Cell Earth LLC, Stoneham, MA) and fastened to the exterior wall of the Ultrax membrane with a nickel strip. The nickel strip acted as current collector at the cathode.



3.3.4 Operation

Here, 2% (v/v) of anolyte (OD_{600} of 2.85) from an eight month old MFC was incubated in acetate media for 24 h at 150 rpm and 24 °C. Each six new MFCs were filled with the incubated culture and topped up with acetate media. Two of the MFCs were bubbled with nitrogen while the other two were bubbled with air. Two of the MFCs were made as control, free from flowing of gas. Except for the controlled MFCs, most of the enrichments had their anodes poised at potential of +200 mV (vs. Ag/AgCl) for seven days and operated in controlled temperature of 28 °C. From eight day onwards, the anode poisoning were discontinued and the MFCs were connected to external resistors of 1,000 Ω .

3.3.5 Analytical methods and calculation

Cell voltage (E) across the external resistor and cell current generated from the anode fixed potential poised were measured every twice a day using a Digitech QM 1326 multimeter or every 30 s to 30 min using a four channel Quadstat 164 potentiostat (eDAQ Pty Ltd, NSW, Australia) and continuous recording using an e-corder 1621 (eDAQ Pty Ltd, NSW, Australia) data acquisition system. Current (I) and power (P) were calculated using the Ohm's law, where E represents circuit's potential and R_{ext} represents circuit external resistance, with the current density, $I_{density}$ and power density, $P_{density}$ normalized by the projected area of the anode (Luo et al., 2011):

$$I = \frac{E}{R_{ext}}, I_{density} = \frac{I}{Anode\ area} \quad \text{-----} \quad (1)$$

$$P = I \times E, P_{density} = \frac{P}{Anode\ area} \quad \text{-----} \quad (2)$$

Dissolved oxygen concentration in the anolyte was determined before the gas swapping activity from the aerobic MFCs as 7.5 ppm, by HQ40d portable multi-parameter meter (pH/ conductivity/ dissolved oxygen/ ORP/ ISE) (Hach Company, Colorado, US). The polarization curve and the power density curves were produced by using method in Luo et al. (2011) and Watson and Logan, (2011) to obtain the open circuit voltage (OCV), P_{max} , I_{max} and R_{int} of the system (Luo et al., 2011; Watson & Logan, 2011). In this study, the polarization curves were obtained using multiple resistors (820 k Ω to 18 k Ω), with each resistance changed in decreasing order after every pseudo steady-state achieved or not more than 20 min intervals (which ever comes first) over a complete fed batch cycle. Analysis was conducted once the voltage output was stabilised after replenishing the media. The analysis was done for two consecutive cycles to ensure that the voltage response was unchanged with successive cycles.

3.4 Results and discussion

Current density shows that once the anode poisoning was discontinued, only anaerobic MFCs show high current density with total daily average from day-8 till day-25 of 38.26 ± 0.13 mA/ m² and lowest by aerobic MFCs of 2.08 ± 0.01 mA/ m² while the control gave an average of 20.65 ± 0.28 mA/ m² (Figure 3.2). As soon as the MFC characterisation started (day 23 24 and 25), the aerobic MFCs began to show significant in current density (t-test, $p < 0.05$), which is higher than anaerobic MFCs with total daily average from day-26 till day-30 of 70.93 ± 0.19 and 67.49 ± 0.32 mA/ m² respectively. In the control, there was not much increase in current density recorded after day-26, 30.69 ± 0.68 mA/ m².

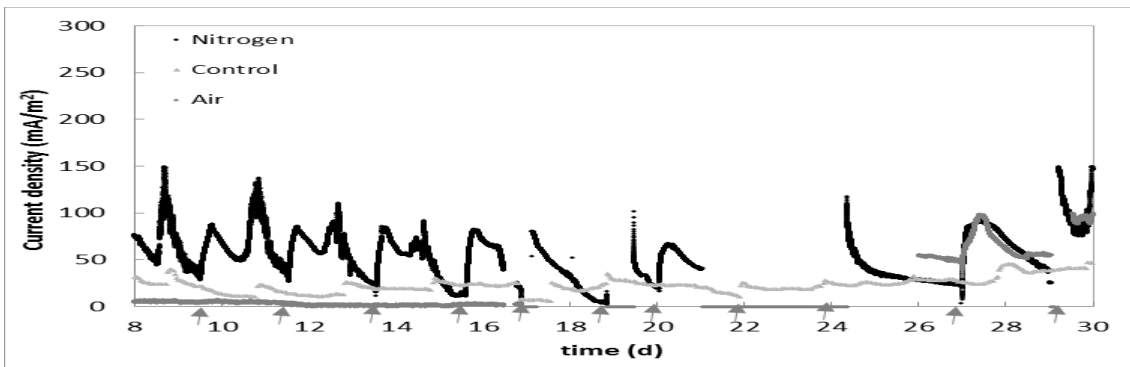


Figure 3.2 Biocatalytic current generation compared between aerobic and anaerobic environment.

The air-cathode MFCs were inoculated with anolyte from operating 8-months old enriched MFC originated from sludge of trickling filter's plastic media and fed with 7 mM acetate (pH 7). The frequency of batch feeding mode was in average every day (represented by \uparrow). The MFCs were kept at 28 °C. Graph plotted based on current density average of each replicates. (n=2)

The reason of nitrogen bubbling into the anode compartment was to accelerate the anaerobic condition in the system simultaneously increase the MFC electrochemical performance. The control MFCs were solely depending on the bacteria in the anode chamber to create anaerobic environment by gradually consuming the soluble oxygen in the anolyte (Ringeisen et al., 2007). The current density generated via control MFCs was almost 2-fold less than that generated by nitrogen bubbled MFCs. The high mass of bacteria inoculated in the anode compartment of the control MFCs, capable to consume most of the oxygen available in the chamber for a short time. When the area is suitable for anaerobic bacteria to survive and perform anodophilic transfer, then only current density started to gain pace. This was mentioned by Hutchinson et al. (2011), stated about the importance of having the anode compartment free of diffused oxygen from the cathode especially during startup (Hutchinson et al., 2011). In this study, feeding was done manually through a designated cavity at the top of the MFC reactor. This action will allow air to seep into the control MFCs, while for the anaerobic MFCs, the pressure created by the nitrogen bubbled MFC will push the air out during feeding. Therefore, the nitrogen bubbled MFCs could easily generate high current without the interference of air. In contrast, air bubbled MFCs remained at much lower current density than the control MFCs before the MFC characterisation activity. The characterisation activity conducted on the MFCs for power and polarization curves, appeared to increase the current intensity of the aerobic and the anaerobic MFCs. From the Ohm's law in equation 1, new voltage at the electrodes can be obtained through changing the R_{ext} . At the beginning of the MFC characterisation activity, the MFC electrodes were disconnected, which creates an infinite resistance in the cell. When this

happened, the current generated will be low since the anode potential will be much too low to attract the bacteria to release electrons to the anode. This might attributed to the moment surged in current intensity once the MFC characterisation was stopped. Similar incident was experienced by Aelterman et al. (2008), in their studies on the effect of R_{ext} ranges towards MFCs current generation (Aelterman et al., 2008). They found that the current intensity of their MFCs increased by 3.29-fold when they changed the R_{ext} from 50 to 10.5 Ω .

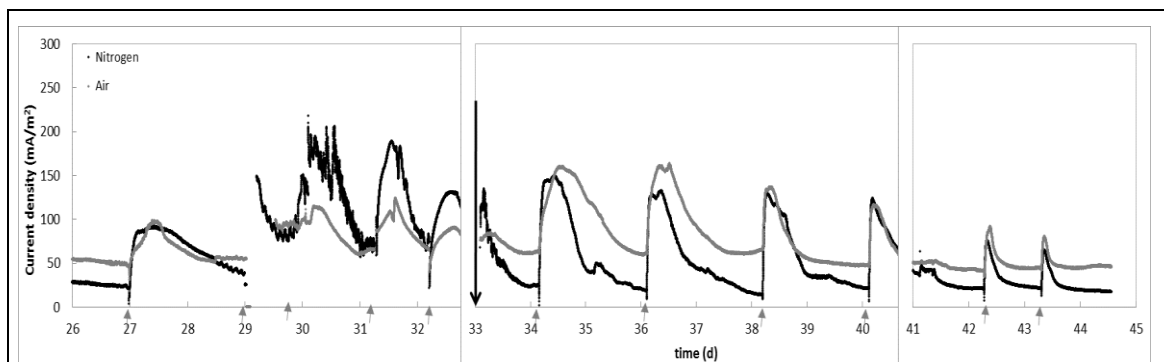


Figure 3.3 Effect of gas swapping (↓) between the aerobic and anaerobic MFCs.

The air-cathode MFCs were inoculated with anolyte from operating 8-months old enriched MFC and fed with 7 mM acetate (pH 7). The frequency of batch feeding mode was in average every two days (represented by ↑). The MFCs were kept at 28 °C. (n=2)

The switching of gasses between the anaerobic and aerobic MFCs began on day-33 until day 44. The total daily average current calculated for the 11 days after gas swapping did not show any significant in current density (t-test, $p > 0.05$) between before (day-26 to 30) and after gas swapping for each MFC conditions (day-33 to 44): 49.89 ± 0.19 mA/ m^2 (anaerobic MFCs) and 74.81 ± 0.18 mA/ m^2 (aerobic MFCs) (Figure 3.3). However, when looking at the individual daily average in current density (Table 3.1), there seems to be clear decreasing trend for the anaerobic MFCs from the beginning of the swapping till day-43. For aerobic MFCs, the effect of nitrogen bubble seems to be rather slow in comparison to the anaerobic MFCs.

Table 3.1 Daily average current calculated after gas swapping (\pm standard error of mean) (n=2).

Day	Anaerobic MFCs bubbled with air (mA/ m^2)	Aerobic MFCs bubbled with nitrogen (mA/ m^2)
33 -34	53.40 ± 0.58	71.92 ± 0.16
34 (feed) -35	97.89 ± 0.85	127.57 ± 0.63
35 -36	33.89 ± 0.17	85.28 ± 0.39

36 _(feed) -37	82.84 ± 0.69	124.66 ± 0.59
37 -38	30.68 ± 0.17	69.21 ± 0.17
38 _(feed) -39	74.19 ± 0.75	87.11 ± 0.53
39 -40	30.70 ± 0.08	50.43 ± 0.04
40 _(feed) -41	69.36 ± 0.54	72.69 ± 0.44
41 _(feed) -42	31.66 ± 0.16	47.88 ± 0.07
42 _(feed) -43	33.08 ± 0.29	52.23 ± 0.25
43 _(feed) -44	28.49 ± 0.23	49.15 ± 0.17

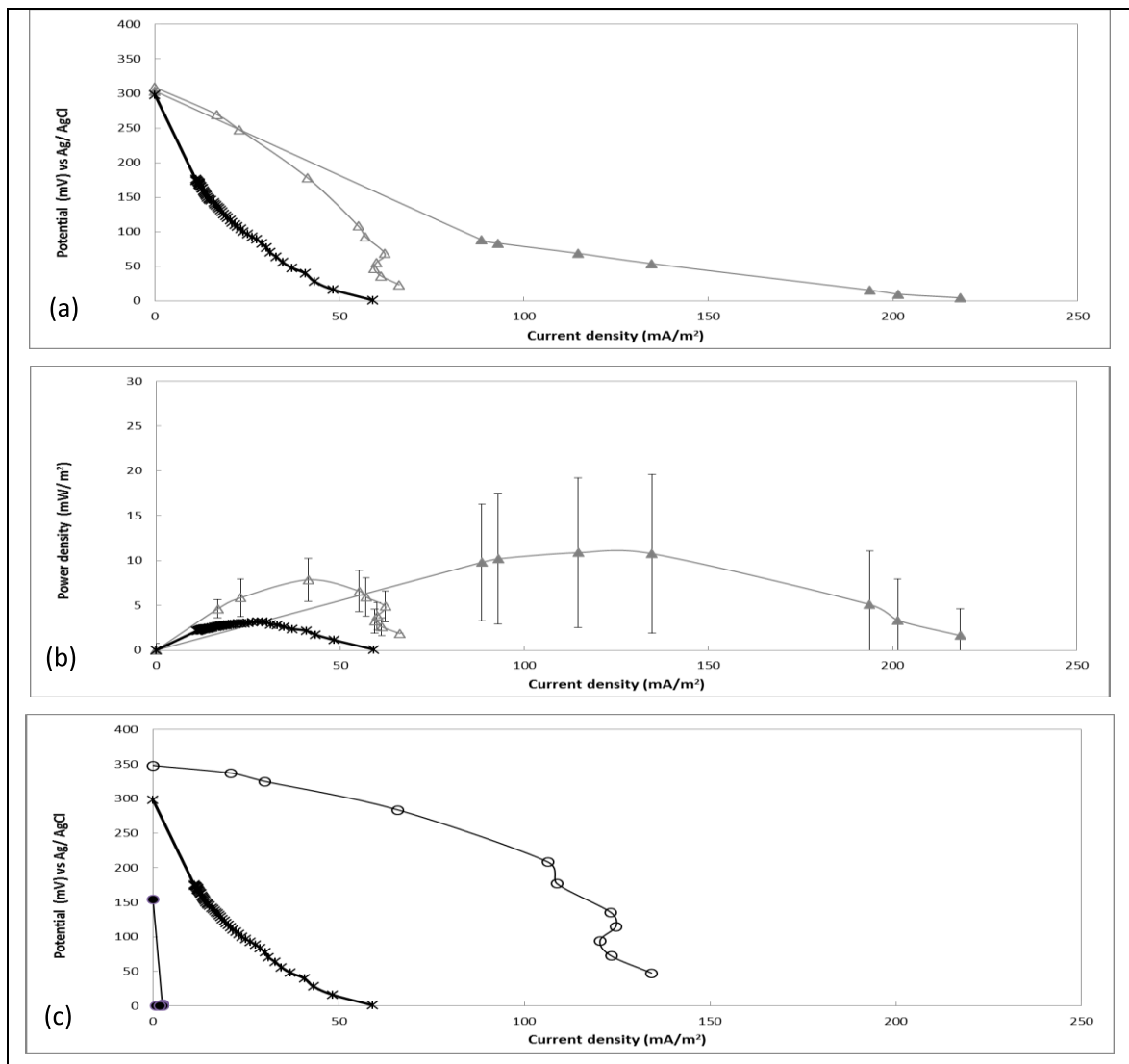
The impact of the gas swapping before and after can be observed through the polarization and the power curves. Comparisons done on the OCV from the polarization curves between the aerobic and anaerobic MFCs before and after the gas swapping (Figure 3.4a), which was about 20 days apart and the control, shows that the aerobic MFCs possessed 2.3 fold higher OCV than before the gas swapping (150 mV, vs. Ag/ AgCl), and 1.2 fold higher OCV than both the anaerobic (before and after gas swapping) and the control MFCs (300 mV, vs. Ag/ AgCl)(Figure 3.4a). The OCV zone is known as the activation loss zone and refers to the electron transfers reaction at the electrode surface. The OCV is the highest voltage produced in an MFC, measured in the absence of current and take into consideration various potential losses as follows (Logan et al., 2006; Osman et al., 2010) (Equation 3 and 4).

$$OCV = E_{cell} + IR_{int} \quad \text{-----} \quad (3)$$

$$E_{cell} = E_{emf} - (\sum \eta_a + |\sum \eta_c| + IR_{\Omega}) \quad \text{-----} \quad (4)$$

Where the E_{cell} is the measured cell voltage, IR_{int} is the sum of all internal losses of the MFC, $\sum \eta_a$ and $|\sum \eta_c|$ represents the overpotentials of the anode and cathode respectively. The overpotential of the anode and cathode reflect the influence of slow kinetics of heterogenous electron transfer, which is the movement of electrons between a chemical species and a solid-state electrode, together with ohmic resistance and concentration gradients (Tayhas et al., 1994). E_{emf} is the cell electromotive force from the difference of cathode potential, E_{cat} to anode potential, E_{an} , and IR_{Ω} represents the sum of all ohmic losses. Hence, apart from the low concentration of oxygen in air (ca. 21%), the reduced in OCV could be attributed to factors, such as potential generated by the exoelectrogen that formed the anodic biofilm, diffused oxygen into the anode compartment that interrupts the anodic biofilm and inefficient oxygen reduction reaction (ORR) occurs at the cathode site (Cheng et al., 2006). Ideally, an OCV of an air-cathode MFC should be around +595 mV (vs. Ag/AgCl) (+800 mV, vs. SHE) when pure oxygen is used. However when air is used at the cathode

side, OCV obtained are much lower than the ideal. In an MFC study done by Li et al. (2013) using anaerobic wastewater as inoculum in a 75.6 mL dual chambered MFC with air bubbled in deionized catholyte, OCV was within the range of +419 to +489 mV (vs. Ag/ AgCl) (Li et al., 2013). In other study done by Khan et al. (2015) using anaerobic digester from palm oil waste as inoculum in 20 mL single chamber air-cathode, found that the OCV also dependent on the catalyst applied onto the cathode, which could ranged from +385 to +626 mV (vs. Ag/ AgCl) (Khan et al., 2015). In this study, however, the high OCV recorded for the aerobic MFCs after the anolyte was continuously bubbled with nitrogen for 11 days, might have increased the population of the exoelectrogens in the anode compartment, thus reduce the overpotential of the anode and the internal losses in the MFC.



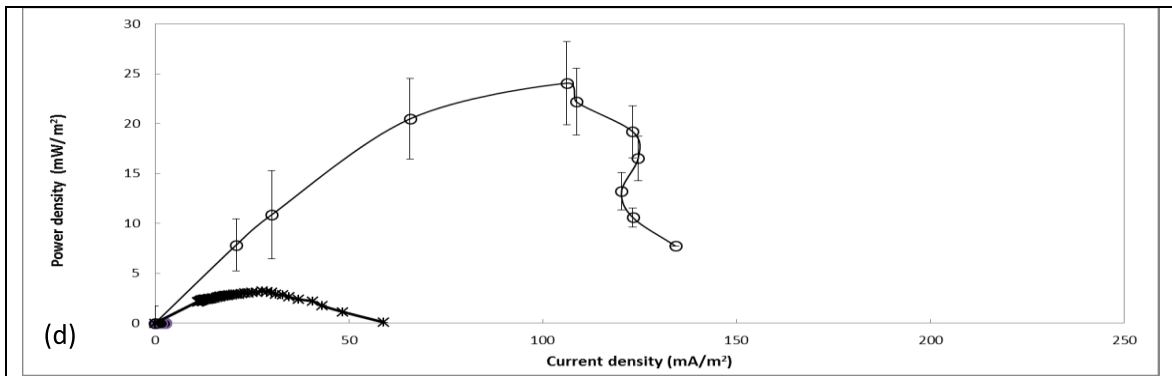


Figure 3.4 Polarization (a) and power density (b) curves recorded.

The external resistance used were from 18 – 820 kΩ. Symbols in the figure represent anaerobic MFCs before (▲) and after (△) gas switching (a & b) and aerobic MFCs before (●) and after (○) gas switching (c & d) as well as controls (x) (a-d). (n=2)

From the MFC characterisations (Table 3.2), positive changes were seen on the aerobic MFCs where the P_{max} increased by more than 1,000-fold, increased in I_{max} by 42-fold, once the air in the anolyte was replaced with nitrogen. The change in the anaerobic MFCs after the nitrogen bubble replaced with air was small, about 1.4-fold decrease in P_{max} along with a slight decrease in I_{max} by 2.8-fold. This increase in both I_{max} and P_{max} for the aerobic MFCs after the gas swapping shows that when MFCs were in the aerobic state, the exoelectrogens were already there, and these became active once the environment turned to anaerobic. Exoelectrogens are believed to be facultative bacteria that could survive in both conditions, aerobic and anaerobic (Lefebvre et al., 2011). In the air bubbling anode chamber, the small number of exoelectrogenic bacteria near the anode still survive because concentration of oxygen lessens with the increasing depth of biofilm (Figure 3.5a); while the centre is already anaerobic. Diffused oxygen is consumed in the outer layers of biofilm, providing favourable conditions for growth of facultative and strict anaerobes in the deep layers of the biofilm (Pastorella et al., 2012). Similar to oxygen, substrate diffusion also decreases with the increase of biofilm mass depth from bulk fluid to the interior biofilm (Figure 3.5b). Effect of oxygen concentration on MFC electrochemical performance was also observed by Ringeisen et al. (2007) in their study using 1.2 mL aerobic miniature MFC, with 611 cm² of graphite felt anode and applying *Shewanella onedensis* as inoculum (Ringeisen et al., 2007). They discovered that once they discontinued the source of air into the system with measured dissolved oxygen of 8 ppm, the concentration of the dissolved oxygen rapidly declined to below 2 ppm in less than 30 s and slowly became anaerobic within 7 minutes. As a result, they observed an improvement of about 10% in current over the first minute after the discontinuation of the aerobic feed flow. For the anaerobic MFCs, the effect of gas swapping was not as significant as changing the aerobic MFCs to anaerobic

state and the reduction in current density was gradual. This could be due to the bacteria adapting to an aerobic state. Hence, the multi-cultured exoelectrogenic bacteria in MFCs originated from aerobic wastewater system after exposure to oxygen in air for a long duration (30 days) has the potential to produce high electricity performance when introduced into an anaerobic environment.

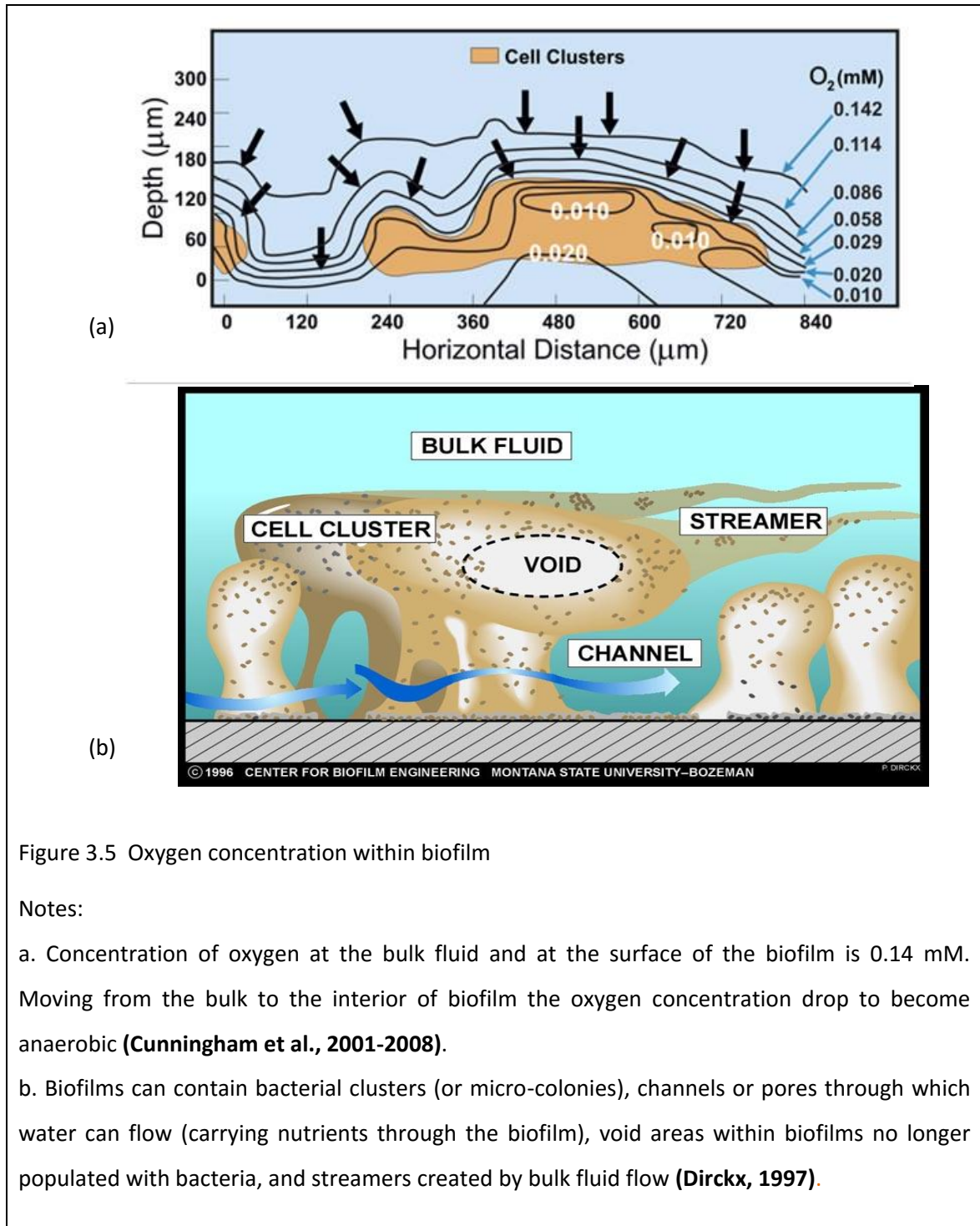


Figure 3.5 Oxygen concentration within biofilm

Notes:

- Concentration of oxygen at the bulk fluid and at the surface of the biofilm is 0.14 mM. Moving from the bulk to the interior of biofilm the oxygen concentration drop to become anaerobic (Cunningham et al., 2001-2008).
- Biofilms can contain bacterial clusters (or micro-colonies), channels or pores through which water can flow (carrying nutrients through the biofilm), void areas within biofilms no longer populated with bacteria, and streamers created by bulk fluid flow (Dirckx, 1997).

Although both the P_{max} and the I_{max} showed expected results with the swapping of gasses, the R_{int} for aerobic MFCs showed an increment of 2.1-fold after the gas swapping. Comparison between the R_{int}

of aerobic and anaerobic MFCs after the gas swapping however shows that the nitrogen replacing the air in aerobic MFCs, reduced its R_{int} lower than that of anaerobic MFCs. This effect can be seen clearly in the power curves where the curve of aerobic MFCs after the swapping was not symmetrical as the power curve of the anaerobic MFCs (Figure 3.4b). Based on Logan et al. (2006), the symmetric nature of the power density curve obtained from the MFC characterisation analysis, which was also seen in this study represents a high R_{int} in an MFC mostly due to the ohmic resistance (R_{Ω}) at the point of P_{max} (Logan et al., 2006). R_{Ω} can be derived from any material that creates resistance in the system, such as substrates, bacteria, gap between electrodes, loose contacts between components, and low ionic conductivity in the substrate. The continuous air bubbling in the anode chamber probably helped with the growth of aerobic microbes due to a direct reduction of oxygen in the cell to increase biomass production. Although increase in biomass means increase in the NADH production, which leads to increase in electrons production, most of these electrons however will be consumed for biomass before able to generate electricity (Li et al., 2010). This could be the reason for the high R_{int} observed from aerobic MFCs before the gas swapping with very poor I_{max} and P_{max} (Logan, 2008).

Table 3.2 Details obtained from MFC electrochemical characterizations.

MFC	P_{max} (mW/ m²)	I_{max} (mA/ m²)	R_{int} (kΩ)
Anaerobic- before gas swap	10.88 \pm 8.33	114.61 \pm 49.97	30.55 \pm 0.00
Anaerobic- after gas swap	7.87 \pm 2.13	41.29 \pm 5.35	226.40 \pm 2.45
Aerobic- before gas swap	0.02 \pm 0.02	2.50 \pm 2.25	50.92 \pm 0.00
Aerobic- after gas swap	24.07 \pm 4.06	106.22 \pm 11.20	107.79 \pm 3.89
Control	2.91 \pm 2.52	31.09 \pm 17.94	2.41 \pm 0.00

Although this study was able to culture exoelectrogen from aerobic sludge originated from trickling filter, the electrochemical performance was way too low from results that have been reported in other publications, which is no less than 100 mW/m². According to (Haslett, 2012; Rahimnejad et al., 2011a), the performance of MFCs are commonly associated with the following: 1) Substrates oxidation in the anode compartment, 2) Microorganism used for inoculum, 3) Mediator, 4) Permeability of cation exchange membrane (if any), 5) Electrode material and their surface area, 6)

Electron acceptor at the cathode chamber, 7) Electron transport pathway to anode surface, 8) Overpotential at the electrodes, 9) External load applied, 10) Distance between electrodes, 11) Mass transport, and 12) Operational temperature (Haslett, 2012; Rahimnejad et al., 2011a). For instance Feng et al. (2010b) analysed the effect of acid modified carbon fiber brush in 28 mL air-cathode MFC having 20% inoculum from domestic wastewater with external load of 1 k Ω , achieved P_{max} of 1,370 mW/ m² (Feng et al., 2010b). Watson and Logan (2011) adapted similar MFC design with an increased of inoculum concentration upto 50%, different type of microorganism and used a non modified carbon fiber brush, had achieved 1.6 fold lower P_{max} than the later (Watson & Logan, 2011). Santoro et al. (2012) on the other hand with completely different MFC design, used 4.6 fold more volume and non modified carbon cloth for anode and cathode, only achieved 268 mW/m² of P_{max} (Santoro et al., 2012). To identify the reason of poor electrochemical performance in this study and to reduce such high R_{int} , the variables affecting the performance of MFCs listed above need to be analyzed and compare them with those having similar MFC designs.

3.5 Conclusions

The goal of this study was to analyse the effect of long-duration exposure towards oxygen in air through gas swapping on the electrochemical performance of enriched multi-cultured bacteria in air-cathode MFCs. The results showed that prolong exposure in 7.5 mg/L (ppm) of dissolved oxygen MFCs for a month on the enriched multi-cultured bacteria culture, will produce only low power and current generation. This however is not permanent since it could easily and quickly be rectified with improvements up to 100% in P_{max} and I_{max} and a reduction in R_{int} of up to 53%, when introduced into an anaerobic environment. Future studies could be carried out to gain a more in-depth understanding on electrochemical performance of MFCs before and after gas swapping, and also understanding of its effect on microbial community in the biofilm and half-wave redox potential ($E_{1/2}$). Further research can also be carried out on electrode polarization and the effect of different oxygen concentration ranges on MFC performance.

Chapter 4

9,10-Anthraquinone-2,6-disulfonic acid disodium salt/ epoxy graphite composite for anode in microbial fuel cell[#]

Mimi Hani Abu Bakar^{a,b,c*}, Neil F Pasco^b, Ravi Gooneratne^c, Kim Byung Hong^a

^a Fuel cell Institute, Universiti Kebangsaan Malaysia (UKM), 43000 Bangi, Selangor, Malaysia

^b Lincoln Ventures Ltd, PO Box 133, Lincoln, Christchurch 7640, New Zealand

^c Lincoln University, PO Box 84, Lincoln, 7647, New Zealand

[#] For submission to the Journal of Bioresource Technology

*Corresponding author: Mimi Hani Abu Bakar, email: mimihani@ukm.edu.my

4.1 Abstract

Properties such as electrical conductivity, low resistivity, chemicals and corrosion resistance are mostly found in carbon based materials. Epoxy resin is excellent for electrical insulation and can be used as a conductor with the addition of conductive filler. Combinations of carbon and epoxy show qualities of a conductive electrode, mechanically strong with design flexibility and thus makes them suitable as electrodes in microbial fuel cell (MFC). In this study, graphite-epoxy composites were fabricated with multi-walled carbon nanotube (MWCNT) embedded in the matrix surface. 9,10-Anthraquinone-2,6-disulfonic acid disodium salt / polypyrrole (PPy/AQDS) was used as mediator, covalently electrografted on electrode's surface. Electrochemical stability of anodes during continuous operation were measured in air-cathode MFCs. It appears that maximum power in MFC could be increased up to 42% with surface modification using PPy/AQDS. Internal resistance (R_{int}) could be reduced up to 66% with the inclusion of MWCNT. These findings show that a one-day fabrication of a-ready-to-use conductive electrode is possible for graphite content between 70-80% (w/w).

Keywords: *anode, 9,10-Anthraquinone-2,6-disulfonic acid disodium salt/polypyrrole, graphite-epoxy composite, microbial fuel cell*

4.2 Introduction

In general, an electrode should have qualities such as good electrical conductivity, low resistivity, stable against chemicals and corrosion (Nandy et al., 2015). These features are mostly found in carbon based materials, such as graphite, thus making it popular material for electrodes (Corb et al., 2007). Carbon with biological catalysts in many aspects also conforms to requirements of a biosensor, thus making it acceptable material for electrode fabrication in a microbial fuel cell (MFC). Epoxy resins on the other hand are polymers with good electrical insulation properties (Bhatnagar, 1996), which is valuable in the electronics industry. This trait however is adjustable to conductor or semiconductor with the addition of conductive filler (Martin et al., 2005). Therefore, a combination of carbon as filler and epoxy resin offers fabrication of a polymer composite, which are conductive (Du & Jana, 2007), effortless in processing as well as moulding, and corrosion resistance (Kirgoz et al., 2006; Vahedi et al., 2014).

Studies conducted on carbon-epoxy composite within the field of fuel cell and biology shows its favourable applications in bipolar plates of proton exchange membrane fuel cell (PEMFC) and biosensor. In the area of bipolar plates, Du and Jana (2007) found that their fabricated carbon-epoxy with the total filler loading greater than 50 wt% showed good conductivity, mechanical integrity and chemical stability at temperature above 150 °C and at pH 4, much suitable for PEMFC application (Du & Jana, 2007). Llopis et al. (2005) showed that their amperometric glucose biosensor worked more efficiently when a mixture of glucose oxidase (GOD) powder, epoxy resin, graphite powder and tetrathiafulvalene-tetracyanoquinodimethane (TTF·TCNQ) were applied at a ratio (wt%) of 5:76:9.5:9.5 for automated detection of glucose (Llopis et al., 2005). Kirgoz et al. (2006) discovered that combination of the composite biosensor with a thin layer solution of *Pseudomonas putida* cells modified the surface could give minimum detection limit on phenol almost 1,000 times lower than thick film microbial biosensor and conventional oxygen electrode (Kirgoz et al., 2006). Later, Ocaña et al. (2014) found that aptamer when immobilized on the surface of graphite-epoxy composite gave good detection range for cytochrome c and high sensitivity, which is suitable for an aptasensor (Ocaña et al., 2014). Pumera et al. (2006) learnt that carbon nanotube-epoxy composite exceeded in both electrochemical and mechanical qualities when compared to graphite-epoxy composite for sensor application (Pumera et al., 2006). Based on Ma et al. (2010) and Vahedi et al. (2010), carbon nanotubes as filler in the epoxy system had the ability to improve conduction pathway in the epoxy matrix and increased conductivity at loading as low as 0.5 wt. % (Ma et al., 2010; Vahedi et al., 2014). These qualities; strong mechanical properties in bipolar plates and good conductivity as biosensors, gave the indication that the graphite-epoxy composite has the potential to be applied in an MFC application. Unfortunately, it is not known whether there had been studies done more than seven

days on the performance of the graphite-epoxy composite as electrodes in MFC. In addition to that, the composite ease of shapes gives more opportunities to flexibility in reactor and electrode designs for MFC performance study.

In this study, graphite-epoxy composites were fabricated with multi-walled carbon nanotube (MWCNT) embedded in the matrix surface. 9,10- Anthraquinone-2,6-disulfonic acid disodium salt/ polypyrrole (AQDS/ PPy) was used here as external mediator electrochemically grafted to the composites' surfaces to induce preferred orientation on the active site and increased the electron transfer rates (Kumar et al., 2013; Tasca et al., 2011a). Performance of the graphite-epoxy composites in terms of electrochemical stability as anodes during continuous operation were measured in air-cathode MFCs. For this purpose, characterization of the MFC systems were measured through the polarization and power density analyses.

This study was designed to analyse the graphite-epoxy composite with more than 50% graphite contents, fabricated in a day using simple technique, on its capability when operated as anode in air-cathode MFCs' environment. In addition to that, the effect of embedded MWCNT in composite matrix and its compatibility with AQDS/ PPy electropolymerised on its surface were also assessed through the MFC performance.

The results generated showed that it is possible to make a ready-to-use conductive electrode at par with commercial graphite rod within 24 h using simple technique, provided the graphite content was between 70-80% (w/w). The anode performance in MFCs to generate maximum power, could be increased up to 42% with surface modification using PPy/AQDS solution. Through AQDS/ PPy surface modification, internal resistance (R_{int}) of the MFC system could be reduced by up to 48%, while a further 18% reduction was achieved when the graphite-epoxy composite was embedded with MWCNT. More data on this chapter is shown in Appendix B.

4.3 Methods

4.3.1 Inoculation

Working buffer was a 50 mM phosphate buffer solution (PBS) containing NH_4Cl (0.31 g/L), $\text{NaH}_2\text{PO}_4 \cdot 2\text{H}_2\text{O}$ (3.12 g/L), Na_2HPO_4 (4.58 g/L), and KCl (0.13 g/L) at pH 7 used for preparing acetate media and for analysis (Kim et al., 2005; Rader & Logan, 2010). Basal media of 7 mM acetate containing CH_3COONa (1 g/ L), peptone of casein (1 g/ L) and yeast extract (2 g/ L) was dissolved in PBS (Atlas, 2005). The media was autoclaved at 121 °C for 15 min prior to use. Analytical solution were made using Milli-Q water from EASYpure UV unless otherwise stated. All MFCs were inoculated with effluent from an existing MFC acetate batch fed operated for approximately two years, at 28 °C with an external resistor of 500 Ω .

4.3.2 Anode construction

The base for the anodes were made from graphite powder mixed with epoxy resin in four different ratios by adjusting the weight of the graphite powder (% w/w): 53 (total weight of 430 g), 73 (total weight of 730 g), 78 (total weight of 930 g) and 84 (total weight of 1,250 g). The total filler loading was more than 50 wt% to get desired low inherent resistance of fabricated electrodes. Ratio between the resin (norSKI® part A) and its hardener (norSKI® part B) followed Pumera et al. (2006) at (w/w) of 20:3 (Pumera et al., 2006). The combined material was manually blend using spatula until the texture turned flaky and packed into the PCR tubes (\varnothing 0.4 cm) at the length of 1.5 cm.

For the embedding of MWCNT into the matrix of graphite epoxy composite, only two ratios of graphite powder were used (% w/w): 73 and 78. This was because graphite powder ratio of 53% (w/w) required longer curing hours while graphite powder ratio of 84% (w/w) could not produce detectable redox peaks when analysed using cyclic voltammetry (CV). MWCNT was prepared through mixing of 1 mg of MWCNT with a 0.4 mL N,N-dimethylformamide (DMF) in a vibrator for one min. The mixture was later topped up with 0.6 mL of 70% ethanol and sonicated in water bath for five minute. Loading of the MWCNT ink into the base of graphite-epoxy composite was done at different ratios of MWCNT (% w/w): 0.04 and 0.06. The MWCNT mixtures were manually blend using spatula and dried under room temperature until the texture became muddy dry. The mixture paste was topped up about 0.3 cm high on the packed graphite- epoxy resin mixture in the PCR tube, to become the electrode's surface.

Prior to the surface modification methods, each of the packed PCR tubes was centrifuged at 14, 000 g for 1.5 min to compress and remove remaining air in the paste. A copper wire was inserted at the bottom of each tube for electrical contact. The filled PCR tubes were then cured at 80 °C for 12 h. They were then allowed to cool at ambient temperature for 30 min. Later, each excess PCR tube wall was cut until the wall was at the same level with the surface of the fabricated graphite-epoxy composite electrodes. The electrode surface area was polished, first on a wet fine emery paper (Norton, P400), then rinsed with Milli-Q water and dried on paper towel before polished on white paper until mirror like surface appeared.

4.3.3 Electrografting with 9,10- Anthraquinone-2,6-disulfonic acid disodium salt (AQDS)/ polypyrrole (PPy)

Polypyrrole (PPy) was purified before used (Kumar & Swetha, 2011; Reiter et al., 2001). PPy was chosen in this study because of its high electronic conductivity and relatively long period of stability (Karami & Nezhad, 2013) to provide good support for AQDS. PPy was passed to a column of alumina about 4 cm in height stuffed in a glass pipette. Surface modification of AQDS was done using method described in Feng et al. (2010) (Feng et al., 2010a). Here, 4 mM PPy was added to 4 mM AQDS in 70%

ethanol and 120 mM hydrochloric acid (HCl) (Feng et al., 2010a; Karami & Nezhad, 2013). The mixture was mixed under nitrogen environment for 5 minutes prior to the electropolymerization. Surface of the electrodes were then modified through electropolymerization in a three-electrode configuration electrochemical cell, free from mixing, yet still under nitrogen environment. An Autolab potentiostat was used to control the constant potential of +1,100 mV applied to the anode for about 1 h ($t_{\text{Quiet}} = 5$ s, $t_{\text{1st step}} = 1$ s and $t_{\text{2nd step}} = 1$ s). The freshly prepared AQDS/ PPy- modified electrode was first rinsed with 100 mM HCl and water before thoroughly rinsed in 100 mM PBS.

4.3.4 Single chamber air-cathode MFC

Four cyclones shaped MFCs with anode compartment capacity of 25 mL were constructed from a 50 mL Falcon tube (ϕ 3 cm) (Figure 4.1a). Tube wall of 3.5 cm x 2.4 cm was cut and glued with cation exchange membrane (Ultrax) from BASF Fuel Cell Inc. (Somerset, NJ, USA) while its opposite wall was cut at 1.4 cm x 1.4 cm and glued with butynol Dunlop sheet with one small hole punctured for working electrode. The Falcon tube cap was used to cover the cyclone MFC and was equipped with three holes: a small square about 1 cm x 1 cm for reference electrode (Ag/ AgCl) during the working electrode potential poisoning and electrochemical analysis, and one small circle of ϕ 0.15 cm for incoming gas. An air-cathode from a 10% Pt-carbon cloth (Fuel Cell Earth LLC, Stoneham, MA) was fastened to the exterior wall of the Ultrax membrane with a nickel strip and insulated garden wires. The nickel strip acted as current collector at the cathode. The anode compartment was kept anoxic through continuous gassing with oxygen-free nitrogen. The working electrode was the fabricated graphite -epoxy composite electrodes of ϕ 0.4 cm (Figure 4.1b). The graphite -epoxy composite electrodes were placed almost 90° facing the Ultrax membrane interior wall at a constant distance of about 1-2 mm.

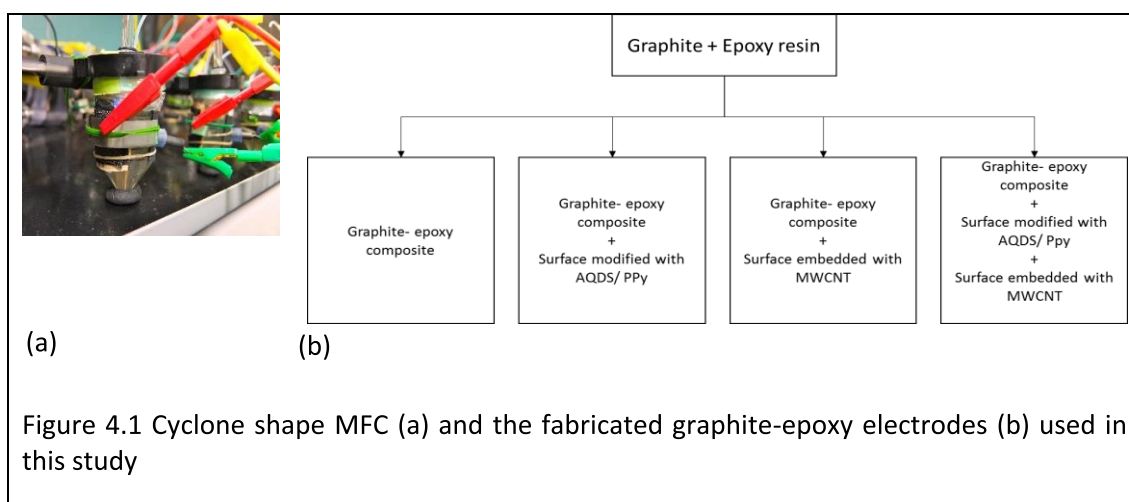


Figure 4.1 Cyclone shape MFC (a) and the fabricated graphite-epoxy electrodes (b) used in this study

4.3.5 Operation

Inoculation method was adapted and adjusted from the method in Watson and Logan (2011), who studied the effect of AQDS/ PPy on carbon felt in dual chambered MFC (Watson & Logan, 2011). Here, about 50% of each 12 new MFCs were filled with anolyte and topped up with acetate media. The anolyte came from a two year old acetate fed MFC, where its early culture originated from aerobic trickling filter. The electrodes were then connected with a 1,000 Ω resistor.

4.3.6 Analyses

Cell voltage (E , mV) across the external resistor were measured every six times daily using a four channel Quadstat 164 potentiostat (eDAQ Pty Ltd, NSW, Australia) with continuous recording using an e-corder 1621 (eDAQ Pty Ltd, NSW, Australia) data acquisition system. Current (I , mA) and power (P , mW) were calculated using the Ohm's law, $I = E/R_{ext}$, where R_{ext} is the applied external resistance. The current density (I/A anode area, mA/ cm²) and power density ($I E/$ Anode area, mW/ m²) are normalized by the projected area of the anode.

Cyclic voltammetry (CV) was measured using a BASi epsilon C3 cell stand with potentiostat (BASi, Indiana, US). A three-electrode system was used, comprising a coiled platinum wire as auxiliary electrode, a Ag/AgCl electrode as reference electrode and the fabricated anodes as working electrode. The experiment was performed at room temperature in a Faraday's cage.

Polarization curve and the power density curves were produced by using anode potential poisoning method, adapted from linear sweep voltammetry method of Lanas and Logan (2013) (Lanas & Logan, 2013). In this study, anode became the working electrode and cathode as the counter and reference electrode. The polarization curves were obtained starting with open circuit voltage (OCV) with each potential changed in decreasing order after every pseudo steady-state achieved, or not more than 20 min intervals (whichever comes first) over a complete fed batch cycle. Analysis was conducted once the voltage output was stabilised after replenishing the media.

4.4 Results and discussion

4.4.1 Fabrication of graphite-epoxy composite anodes

The inherent resistances measured for the fabricated graphite-epoxy composites in this study were also compared to the commercial graphite rod and a 20% (w/w) graphite-epoxy composite fabricated by Corb et al. (2007), which was fabricated using a hot press machine at 80 °C for 40 min (Table 4.1) (Corb et al., 2007). Samples from 53% graphite had much higher resistance than the other graphite-epoxy composite samples in this study. At the same time, the curing time applied in this study proved not to be sufficient for 53% graphite where the surfaces were easily penetrated from the prodding of

the multimeter probes. The incomplete curing might have built the high inherent resistance for the 53% graphite. All the fabricated samples showed significant differences (t-Test, $p > 0.05$) in inherent resistance from the commercial electrode, however showed comparable inherent resistance with the graphite-epoxy composite electrode consisting of 20% graphite (Corb et al., 2007). Sandler et al. (1999) reported that the critical filler volume fraction for percolation, a conductive path created through three-dimensional network of conductive filler particles, is between 5 and 20 vol. % (Sandler et al., 1999). Llopis et al. (2005), Corb et al. (2005) and Ocaña et al. (2014) used a filler as low as 20% (w/w) to fabricate good graphite-epoxy composite biosensors that exhibited good conductivity (Corb et al., 2007; Llopis et al., 2005; Ocaña et al., 2014). However, to fabricate an epoxy composite with very low filler contents, either a long curing time period is required (more than two days) (Llopis et al., 2005; Ocaña et al., 2014) or require the help of expensive machinery, such as hot pressed machine (Corb et al., 2007).

Table 4.1 Inherent resistance measured for graphite-epoxy composite anodes

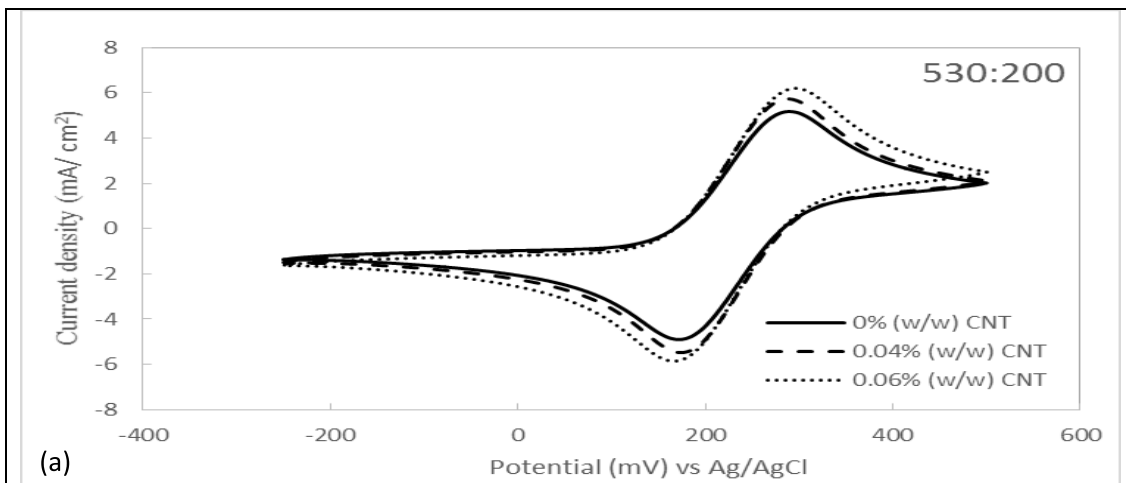
Graphite % (w/w)	Inherent resistance (Ω)		
	0% MWCNT	0.04 % MWCNT	0.06% MWCNT
20*	7.3	-not available-	-not available-
53	34.0	-not available-	-not available-
73	6.1 \pm 0.3	5.7 \pm 0.4	5.8 \pm 0.4
78	4.3 \pm 0.3	4.0 \pm 0.3	4.4 \pm 0.5
84	4.6 \pm 0.5	-not available-	-not available-
ϕ 3 mm commercial graphite rod	0.4 \pm 0.0	-not available-	-not available-

*Corb et al. (2007) evaluated the inherent resistance at sample thickness of 1 mm over sample area of 81 mm². All the fabricated electrodes in this study were evaluated at sample thickness of 1.5 cm over sample area of 12.6 mm².

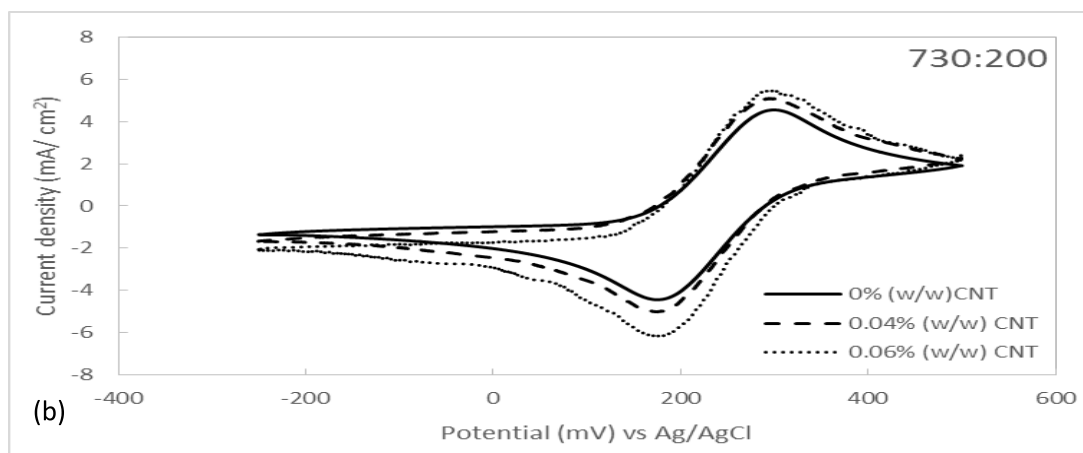
O'Hare et al. (2002) however, had used filler contents ranging between 40 to 60% for their electrodes and cured them by degassing in vacuum oven (O'Hare et al., 2002). They discovered that only the

electrode with 60% filler gave voltammetric peaks response similar to the classic peaks shaped of a solid macroelectrode. By increasing the volume filler fraction to more than 60% (w/w) in this study, a graphite-epoxy composite was able to be fabricated in less than a day, without using expensive machinery and complex method, while at the same time able to show good conductive behaviour. Introduction of 0.04% MWCNT into the surface matrix had reduced the inherent resistance of the plain graphite-epoxy composite samples, although not significantly (t-Test, $p > 0.05$) by 7% less for both 73 and 78% samples (Table 4.1). For samples with 84% graphite, the addition of 0.04% MWCNT into the surface matrix had turned the surface very dry and brittle. After increasing the concentration of MWCNT to 0.06%, the inherent resistance of each samples had increased to 2% for 73% graphite, 9% for 78% graphite and had caused very brittle surface for 84% graphite. The embedding of 0.04% MWCNT within composite matrix that consists of graphite more than 70%, was able to bring down the inherent resistance of the graphite-epoxy composite slightly. However, adding another 0.02% more had proven to give unfavourable effect through increasing the inherent resistance for the samples. Both samples from the 73 and 78% graphite might end up like the 84% graphite samples if more than 0.06% MWCNT added into its system. Though the MWCNT could contribute towards reinforcement of a MWCNT-epoxy composite system (Allaoui et al., 2002), too much filler in an epoxy system will create non-homogeneity in dispersion, especially when using simple hand shearing as applied in this study. This may have a lesser effect on conductivity (Allaoui et al., 2002) but increases the possibility of mechanical failure. It was reported that the structural failure in one of the studies of MWCNT-epoxy composite system, was due to the addition of MWCNT from 0.05 to 0.5% (w/w) (Vahedi et al., 2014). They explained that the increased in fillers will prevent the movement of polymer chains from the epoxy causing the system to become brittle. The amount of low loading however, is dependent on epoxy system, aggregation mechanism and the type of filler applied (Martin et al., 2004). In this study, the MWCNT was added into an epoxy mixture that already had graphite as its filler. Therefore the reason of too much filler might have led to the surface failure of 84% graphite samples.

The ability of the fabricated epoxy composite electrodes to deliver current response from the reaction of electrolyte can be measured through CV. The redox potential of the ferricyanide / ferrocyanide calculated from the half waves, $E_{1/2}$ obtained from the plain graphite-epoxy composite electrodes when compared to standard reduction potential, $E^{o'}$ of ferricyanide / ferrocyanide, which is +162 mV (vs Ag/ AgCl) (Logan et al., 2006), shows astray from the $E^{o'}$: 73% graphite detected about 69 mV more while 78% and 84% graphite detected more than 72 mV (Figure 4.2). There was no significant difference (t-Test, $p > 0.05$) for $E_{1/2}$ detected between the 78% graphite samples and ϕ 3 mm commercial graphite ($E_{1/2} = 234 \pm 0.3$), which was used for comparison.



(a)



(b)

Figure 4.2 Cyclic voltammograms between different MWCNT loadings in graphite-epoxy composite anodes at scan rate 20 mV/ s and in 50 mM ferricyanide/ferrocyanide electrolyte at room temperature (n=3)

$E_{1/2}$ for:

73% (w/w) graphite (a):

No CNT = 231 ± 0.3

0.04% (w/w) CNT = 236 ± 0.3

0.06% (w/w) CNT = 231 ± 0.2

78% (w/w) graphite (b):

No CNT = 239 ± 2.0

0.04% (w/w) CNT = 236 ± 1.2

0.06% (w/w) CNT = 236 ± 4.6

This shows the likeness in current response ability between the 78% graphite samples to the \varnothing 3 mm commercial graphite. However, there were significant differences (t-Test, $p < 0.05$) when the $E_{1/2}$ of the commercial graphite was being compared to both 73 and 84% graphite samples. No $E_{1/2}$ was detected for electrodes with 53% graphite, which might be due to the incomplete curing. For 78% graphite samples, the addition of MWCNT on those two MWCNT loadings did not give significant difference (t-Test, $p > 0.05$) in $E_{1/2}$ when compared to its respective plain samples, between the two MWCNT loadings and the \varnothing 3 mm commercial graphite. Meanwhile, for 73% graphite samples, the addition of 0.06% (w/w) MWCNT had given significant difference (t-Test, $p < 0.05$) in $E_{1/2}$ when

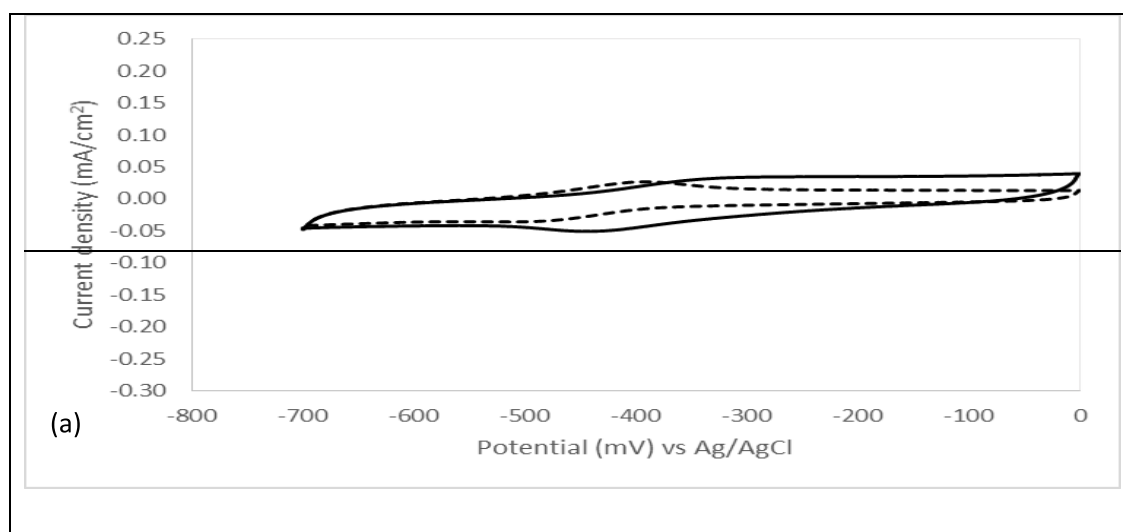
compared to the 0.04% (w/w) MWCNT loading and the ϕ 3 mm commercial graphite. No $E_{1/2}$ analysis was done to 84% graphite samples due to the surface failure after the incorporation of MWCNT into the surface matrix. From the $E_{1/2}$ analysis, the 78% graphite samples show as if the addition of MWCNT into its system did not improve nor worsen the current response ability, unlike 73% graphite samples where 0.04% loading was able to improve its current detection. This could be due to the effect of the filler agglomerating during blending and curing, creating conductive network, which covers the nonconductive epoxy area (Martin et al., 2004). Although the inherent resistance results show the ϕ 3 mm commercial graphite had the lowest resistance, the $E_{1/2}$ performance of the fabricated graphite-epoxy composites (73 and 78% graphite contents) had showed to be comparable in current response to the ϕ 3 mm commercial graphite in this study albeit the inherent resistances.

For surface modification with PPy and AQDS, 78% graphite samples and MWCNT loading of 0.04% (w/w) were applied due to not much difference in current response between the two MWCNT loading as well as the low inherent resistance and consistent $E_{1/2}$ showed by 78% graphite samples. Figure 4.3 shows that the electrografting technique had successfully modified the electrode surfaces. For the embedded MWCNT with AQDS through the formation of redox potential, was seen at $E_{1/2}$ close to $E^{o'}$ of AQDS, -395 mV (vs Ag/AgCl) (Du et al., 2007). This is promising for application as mediated anode in MFC, due to the $E^{o'}$ reported for NAD^+/NADH is -525 mV (vs A/AgCl) (Logan, 2008), which is lower than the surface modified electrodes. The results in this study agrees with Feng et al. (2010a), who had obtained $E_{1/2}$ at -451 mV (vs Ag/AgCl) when using pretreated carbon felts as base for the electrodes (Feng et al., 2010a). Although the peaks were not clear for the plain graphite-epoxy composite samples, there are evident current size and $E_{1/2}$ differences between the initial modified electrodes and after 24 h rinsing in PB solution, where the current size and $E_{1/2}$, became smaller in current and slightly more negative in $E_{1/2}$ potential. Feng et al. (2010a) also observed the difference in peaks size and clarity between two different materials, glass carbon and carbon felt, after their surface modified with AQDS/ PPy (Feng et al., 2010a). They explained that curves with larger currents represented enhancement made by PPy/AQDS on the modified surfaces while good peak clarity denotes the low charging inherit current by the electrode. The shift of waves to negative potential in voltammetry analysis reflected the change in the equilibrium of the active redox couple as a function of the equilibrium constant, $K_{eq} = [\text{OH}][\text{H}^+]/[\text{H}_2\text{O}]$, and can be mathematically explained by the Nernst equation, $E = E^{o'} - (RT/F) \cdot \ln([C]/K_{eq}[A])$ (Compton et al., 2012). The R represents the gas constant of 8.3147 J/K mol, T represents the temperature, F represents the Faraday constant of 96,485 C/ mol and $[C]$ represents the reduced concentration of substrate $[A]$ in mol/ dm^3 when species A is in equilibrium with species B from $A \rightleftharpoons B, B + e \rightleftharpoons C$. The rinsing had removed the excess modification from the electrode surface. This might have caused the electrode surface to

become less acidic, subsequently reducing the K_{eq} and eventually pushing the wave towards negative potential.

4.4.2 Power generation

The main aim of this study was to fabricate strong and easy- to- mould graphite-epoxy composites using simple methods described in section 4.3.2. The prepared electrodes were used as anodes in MFC operations and the performance was measured through anodes polarization and power density on the 13th day after start up. The electrodes polarization results (Figure 4.4a & b) showed that between the fabricated anodes, open circuit potential (OCP) for anodes from MFC2 and MFC2m, gave lower OCP (more negative), -192 mV (vs. Ag/AgCl) less by 62% than MFC1 and MFC1m. The lower OCP observed from these anodes show the contribution of MWCNT in keeping down the anode potential regardless with or without the AQDS/ PPy for surface modification. Low anode potential, as close to the E° of NAD^+/NADH is necessary to prevent the bacteria from gaining metabolic energy, thus reducing maximum attainable voltage for MFC (Logan et al., 2006). These OCP for anodes however are 56% more shifted to the positive potential than $E_{1//2}$ of surface modified graphite-epoxy with AQDS/ PPy recorded in CV using 0.1 M PB, free from bacterial cell (Figure 4.3). This occurrence was also reported by Feng et al. (2010a) where the CV analysis showed that peak waves for their AQDS/ PPy modified carbon felt as anodes in MFC were shifted towards the positive potentials when compared to the surrounding without bacterial cell (Feng et al., 2010a). Based on Logan (2008), bacteria regulate the concentration ratio of the reduced/ oxidized species to maximise the degradation of substrate through NAD^+/NADH , and to transfer the electrons to the anode electrode through other terminal enzymes, which has different potentials (Logan, 2008).



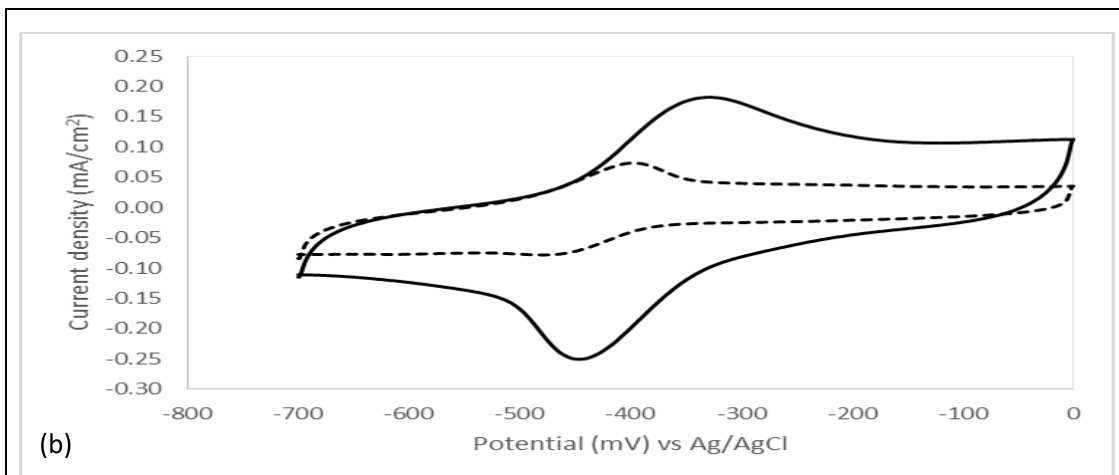


Figure 4.3 Cyclic voltammograms of AQDS/ PPy surface modified on 78% graphite samples (a) without and (b) with 0.04% (w/w) MWCNT loading embedded in the surface of composite matrix before (—) and after 24 h rinsing (- - -) in 0.1 M PB electrolyte at room temperature. Scan rate used was 20 mV/ s.

$E_{1/2}$ for:

Without MWCNT (a):

With MWCNT(b):

0 h rinsing = not available

0 h rinsing = -389 ± 0.6

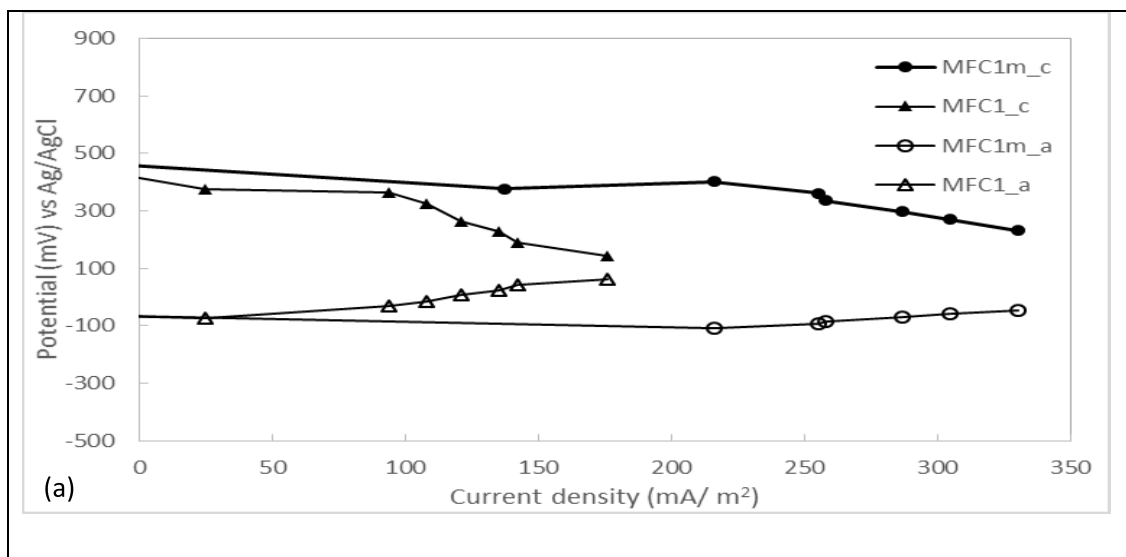
After 24 h rinsing = not available

After 24 h rinsing = -438 ± 0.9

Therefore, it seems that the anode potential will vary according to the bacterial strain dominating the electrode and whether the electrode is with or without biofilm on it. The existence of MWCNT in the anode matrix however did not show any improvement (decreasing) in the overpotential. It gave a significant increase in anode potential, about 214.5 mV (from -164 to +50.5 mV). In fact, this is 38% higher than MFC1 to drive similar current densities from 0 to 176 mA/ m². With the introduction of AQDS/ PPy for surface modification, a low overpotential of 24 mV (from -72 to -48 mV) was achieved by MFC1m, while the current densities were pushed further from 0 to 330 mA/ m² (Figure 4.4a). The surface applied mediator acts as catalyst on the electrode and at the same time reduced the large overpotentials of the electrodes (Feng et al., 2010a; Ramakrishnappa et al., 2011). For the cathode, the application of commercial Pt on carbon clothes were made consistent for each MFCs in this study, and the overpotential from cathode electrodes due to the oxidation reduction reaction were much higher than the anode electrodes (Ghasemi et al., 2013). Therefore, the cathode electrodes with large overpotentials became the limiting factor, which indicates the domination on the cell voltage output (Feng et al., 2011). It is necessary to get low overpotential since electrode overpotential in an MFC is a constitution of three basic losses, 1) activation due to energy lost during electron transfers, 2) bacterial metabolism through substrate oxidation, and 3) mass transport

referring to flux of reactants and products during the reaction (Logan, 2008). In addition to that, these high overpotentials are shown clearly in the power curves (Figure 4.4c). The MFC1m samples that had low anode electrode overpotentials, gave high maximum power density of 59 mW/ m² at the current density of 255 mA/ m²; and followed by MFC1 with 42% less, MFC2m with 47% less and MFC2 with 56% less in power density than MFC1m.

Apart from that, the power density curves also gives quick indication on internal resistance (R_{int}) of the MFC system, where a power curve leaning more to the right will have lesser R_{int} than those with symmetrical curves (Logan et al., 2006). R_{int} of an MFC system could refer to resistance experienced by the electrons through the electrodes and interconnections, resistance experienced by the ions through the membranes, the ionic strength in the electrolytes and many more occurred within the MFC system. Using R_{int} calculation method from Logan (2009), $R_{int} = P_{max} / I^2$, where P is maximum power generated and I is current obtained at P maximum (Logan, 2008), MFC1m and MFC2m samples showed $R_{int} < 100$ k Ω , while MFC1 and MFC2 had $R_{int} > 100$ k Ω . This shows that the AQDS/PPy surface modification had successfully bring down the R_{int} of plain graphite epoxy anodes by 48% and plain graphite epoxy anodes with embedded MWCNT by 66%. Further comparison of R_{int} between fabricated anode without surface modification shows that anode embedded with MWCNT had 22% lesser R_{int} than the anode samples without MWCNT. This shows the ability of graphite-epoxy composite with embedded MWCNT anodes to bring down the R_{int} in the MFC system.



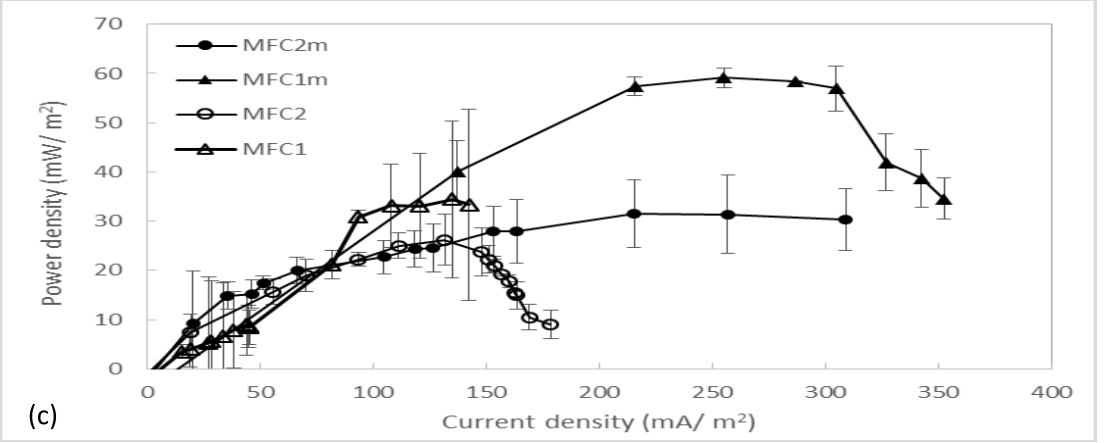
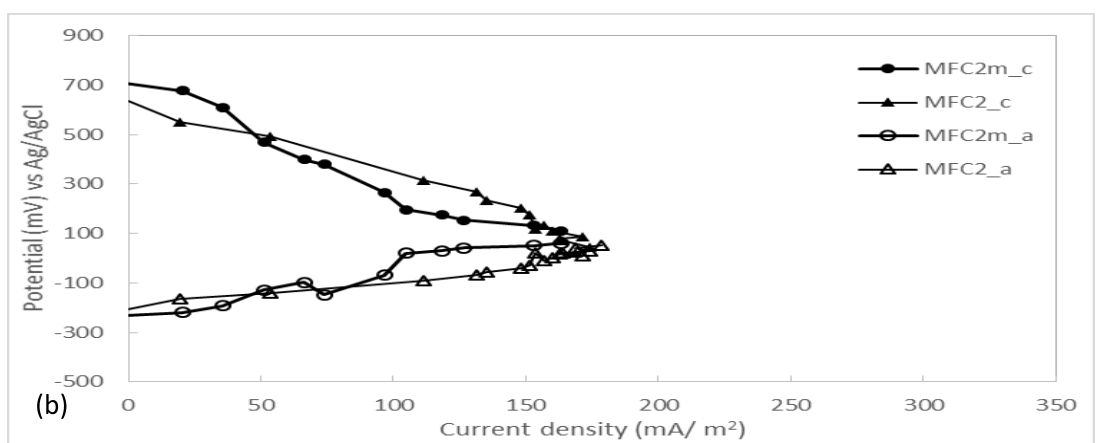


Figure 4.4 Power generation for MFCs operated with (MFC_{Cy}, $y= 1, 2$) and without (MFC_{Cy}, $y= 1, 2$) the AQDS/ PPy surface modified anodes on plan graphite-epoxy anodes and on anodes with embedded MWCNT (MFC_{2x}, $x= m, 0$) and without the embedded MWCNT (MFC_{1x}, $x= m, 0$). (a) Anode and cathode polarization curves when using plain graphite as base, (b) when using graphite-epoxy composite embedded with MWCNT as base, and (c) power density curves of four MFCs. Data presented in this figure are representative of at least three independent experiments.

Note:

c = cathode electrode, a = anode electrode and m = AQDS/ PPy surface modification

The reason for the low maximum power generated by these embedded MWCNT anodes relative to the non-embedded MWCNT, however requires further investigation. The obtained maximum power is much lower in performance than reported, 1,303 mW/m² (Feng et al., 2010a), where their surface modification technique of AQDS/ PPy on carbon felt was adopted onto this study’s fabricated graphite-epoxy composite samples. Since the only similarity between this study and Feng et al. (2010a) is the surface modification technique (Feng et al., 2010a), the inferior performance observed in my study could be due to the differences in the electrode material used, bacterial culture applied as the inoculum and the catholyte used in in MFC.

4.5 Conclusion

We have demonstrated that it is possible to prepare a ready to use electrode within one day from graphite-epoxy composite with more than 70% graphite using a simple and cheap technique, while showing similarity in current response close to the conductive commercial graphite rod. We have also shown that the fabricated electrodes are capable to be used as anodes in MFCs, while the P_{max} could be increased by 42% and R_{int} reduced by 48% through simple surface electrografting with AQDS/ PPy solution. Although anode samples with embedded MWCNT were not superior in maximum power density compared to samples without MWCNT, the R_{int} however showed a reduction by up to 66% for the anode with PPy/AQDS surface modification. Further studies are required to determine whether the anode with embedded MWCNT will show a higher maximum power density if allowed to operate for a much longer duration.

Chapter 5

Cellobiose dehydrogenase/ epoxy-graphite composite with aryl diazonium reduction for lactose detection[#]

Mimi Hani Abu Bakar^{a,b*}, Neil F Pasco^b, Ravi Gooneratne^c, Kim Byung Hong^a

^a Fuel cell Institute, Universiti Kebangsaan Malaysia (UKM), 43000 Bangi, Selangor, Malaysia

^b Lincoln Ventures Ltd, PO Box 133, Lincoln, Christchurch 7640, New Zealand

^c Lincoln University, PO Box 84, Lincoln, 7647, New Zealand

[#] For submission to the Journal of Sensors and Actuators B

*Corresponding author: Mimi Hani Abu Bakar, email: mimihani@ukm.edu.my

5.1 Abstract

Milk is an important ingredient in our day to day diet because of the high quality nutrients in it. In the dairy industry including cheese fermentation processes, there is a need to control the release of lactose into wastewater streams. There are methods adopted to recover the lactose and to transform the lactose into energy through renewable energy (RE) pathways. In this study, graphite-epoxy composite electrode was surface modified with cellobiose dehydrogenase (CDH) enzyme using aryl diazonium. These designed composite electrodes were tested on its capability as biosensor for sensitivity on detecting the lactose as well as its capability as an anode in enzymatic fuel cell (EFC) on long term electrochemical stability in generating electricity from lactose oxidation. The results showed that the CDH-Aryl diazonium modified on surface of fabricated graphite-epoxy electrodes are conductively sensitive and the Michaelis Menten constant K_m for CDH is comparable to available commercial electrodes reported in the literature. The current intensity was 86% more with the above mentioned electrodes when modified with embedded multi-walled carbon nanotube (MWCNT) and gave a high reproducibility signal. These electrodes are stable up to a month when continuously operated. The maximum lactose detection using the above mentioned electrode with embedded MWCNT is higher than the already existing electrodes with MWCNT on surface. However, the current intensity was high with MWCNT on surface than the electrodes with embedded MWCNT in fabricated graphite-epoxy electrodes.

Keywords: *anode, biosensor, cellobiose dehydrogenase/aryl diazonium, enzymatic fuel cell, graphite-epoxy composite, lactose*

5.2 Introduction

Milk is an important constituent of our daily because of its inherent nutrients, such as carbohydrates, fat, protein, vitamins and minerals and enzymes. In the dairy industry, there is a need to control the lactose effluent polluting the wastewater streams. Raw milk has a BOD₅ of about 100 g/ L (Janni et al., 2007) while the soluble carbonaceous tolerance adopted by the New Zealand government is less than 0.002 g/ L daily (Barnett et al., 1998). This standard was set to reduce water pollution by bacteria while ensuring the accessibility of aquatic ecosystem to soluble oxygen in waterways. For this reason, there have been reports published on methods to remove lactose from the waterways including recovering lactose from dairy waste streams using filtration techniques, ultra and nano and reverse osmosis (Chollangi & Hossain, 2007; de Souza et al., 2010), and converting lactose and other organic matters to biogas by using the up flow anaerobic sludge-fixed film (UASFF) (Najafpour et al., 2008). The latter technique is a branch of renewable energy where it uses the internal energy from unwanted biomass and transforms it into a useful source of energy. Another branch in renewable energy, which also is an extension from biosensor technology that directly converts energy through electrochemical pathway from biomass into electricity is the enzymatic fuel cell (EFC). Enzyme applied in EFC would have specific activity and highly selective in choices of substrates. For instance, lactose can be determined using biosensors employing a single cellobiose dehydrogenase (CDH) enzyme. CDH is an extracellular enzyme with narrow substrate specificity: active on cellobiose and lactose while showing distinct discrimination over glucose and maltose (Tasca et al., 2009). The enzyme has two prosthetic groups, the dehydrogenase (FAD domain) and a cytochrome (heme domain). During lactose oxidation to lactobionic acid in an external mediator- free environment, the FAD domain with the maximum capacity of accepting two electrons, will oxidized the lactose while reducing itself to FADH₂. The electrons on the other hand will be channelled one at a time via a flexible linker through the heme domain, which lies about 15 Å away from the FAD domain and get transferred to the electron acceptors, an electrode (Henriksson et al., 2000). Various studies were done on the CDH- modified electrodes for biosensor and EFC applications with lactose as the target substrate with trend to investigate and improve the electron transfer from the CDH to the electrodes. The CDH capability in performing DET and high substrate specificity without need to compete with oxygen makes the enzyme a preferred choice (Wang et al., 2012) when involving lactose / and cellobiose as substrate.

Table 5.1 Some publications on interaction between lactose and CDH-modified electrodes for biosensor and EFC applications.

Electron acceptor	Interest	Source	Year
Graphite rod (\varnothing 3.05 mm)	Investigate the performance of DET between whole CDH / FAD fragment adsorbed directly on electrode surface and whole CDH / FAD fragment cross-linked in a mediator on electrode surface for biosensor application (CDH source: <i>Phanerochaete chrysosporium</i>)	(Larsson et al.)	1996
Graphite rod (\varnothing 3.05 mm)	Effect of pH and ionic strength on the bioelectrocatalysis of cellobiose and lactose at CDH-modified graphite electrodes for biosensor application (CDH source: <i>Phanerochaete chrysosporium</i>)	(Larsson et al.)	2000
Graphite rod (\varnothing 3.05 mm)	Evaluating detection limit, linear range, sensitivity of sensor and long term stability of CDH-modified graphite electrodes for lactose and cellobiose in flow injection mode: in the presence and absence of 1,4-benzoquinone for biosensor application (CDH source: <i>Myriococcum thermophilum</i>)	(Harreither et al.)	2007
Graphite rod (\varnothing 3.05 mm)	Investigate the DET performance of CDH from different sources of fungi in the presence and absence of SWCNT modified to anode surface for EFC application (CDH source: <i>Phanerochaete sordida</i> , <i>Sclerotium rolfsii</i> , <i>Myriococcum thermophilum</i> , <i>Trametes Villosa</i> and <i>Phanerochaete chrysosporium</i>)	(Tasca et al.)	2008
Graphite (3 mm x 3 mm)	Comparing DET and MET between CDH and anode in a membrane-less EFC (CDH source: <i>Phanerochaete sordida</i>)	(Tasca et al.)	2009
Graphite rod (\varnothing 3.05 mm)	Investigate the performance of integrating CDH with specifically developed polymer mediator with respect to conversion of lactose for EFC application.	(Stoica et al.)	2009

Graphite based SPE (Ø1.80 mm)	Improve efficiency of direct bioelectrocatalysis by CDH-electrosynthesised PANI –graphite based SPE (CDH source: <i>Myriococcum thermophilum</i>)	(Trashin et al.)	2009
Carbon based SPE (Ø na)	Improve a lactose biosensor designed by Stoica et al. (2006) using graphite rod as based with cross-linked CDH-MWCNT modified carbon based SPE to make it small, more sensitive and suitable for on-line mode (CDH source: <i>Phanerochaete sordida</i>)	(Safina et al.)	2010
Glassy carbon electrode (Ø3.00 mm)	Investigate the effect of negatively/ positively charged SWCNTs on DET interaction between heme and electrode with respect to current density and stability of the produced electrodes for EFC application (CDH source: <i>Phanerochaete sordida</i>)	(Tasca et al.)	2011
Graphite (Ø na)	Investigate the influence of different concentrations of sodium chloride on the performance of CDH from various sources in solution and immobilised on electrode area for EFC application (CDH source: <i>Phanerochaete chrysosporium</i> , <i>Myriococcum thermophilum</i> , <i>Pichia pastoris</i> , <i>Humicola insolens</i> and <i>Aspergillus oryzae</i>)	(Schulz et al.)	2012
Graphite rod (Ø na)	Combined thermometric/amperometric biosensor, which is separated from immobilised CDH on pore glass in a flow system assisted by benzoquinone (BQ) as mediator (CDH source: <i>Phanerochaete chrysosporium</i>)	(Yakovleva et al.)	2012
Carbon based SPE (Ø 4.00 mm)	Developed an automated at-line lactose biosensor for monitoring dairy wastewater streams using SPE modified with MWCNT using a prototype design, Lactosenz TM	(Glithero et al., 2013)	2013

Note: DET = direct electron transfer, MET= mediated electron transfer, SPE = screen printed electrode and MWCNT = multi-walled carbon nanotube, CNT = carbon nanotube

Graphite material is a common electrical conductor due to its π bonding between C atoms creating layered, planar structure that allow electrons to move freely (Chang, 1994). At the same time,

graphite gives good electrochemical reversibility to electrode reactions (Zhu et al., 2008). CNT on the other hand is well known for its ability to mediate fast electron transfer kinetics on a wide range of electroactive species (Balasubramanian & Burghard, 2006; Muti et al., 2012; Wang et al., 2011). So far, amalgamation of these two electrical conductive materials; graphite and CNT, has shown good conductivity improvement in electrodes activity (Gong et al., 2012; Larsson et al., 1996; Zhu et al., 2008). In recent advances, graphite-epoxy composites are being studied for improvement in mechanical and electrical features. In view of utilization, research works were done particularly in biosensor (Kirgoz et al., 2006; Llopis et al., 2005; Ocaña et al., 2014; Pumera et al., 2006) and bipolar plate (Du & Jana, 2007; Yu et al., 2011) sectors. Since the epoxy resins have good electrical insulation properties, suitable conductive fillers and curing agents need to be applied to make the resins conductive or semiconductive (Bhatnagar, 1996). The advantages of a conductive graphite-epoxy composites, lie on the versatility in fabricating custom made electrodes, i.e. having various sizes and shapes, simple to prepare and easy adaptation to wide electrode configurations (Kirgoz et al., 2006). From previous research, we were able to quick fabricate conductive graphite-epoxy composites consist of more than 70% (w/w) of graphite content within a day, using cheap and simple technique. Aryl diazonium salts on the other hand is simple to prepare, rapid in electroreduction, large choice of reactive functional groups and provides strong covalent bonding between the aryl and the surface: polymers, biomacromolecules and nanoparticles (Mahouche-Chergui et al., 2011). Tasca et al. (2011) observations on covalent binding of CDH to glassy carbon electrode, it is better to make the electrode's surface positively charged using diazonium salts from amine group, since it will create a better interaction between the modified surface and the negatively charged heme domain (Tasca et al., 2011a).

To our knowledge, there are no reports on the capability and reliability of graphite-epoxy composite for use as an electrode for lactose detection. By combining the graphite-epoxy composite with CDH using aryl diazonium bonding, new insights could be obtained for better and more sensitive lactose detection.

In this study, graphite-epoxy composites were fabricated with MWCNT embedded in the matrix surfaces. Safranin/ aryl diazonium was electrochemically grafted to the composites' surfaces to create strong covalent bonding and induced preferred orientation between the negatively charged CDH and positively charged electrodes' surfaces. The sensitivity of the composite electrodes in detecting lactose was compared to the capability of other published papers on lactose biosensor while the electrochemical stability of the electrodes in continuous operation was monitored through EFC system.

The aim of this study was to investigate performance of immobilized CDH bonded using aryl on graphite-epoxy electrodes with and without embedded MWCNT, for sensitivity in lactose detection and continuous detection stability. Emphasis was on performance of the electrode in increasing the maximum detection of lactose analysis, shorter response time, and sensitivity of the sensor in boosting the amount of electron transfer from the heme domain of the CDH to the electrode and long term operational stability of the electrode performance in continuous flow environment.

The results obtained showed that the CDH-Aryl diazonium modified on surface of fabricated graphite-epoxy electrodes are conductively sensitive and similar in producing Michaelis Menten constant, K_m for CDH similar to electrodes reported in literature. The electrodes modified with embedded MWCNT showed increase in current intensity up to 86% when compared with electrodes without any MWNCT. These electrodes were stable for about a month when operated continuously. However, the electrodes with embedded MWCNT, could not provide a current intensity as high as electrodes with MWCNTs on the surface but electrodes with embedded MWNCT was able to improve the detection of maximum lactose with high reproducibility. More data on this chapter is shown in Appendix C.

5.3 Methods

5.3.1 Chemicals

Chemicals were of analytical grade. Potassium ferrocyanide $K_4Fe(CN)_6$ was purchased from AnalaR®, BDH Laboratory Supplies (Poole, England). Potassium ferricyanide $K_3Fe(CN)_6$ was purchased from UNIVAR, Ajax Finechem (Wellington, NZ). N,N-Dimethylformamide (DMF), sodium nitrate $NaNO_2$ and aryl diazonium were purchased from Sigma (Auckland, NZ). Lactose $C_{12}H_{22}O_{11} \cdot H_2O$ was purchased from Fisher Scientific (New Hampshire, US). Citric acid monohydrate $C_6H_8O_7 \cdot H_2O$ powder, hydrochloric acid (11.7 M HCl) and sodium hydroxide NaOH pellets were purchased from LabServ™, Thermo Fisher Scientific, NZ Ltd. (North Shore City, NZ). Tri-sodium citrate $C_6H_5Na_3O_7 \cdot 2H_2O$ and safranin were purchased from BDH Laboratory Supplies (Poole, England). The 5% functionalized-COOH Multi walled carbon nanotubes (MWCNT) was purchased from DropSense (Spain). Graphite powder with ultra 'F' purity was purchased from Ultra Carbon Corp. (Michigan, US). Resin-norSKI® part A and hardener norSKI® part B were purchased from norSKI® (Wellington, NZ).

All analytical solutions were made using Milli-Q water from EASYpure UV (Barnstead, New Hampshire) unless otherwise stated. The buffer used for lactose analysis was a citrate buffer (CB) (0.1 M $C_6H_8O_7 \cdot H_2O$ / 0.1 M $C_6H_5Na_3O_7 \cdot 2H_2O$, 1.0 M KCl) with pH adjusted to 4.5 using 1.0 M NaOH (Safina et al., 2010; Tasca et al., 2009).

The stock reagent of lactose (0.2 M $C_{12}H_{22}O_{11} \cdot H_2O$) was made into several range of concentrations by diluting lactose solution with CB solution using the following equation: $V_1 = (M_2 \times V_2) / M_1$. The V_1 is the volume to be added in mL from the original lactose source, M_1 is the concentration of the original lactose source, M_2 is the end concentration of lactose while V_2 is the end volume required for testing. All of the prepared lactose with different concentrations were stored in different bottles and stored at 4 °C when not in use.

5.3.2 Enzyme strain

Solution of CDH from *Phanerochaete sordida* was provided by Dr. Roland Ludwig, BOKU, Austria. The CDH has a volumetric activity of 291 U/ mL and a specific activity of 23.9 U/ mg protein. The enzyme unit (U) is a unit for the amount of a particular enzyme. One U is defined as the amount of the enzyme that produces a certain amount of enzymatic activity, that is, the amount that catalyzes the conversion of 1 micro mole of substrate per minute.

5.3.3 Preparation of working electrodes

The base for the anodes were made from graphite powder mixed with epoxy resin in % (w/w) ratio of 78:22. The total filler loading was more than 50 wt% to produce a fast drying conductive electrode with low inherent resistance. Ratio between the resin (norSKI® part A) and its hardener (norSKI® part B) followed Pumera et al. (2006) at (w/w) of 20:3 (Pumera et al., 2006). The combined material was manually blend using spatula until the texture turned flaky and packed into the PCR tubes (\varnothing 0.4 cm) at the length of 1.5 cm. For the embedding of MWCNT into the matrix of graphite epoxy composite, MWCNT was prepared through mixing of 1 mg of MWCNT with a 0.4 mL N,N-Dimethylformamide (DMF) in a vibrator for 1 min. The mixture was later topped up with 0.6 mL of 70% ethanol and sonicated in water bath for five minute. Loading of the MWCNT ink into the base of graphite-epoxy composite was done at % (w/w) ratio of 0.04:1. The MWCNT mixtures were manually blend using spatula and dried under room temperature until the texture became muddy dry. The mixture paste was topped up about 0.3 cm high on the packed graphite- epoxy resin mixture in the PCR tube, to become the electrode's surface. Prior to the surface modification methods, each of the packed PCR tubes was centrifuged at 14, 000 g for 1.5 min to compress and remove remaining air in the paste. A copper wire was inserted at the bottom of the tube for electrical contact. The filled PCR tubes were then cured at 80 °C for 12 h. They were then allowed to cool at ambient temperature for 30 min. Later, the excess PCR tubes wall were cut until the wall was at the same level with the surface of the fabricated graphite-epoxy composite electrodes. The electrode surface area were polished first on a wet fine emery paper (Norton, P400), rinsed with Milli-Q water and dried on paper towel before polished on white paper until mirror like surface appeared. Modification with aryl diazonium adapted

steps from Picot et al. (2011) and Commault et al. (2015) was done on the fabricated electrodes (Commault et al., 2015; Picot et al., 2011). Here, 0.1 M HCl was mixed with 0.01 M safranin and dissolved in Milli-Q water for total volume of 5 mL. The mixture was placed in ice bath and under nitrogen flow while kept in complete darkness. About 0.02 M of NaNO₂ was added into the mixture. Surface of the electrode was then modified through electropolymerization in a three-electrode electrochemical cell consisting of the anode as working electrode, a Pt auxiliary for counter electrode and an Ag/AgCl for reference electrode. A potentiostat (EC epsilon, BASi, IN, USA) was used to control the constant potential of -0.161 V (vs. Ag/AgCl) applied to the anode until total coulombic charge consumed is about 300 mC/ cm² (Initial P= 0 mV, t_{Quiet}= 2s, 1st step = -161 mV; 1,200 s, 2nd step = 0 mV; t= 0s). The freshly prepared modified electrode was rinsed several times in Milli-Q water and absorbed dry on paper towel. The modified electrodes were rinsed with large volumes of water and allowed to air dry. CDH- modified electrodes were prepared by pipetted 10 μL of CDH solution onto each aryl/ graphite-epoxy electrode's surface to adsorb by the surface at 4 °C under controlled humidity, overnight.

5.3.4 Enzymatic fuel cell air-cathode system construction

Stability of the fabricated anodes during continuous lactose detection were analysed using a miniature air-cathode enzymatic fuel cell (EFC) (Figure 5.1). The EFCs consist of a thin drum shaped polyethylene reactor (ø 4 cm) with one wall made from hard polyethylene and the other from Ultrex membrane (BASF Fuel Cell Inc, Somerset, NJ, USA). The air-cathode made from 10% Pt-carbon cloth (Fuel Cell Earth LLC, Stoneham, MA) (12.6 cm²) was fastened to the exterior wall of the Ultrex membrane with a nickel plate (4 cm x 1 cm) and an elastic band. The working electrode had the modified area facing the Ultrex membrane interior wall at a constant distance of about 1-2 mm and was inserted through a small hole made by butynol Dunlop sheet (2 cm x 1 cm) that was fixed onto an opening on the hard polyethylene wall. This is to ensure snug fitting between the electrode and the electrode insertion port at the EFC wall to avoid electrolyte leaking. To enable application of reference electrode (Ag/ AgCl) during the amperometry analysis, a small insertion hole was made at the top of the polyethylene wall, almost parallel to the Ultrex membrane and perpendicular to the inserted graphite rod. The maximum volume of the EFC was 5 mL and the system was equipped with self-drained ability (cut 1 mL polyethylene pipette tip) to naturally maintain the volume of electrolyte and avoid overflow from occurring.



Figure 5.1 The in-house EFC made in this study equipped with self-drained system.

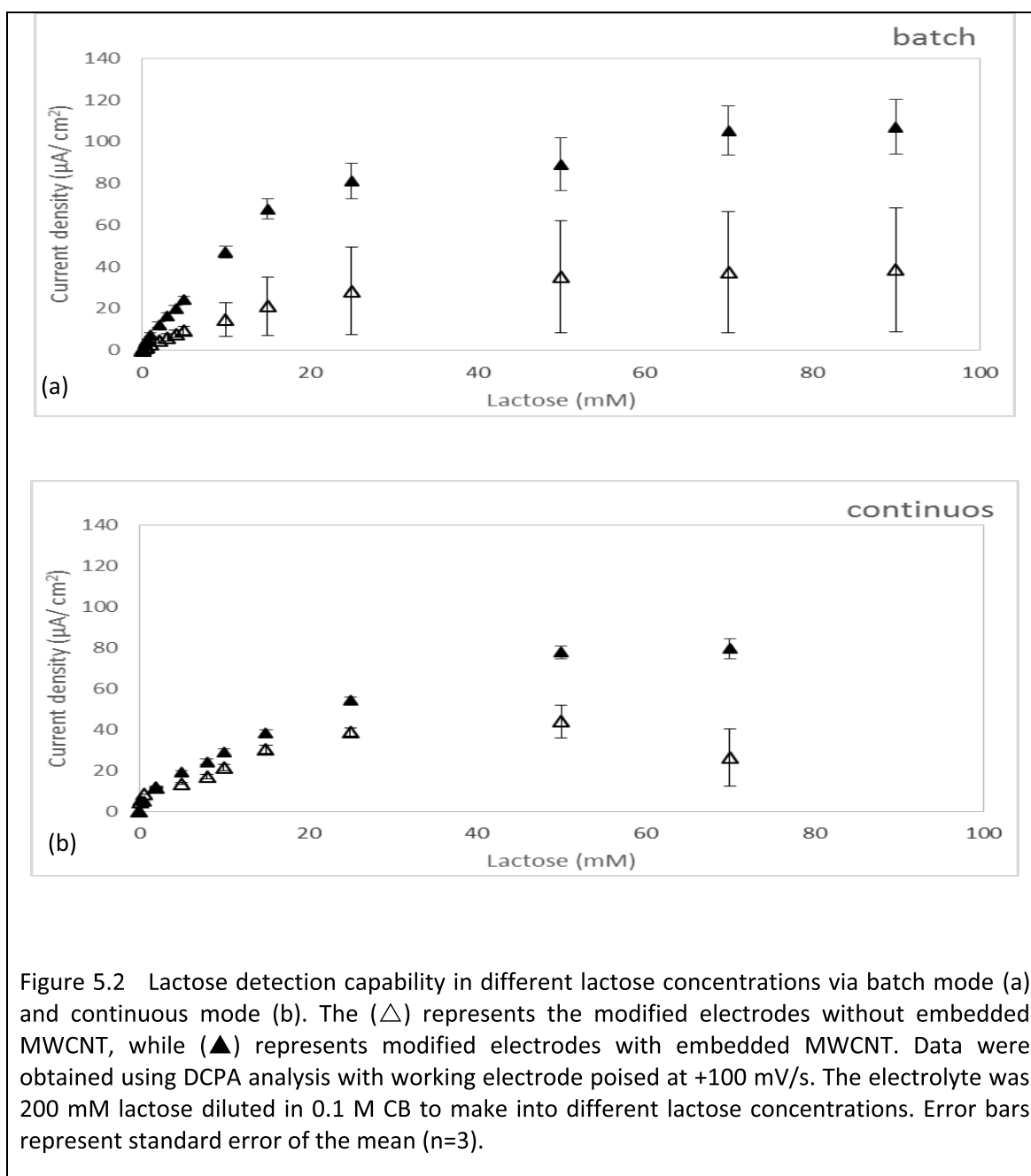
5.3.5 Electrochemical measurements

Electrochemical analyses were conducted using direct current potential amperometry (DCPA) with a four-channel potentiostat (QuadStat 164, eDAQ Pty Ltd, New South Wales, Australia) and data acquisition system (e-corder 1621, eDAQ Pty Ltd, New South Wales, Australia) connected to a computer. A three-configuration electrodes were applied: bioanodes for working electrodes, auxiliary electrodes and Ag/ AgCl (3 M KCl) for reference electrodes. Analyses done in batch mode applied Pt while in continuous mode applied the air-cathode itself for the auxiliary electrodes. Sensitivity in lactose detection was done in both batch and continuous mode. The anode was set at potential +100 mV (vs. Ag/AgCl), which was adapted from Safina et al. (2010) where she found that *Phanerochaete sordida* worked well when the electrodes were poised at +100 mV (vs. Ag/ AgCl) (Safina et al., 2010). Here, 12 different lactose concentrations were tested: 0.04 mM, 0.08 mM, 0.3 mM, 0.5 mM, 1 mM, 2 mM, 3 mM, 4 mM, 5 mM and 10 mM, 15 mM and 25 mM. Analysis in continuous mode introduced flushing with 0.1 M CB in between the lactose detection with the flow rate of 0.5 mL/ min. The anode performance stability analysis was done using a fixed lactose concentration of 5 mM, following Tasca et al. (2011) based on the same K_m value obtained in this study (Tasca et al., 2011a).

5.4 Results and discussion

5.4.1 Sensitivity in lactose detection

The study of maximum detectable lactose concentration could show the highest lactose concentration capable to be oxidized by the enzyme before the enzyme becomes saturated and no longer produce significant current even though there is an availability of substrate.



From Figure 5.2, both mode of analyses, batch or continuous, regardless whether the surface modified graphite-epoxy electrodes are with or without embedded MWCNT, shows having similar capability to detect a wide range of lactose concentrations, up to 70 mM. This shows that the maximum lactose concentration the anode can oxidized under potential poised of +100 mV, would be around 70 mM. Higher than that, there will be no increase in current intensity. In a study done by Stoica et al. (2009) on lactose detection by CDH-osmium/spectroscopic graphite rod, under anode potential poisoning of +205 mV (vs. Ag/ AgCl), the maximum lactose concentration detected was until 34 mM generating about $7.86 \mu\text{A}/\text{cm}^2$ (Stoica et al., 2009). When they applied it as anode in an air-cathode EFC, with 34 mM lactose as anolyte, the maximum current density obtained was 1.7 fold higher than the current at the saturated point. In this study, more than $30 \mu\text{A}/\text{cm}^2$ could be

generated at 34 mM lactose concentration (Figure 5.2). This gives the possibility of the anodes in this study to generate higher maximum in current and power density when operated in EFC. The Michaelis- Menten constants (K_m) obtained from the fabricated electrodes were within the range of 0.65 – 0.78 mM, which is not much different from the K_m obtained for PsCDH in Tasca et al. (2011) (Tasca et al., 2011a) (Table 5.2). K_m focusses on enzyme activity of CDH, measured via the generated current produced by the liberated electrons from the oxidation of lactose concentrations through the external circuit. Study on the K_m when analysed in electrochemical cell upon different concentrations, helps selecting bioelectrodes with a larger K_m value for application in tough condition of continuous lactose detection in an EFC system. A high K_m value will show the capability of the system to operate at higher concentration of lactose before the enzyme became saturated. This would offer the possibility to tap into more electrons out from the oxidation of high lactose concentration to generate current with greater intensity. For the studied bioelectrodes, applying surface modification with embedded MWCNT did not significantly increase the K_m values. This indicates that the high current intensity achieved was due to the contact between CDH and MWCNT located on the electrode's surface (Ludwig et al., 2010). To obtain a high electron transfer rate, the heme domain of the CDH must be in the correct orientation to the electrode surface, which is less than 20 Å away (Tasca et al., 2011a). This was proven by Tasca et al. (2011) in their experiment on glucose biosensor via *Corynascus thermophiles* (CtCDH) (Tasca et al., 2011b). By comparing between the presence and non-presence of SWCNT, they found the performance of CtCDH through application of SWCNT on the surface of the spectrographic graphite electrode, had increased the K_m of glucose concentration higher by 1.2-fold and improved the current intensity by almost two-fold at 300 mM glucose (the maximum glucose concentration analysed in the study) while still having the same maximum linear detection range as the SWCNT-free biosensor. Effect of continuous lactose flow with intermittent buffer flushing had given a slight increase in K_m values. K_m is affected by several factors, such as pH, temperature, ionic strengths and the substrate concentration. The slight increase in K_m could be due to the continuous flow mode maintaining consistent environment for the enzyme by supplying fresh feed every time into the system.

The only difference in observation is the current intensity generated from this study, where the current intensity is greater in batch rather than in the continuous mode (Table 5.2). Significant statistical differences (t-test, $p < 0.05$) however, were seen only in the batch mode at lactose concentrations of 0.5 and 5 mM, where current intensity from the surface modified graphite-epoxy electrodes were higher than the electrodes without embedded MWCNT. At the same time, on average for each electrode types, the current reproducibility is higher (smaller RSD %) on the electrodes with embedded MWCNT, especially in the continuous mode (t-test, $p < 0.05$). This shows that the existence of embedded MWCNT had improved the conductivity of the electrodes. Although

graphite-epoxy composite electrodes have rather high inherent resistance (Kirgoz et al., 2006), the adding of MWCNT into the system however was able to reduce it (Spitalsky et al., 2010). The MWCNT may have dampen the effect of the non-conductive epoxy resin and eventually increased the reproducibility of results, compared to the graphite-epoxy electrodes without embedded MWCNT that had rather low reproducibility. A similar effect due to surface treatment with CNT yet with a different approach from this study, was also observed by Safina et al. (2010)(Safina et al., 2010). Their study on biosensor on the effect of CDH from *Phanerochaete sordida*, when cross- linked directly onto MWCNT on carbon screen printed electrode (cSPE) for lactose detection, showed that the existence of MWCNT on the cSPE showed an improvement in current density by 1.5 to 2.5 times higher than the cSPE without MWCNT. In fact, other studies that had CDH directly linked to SWCNT showed high current intensity (Table 5.2).

Table 5.2 Anode reproducibility test at several lactose concentrations

Anode sample	Lactose (mM)				
	0.5			5	
	K_m (mM)	Current Density (Mean) ($\mu\text{A}/\text{cm}^2$)	RSD (%)	Current Density (Mean) ($\mu\text{A}/\text{cm}^2$)	RSD (%)
MWCNT added					
CDHAryl diazonium/ MWCNT epoxy graphite composite (<i>batch</i>)	~0.65	4.6 ± 0.5	20	24.0 ± 1.5	11
CDHAryl diazonium/ MWCNT epoxy graphite composite (<i>continuous</i>)	~0.75	5.2 ± 2.3	78	19.2 ± 3.8	35
No MWCNT (Control)					
CDHAryl diazonium/ epoxy graphite composite (<i>batch</i>)	~0.75	1.7 ± 0.1	10	9.3 ± 2.0	30
CDHAryl diazonium/ epoxy graphite composite (<i>continuous</i>)	~0.78	8.5 ± 8.3	138	13.6 ± 12.7	132

^a CDHaryl diazonium/SWCNT/ Glassy carbon	0.70	na	na	500	na
^b PEGDGE- CDH/SWCNT/graphite rod	2.3	na	na	80	na

^a(Tasca et al., 2011a) & ^b(Tasca et al., 2008). PEGDGE = poly(ethylene glycol) diglycidyl ether

Note: RSD = (standard deviation/ mean) x 100 = relative standard deviation to express the precision and repeatability of a response. Small RSD% shows good reproducibility (Safina et al., 2010).

In this study, MWCNT was not exposed on the surface of the base electrode, instead the MWCNT was mixed into the matrix graphite composite. The embedded MWCNT in the fabricated graphite composites might create continuous electrical wires to allow easy DET flowing from cytochrome that bonded covalently onto the aryl diazonium compound to the fabricated electrode and all the way to the copper wire, which acts as current collector. Synthesis of aryl diazonium salt from safranin was chosen to obtain protonated state from phenazine-NH₂ when in acidic environment, pH 4.5. The negatively charged cytochrome from the CDH will be attracted to the dangling positively charged -NH₃⁺ with its other end covalently bonded to the graphite surface (Figure 5.3). Hence, these functional charged groups should increase both the interaction forces and orientation of the enzyme on the surface of the electrode (Tasca et al., 2011a) and improve the DET.

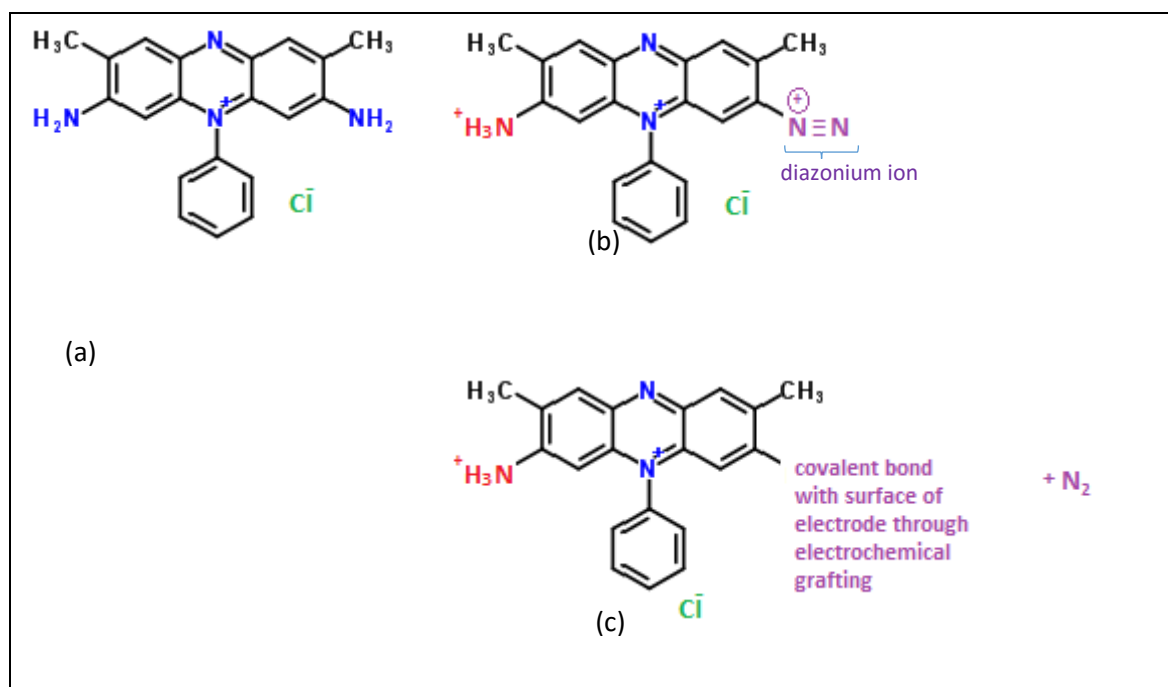


Figure 5.3 Molecular representation of safranin (a), the formed diazonium ion getting ready to make bonding (b) and the attachment of the aryl diazonium salt through covalent bond onto a surface (c).

Safranin = 3,7-Diamino-2,8-dimethyl-5-phenylphenazin-5-ium chloride

Having molecular formula of $C_{20}H_{19}ClN_4$

The fast response time, less than a minute per sample is slightly faster than 2 minutes per sample obtained by Yakovleva et al. (2012) for their lactose biosensor (Yakovleva et al., 2012). This fast sampling obtained through fabricated graphite electrode might be due to the wide electrode active surface area and correct orientation of CDH and $-NH_3^+$ that favours easy flow of electron transfer from CDH to electrode.

5.4.2 Prepared electrodes provide continuous current signal

The duration stability test was done in air-cathode MFCs with 5 mM of lactose continuously flowing into the system. The analysis was carried out onto the fabricated graphite composite electrodes for a length of 25 days (Figure 5.4). Results showed that anodes with MWCNT embedded into the surface matrix gave almost consistent and higher in averaged current density, about 86% more than anodes without embedded MWCNT at the fixed lactose concentration. Due to technical problems, analysis done to anodes without embedded MWCNT was discontinued on the 7th day of EFC operation. Set aside the technical problems, this shows that the fabricated anodes are capable in working within long duration and still sensitive without any significant decrease in analytical response. To our knowledge, continuous stability analysis on lactose detection conducted to a CDH modified electrodes for more than a day (Glithero et al., 2013; Safina et al., 2010; Yakovleva et al., 2012) have been reported on commercial electrodes such as SPEs and graphite rods, however none on graphite-epoxy composite electrodes. Although using the commercial SPE modified with MWCNT could give better performance in RSD% and smaller concentration detection as in Glithero et al. (2013) (0.002 mM to 29 mM), the in-house fabricated graphite epoxy composite electrode in this study offers the flexibility and freedom in designing the electrode shape based on the desired reactor, while maintaining equally fast detection time as the SPEs. In addition, this study targets on high generation of current from the lactose oxidation besides concentration detection for lactose monitoring. Hence, electrode stability analysis on the graphite-epoxy composite while functioning as anode under potential poisoning for lactose continuous detection and generating high currents look promising for further development in real EFC condition without any anode poisoning.

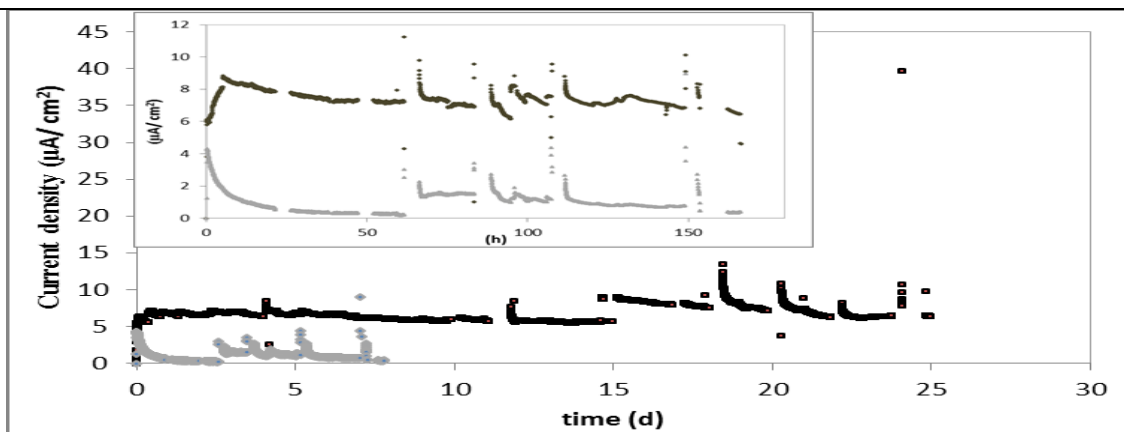


Figure 5.4 Stability test done in an air-cathode EFC for fabricated graphite-epoxy anodes with CDH on aryl diazonium surface modification. (■) represents anodes with embedded MWCNT while (●) represents anodes without embedded MWCNT. Data were obtained using DCPA analysis with working electrode poised at +100 mV/s. The electrolyte was 5 mM lactose in 0.1 M CB at 0.5 mL/min (n=3).

5.5 Conclusion

It is very important and crucial to detect a wide concentration range of substrates and at the same time use them as a stable anode in EFC to generate high current intensity for a long duration (more than 30 days). It serves the purpose of both biosensor and EFC. This study was able to show that the simple and fast drying graphite-epoxy composite electrodes were capable of producing K_m of CDH similar to commercial electrode materials. In addition to that, it was able to detect a higher maximum lactose concentration than achieved by commercial electrode materials and can withstand strenuous long term operation. The embedded MWCNT did not give intense current compared to the MWCNT on the surface due to the non-existence of a direct link between the CNT and the CDH-aryl diazonium. Embedding the MWCNT within the graphite-epoxy matrix however shows that it was able to significantly increase the reproducibility of the signal and intensify the current up to 86% compared to an electrode without embedded MWCNT. In this study, the ability to fabricate anodes gives flexibility to cater with system design. Further studies can be directed to examine the effect of half embedded and half protruded MWCNT on electrode surface for electricity generation.

Chapter 6

General discussion, Conclusions and Future Research

BFCs are categorized into two groups based on the biocatalyst used, the MFC that uses the microbes and the EFC that uses isolated and purified enzymes. Though the catalysts are different, the working mechanisms of these biofuel cells are similar, which is extracting electrons through favoured substrate oxidation, and transferring them to an anode. The electron then travels to the cathode via an outer circuit. At present, the power generated by the BFCs are not substantial, about 2 W/ m² (Nandy et al., 2015) when compared to chemical fuel cell, which is about 550 kW/ m² (Markillie, 2010). Studies are actively being carried out with MFC to improve the power production and reduce cost in a variety of different areas such as electrode material, reactor design, inoculum and substrate rich in electrons. It is also crucial to have the anode compartment free from soluble oxygen and other soluble anaerobic electron acceptors such as, nitrate (NO₃-), sulphate (SO₄²⁻), sulphur (S) or fumarate, which have adverse effect on electricity generation in MFCs (Kim et al., 2004). Among the above mentioned soluble electron acceptors, the most electronegative is oxygen, which accounts for 21% of air in the atmosphere. This study was conducted to achieve three objectives. The first objective was the preparation of enriched exoelectrogen culture exposed to oxygen for an extended time period to provide the inoculum for the second objective. The second objective was focused on graphite-epoxy composite electrode fabrication for better electricity generation and the third objective was immobilization of CDH on the electrodes prepared in the second objective to detect lactose

The first objective (Chapter 3) was to provide an understanding of the long term exposure to oxygen on enriched exoelectrogen culture and this culture was used as the inoculum in the second objective. The results showed that after 30 days of exposure of anolyte in 7.5 ppm of soluble oxygen, the exoelectrogens became inactive from donating electrons to the external anode for electricity production. It is important to have the anode compartment free of diffused oxygen from the cathode especially during start up (Hutchinson et al., 2011). Though the exoelectrogens are believed to be facultative bacteria, only when the area is suitable for anaerobic bacteria to survive and perform anodophilic transfer, then only current density started to gain pace. In the air bubbling anode chamber, the growth of aerobic microbes might have increased due to a direct reduction of oxygen in the cell to increase biomass production. The diffused oxygen is consumed in the outer layer of biofilm, providing favourable conditions for growth of facultative and strict anaerobic in the deep layers of the biofilm. Fortunately, this result was not permanent because on subsequent exposure to an anaerobic environment, the exoelectrogens regained their productivity by generating up to 100%

of P_{max} and I_{max} while reducing the R_{int} to 53%. Ringeisen et al. (2007) showed that single culture exoelectrogens became active once they discontinued the aerobic substrate for seven minutes from reaching the system (Ringeisen et al., 2007). The same phenomenon was also observed by (Li et al., 2010). My study showed that exoelectrogen bacterial community is robust and able to survive for 30 days in aerobic environment and then switch its electron transfer pathway from aerobic to anaerobic.

The exoelectrogens from the first objective was used as the inoculum for the experiments designed to achieve the second objective (Chapter 4). As mentioned in the earlier paragraph, the emphasis of the second and third objectives in this study was to analyse the performance of the fabricated graphite-epoxy composite electrode with a more than 70% graphite content. Attention was given to the composite electrode because of the attractive qualities it offers including improved conductivity, strength and design flexibility. The graphite content of more than 70% was applied throughout the electrode to reduce the inherent resistance and electrode preparation time. The second objective was able to provide evidence that graphite-epoxy composite with more than 70% graphite content could be fabricated within 24 h. The graphite content allowed faster drying thus reducing the time for electrode preparation without using expensive machinery and complex method, while at the same time able to show good conductive behaviour. Samples with 73% graphite and 0.04% MWCNT loading improves $E_{1/2}$ detection in electrochemical analysis, with ferricyanide/ ferrocyanide as electrolyte. This could be due to the effect of filler agglomeration during blending and curing, creating conductive network, which covers the non-conductive epoxy area. When MWCNT was embedded into the composite matrix, lower OCP were recorded from these anodes. This shows the contribution of MWCNT in keeping down the anode potential regardless with or without the AQDS/ PPy for surface modification. Low anode potential, as close to the E° of $NAD^+ / NADH$ is necessary to prevent the bacteria from gaining metabolite energy, thus reducing maximum attainable voltage for MFC. On the other hand, electrodes with embedded MWCNT bring down the R_{int} in the MFC system occurred within the system. R_{int} of an MFC system could refer to resistance experienced by the electrons through the electrodes and interconnections, resistance experienced by the ions through the membranes, the ionic strength in the electrolytes and many more occurred within the system. Up to 22% of R_{int} was reduced in the MFC system, compared to the plain graphite-epoxy electrode. Higher reduction in the R_{int} up to 66% was seen when the graphite-epoxy electrodes had their surface modified with AQDS/ PPy. The surface applied mediator acted as a catalyst on the electrode and at the same time reduced the large overpotentials of the electrodes, which resulted in : 1) activation due to energy lost during electron transfers, 2) bacterial metabolism through substrate oxidation and 3) mass transport referring to flux of reactants and products during the reaction. As for the P_{max} , surface modified plain graphite-epoxy electrode showed a higher P_{max} than the surface modified

embedded MWCNT graphite-epoxy electrodes, and significant differences in P_{max} between the modified and unmodified electrodes were evident. Electrode surface modification acts as a catalyst by reducing the large overpotentials of the electrode (Feng et al., 2010a; Ramakrishnappa et al., 2011), thus improving the P_{max} and R_{int} . The reason for the low P_{max} generated by embedded MWCNT graphite-epoxy electrodes were not clear and requires further study.

In objective 3 (Chapter 5) the graphite-epoxy electrode was surface modified with aryl diazonium to prepare a covalent bond for the CDH enzyme. These electrodes were able to detect a maximum lactose concentration of 70 mM. The slight increase in K_m happened in continuous lactose flow could be due to the continuous flow mode maintaining a constant environment for the enzyme by supplying fresh feed every time into the system. A high K_m value will show the capability of the system to operate at higher concentrations of lactose before the enzyme became saturated. This would offer the possibility to tap into more electrons from the oxidation of high lactose concentration to generate current with greater intensity. The range of lactose detection was similar with or without embedded MWCNT. However, the embedded MWCNT increased the current up to 86% and was stable in long-term operation compared to the electrode without embedded MWCNT. The existence of embedded MWCNT improved the conductivity of the electrodes. The MWCNT may have dampen the effect of the non-conductive epoxy resin and eventually increased the reproducibility of results. Concurrently, the embedded MWCNT might create continuous electrical wires to allow easy DET flowing from cytochrome that bonded covalently to the electrode's surface.

This research has contributed to the advancement of knowledge in the BFCs in the perspective of oxygen effect and alternative anode material. This study has emphasised the detrimental effect of soluble oxygen within the anode compartment of MFC and showed that exoelectrogens could survive when exposed to soluble oxygen of 7.5 ppm for 30 days. These exoelectrogens can rebound when exposed to anaerobic conditions and provide 100% improvement in both P_{max} and I_{max} . Recent studies show the increase of composite electrodes application in BFCs being investigated to reduce the cost of BFCs from using noble metals. However, most of these researchers were unable to completely detach their studies from using non-precious metals such as nickel (Huang et al., 2015; Karthikeyan et al., 2016), iron (Liu et al., 2015), silver and iron (Ma et al., 2015) and manganese and iron (Burkitt et al., 2016) in their electrodes fabrication due to the high current performance they bring. Graphite-epoxy composite gives the ability to fabricate anode material in-house. This study shows that the graphite-epoxy electrodes are cheap and flexible for fabrication when compared to commercial electrodes. These electrodes can be easily fabricated within 24 h to be used as conductive electrodes for the BFCs.

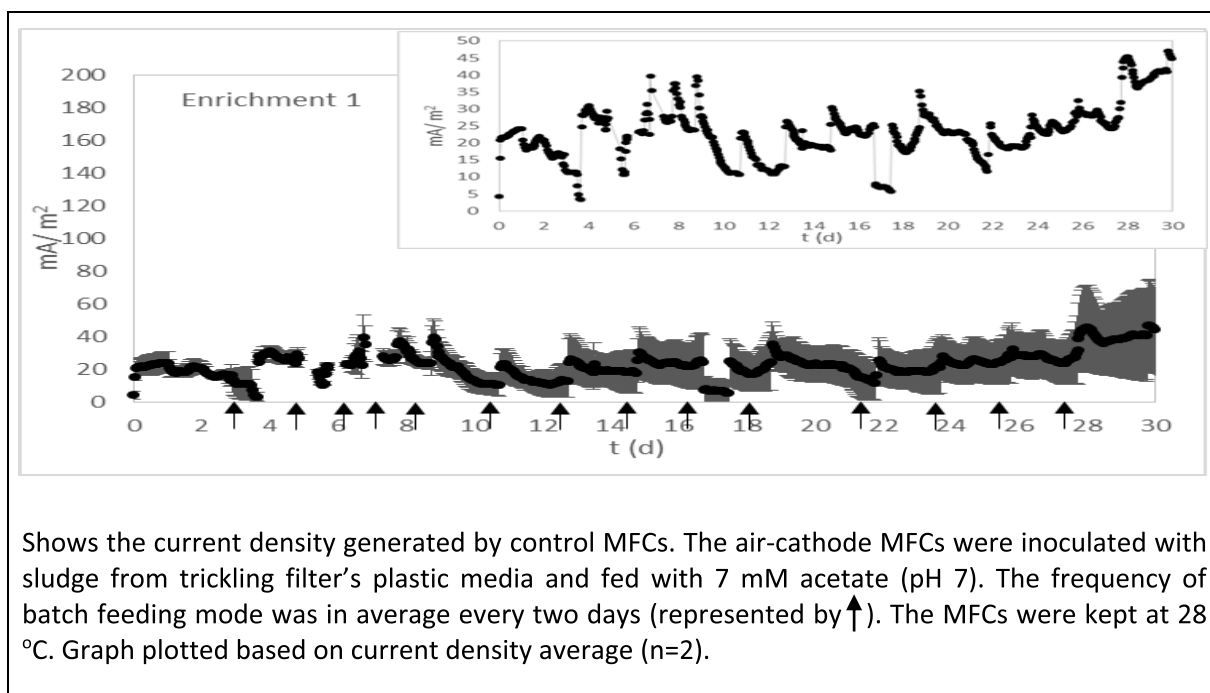
As a way forward, study can be extended to examine long term effects of different oxygen concentrations on the exoelectrogens to identify the maximum tolerable limit of oxygen exposure and understand the effect of MWCNT position. The position of MWCNT play a crucial role in creating a stronger link with the CDH while maintaining strong adhesion within the electrode's matrix. The work can also be extended to reduce the inherent resistance of graphite-epoxy composite electrodes.

APPENDICES

Appendix A

Effect of long time oxygen exposure on power generation of enriched multi-cultured microbial fuel cell (MFC)

A.1 Enrichment of anaerobic MFCs of batch feed modes.

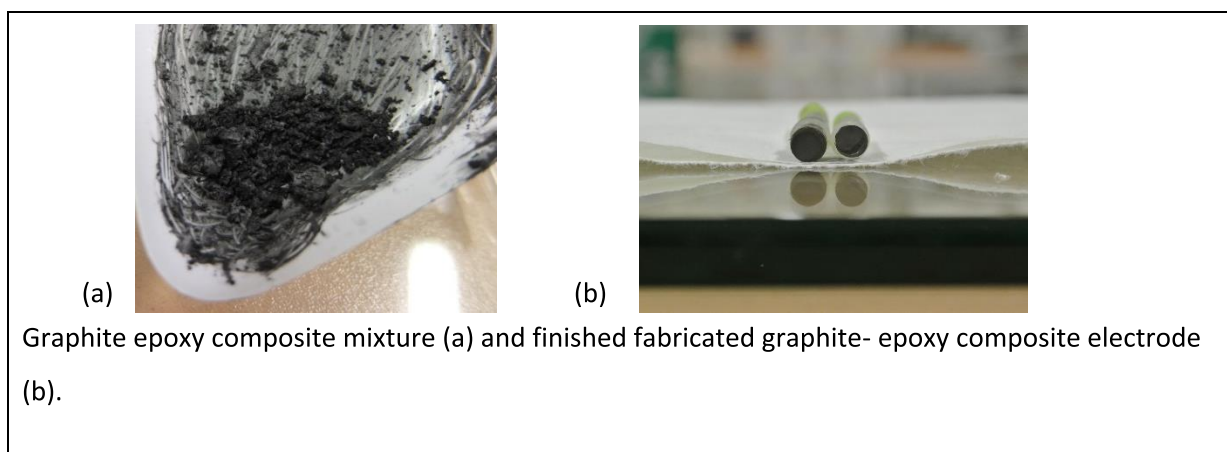


Shows the current density generated by control MFCs. The air-cathode MFCs were inoculated with sludge from trickling filter's plastic media and fed with 7 mM acetate (pH 7). The frequency of batch feeding mode was in average every two days (represented by \uparrow). The MFCs were kept at 28 °C. Graph plotted based on current density average (n=2).

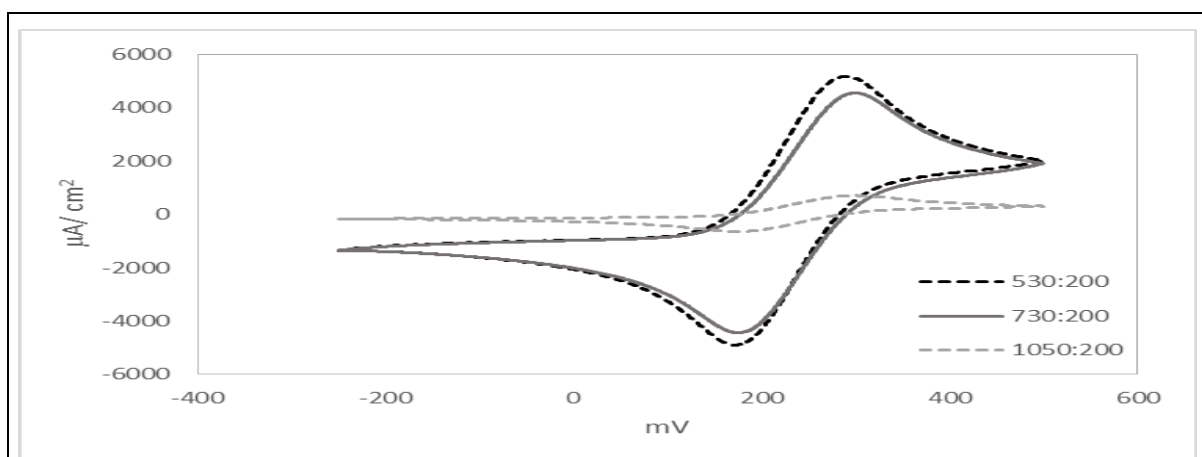
Appendix B

9,10-Anthraquinone-2,6-disulfonic acid disodium salt / epoxy graphite composite for anode in microbial fuel cell (MFC)

B.1 Electrode-epoxy mould from modified polyethylene PCR tube



B.2 Cyclic voltammograms (CV) of unmodified graphite composite anodes at 20 mV/ s.



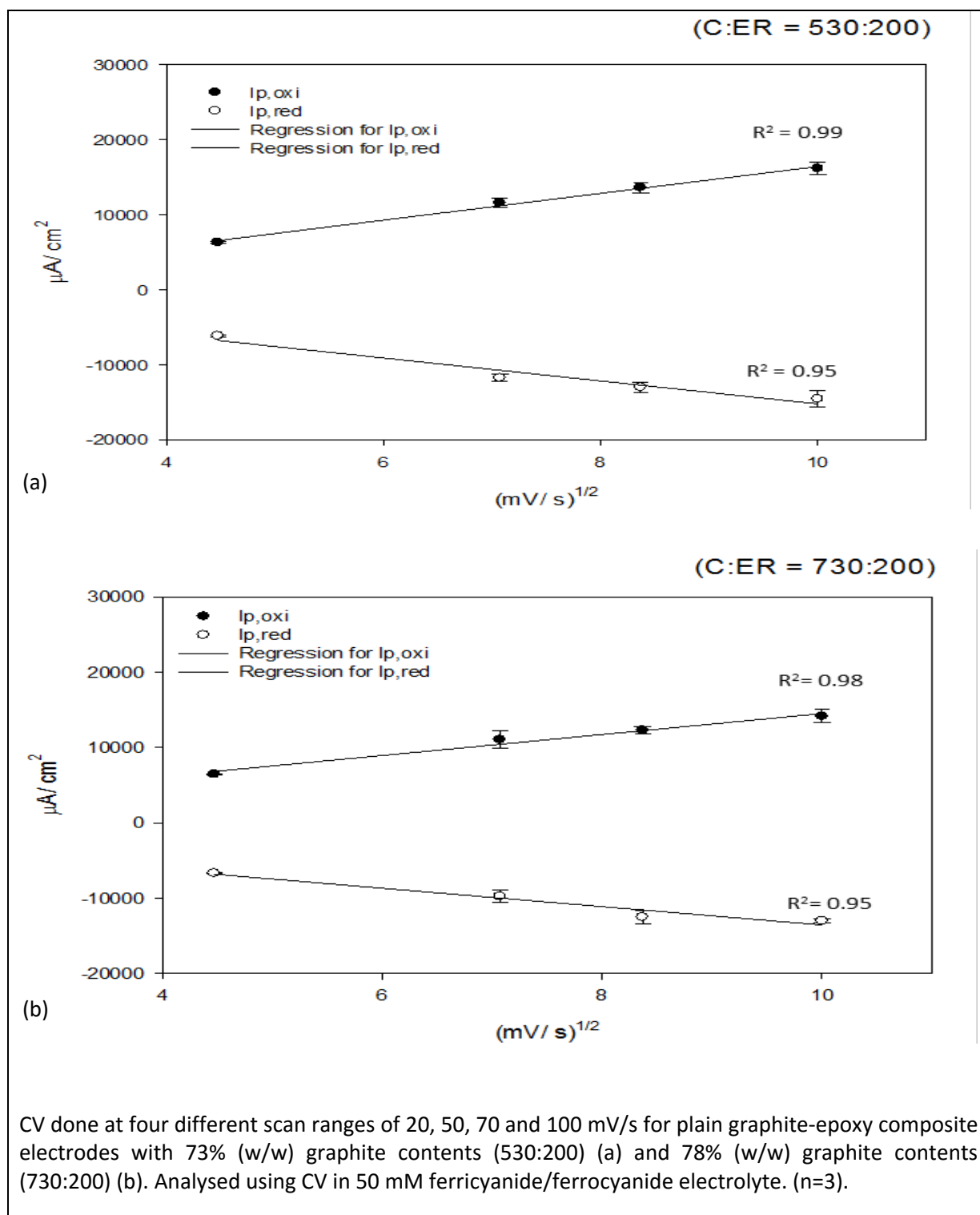
Analysed using CV in 50 mM ferricyanide/ferrocyanide electrolyte. (n=3).

530 mg C: $E_{1/2} = 231$ mV, $I_r/I_f = 0.97$, $\Delta E_p = 116$ mV

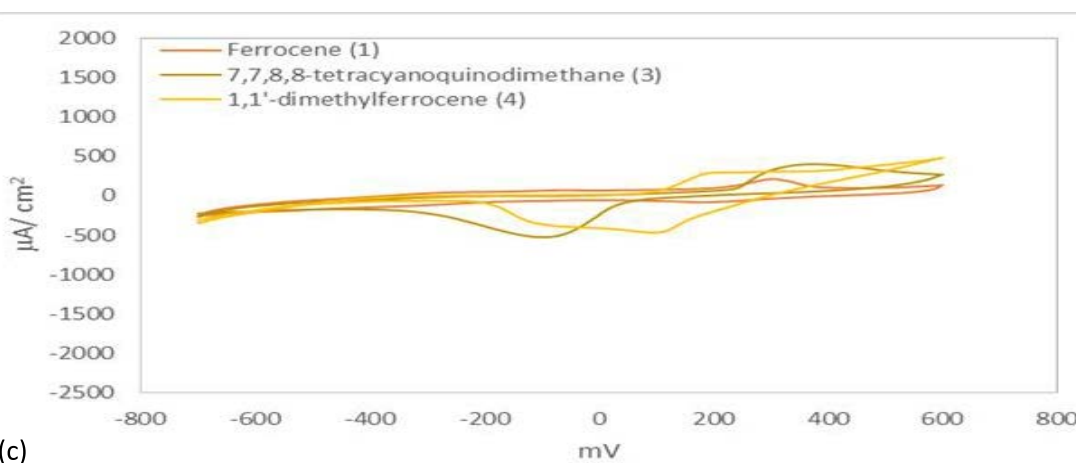
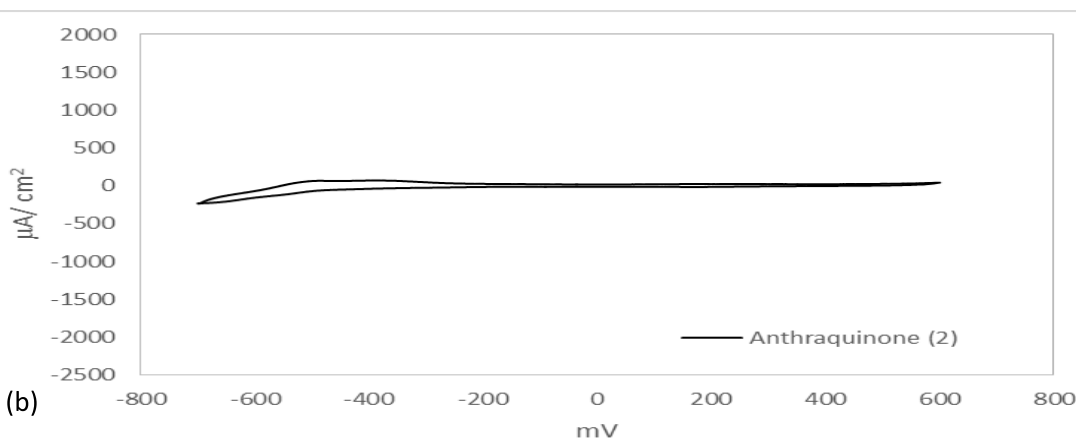
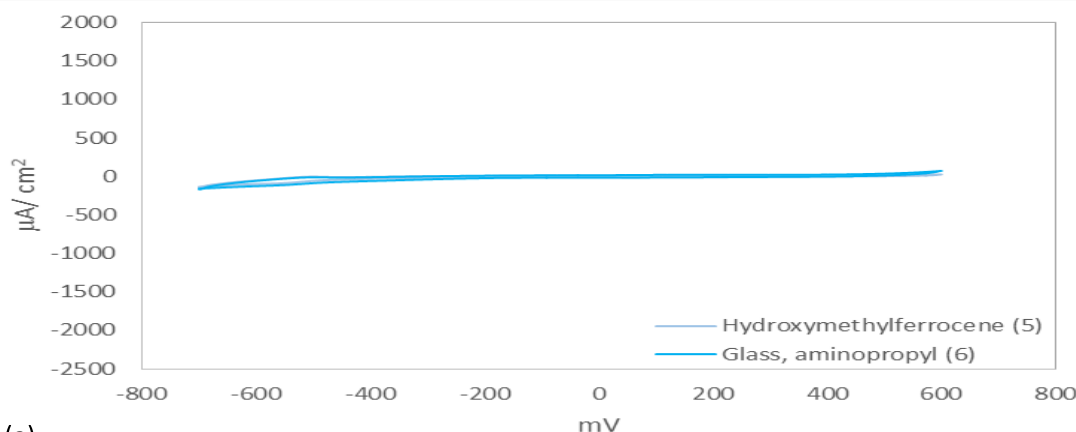
730 mg C: $E_{1/2} = 239$ mV, $I_r/I_f = 0.95$, $\Delta E_p = 127$ mV

1,050 mg C: $E_{1/2} = 237$ mV, $I_r/I_f = 0.95$, $\Delta E_p = 127$ mV

B.3 Cyclic voltammograms (CV) of graphite composite anodes at multiple scan rates.

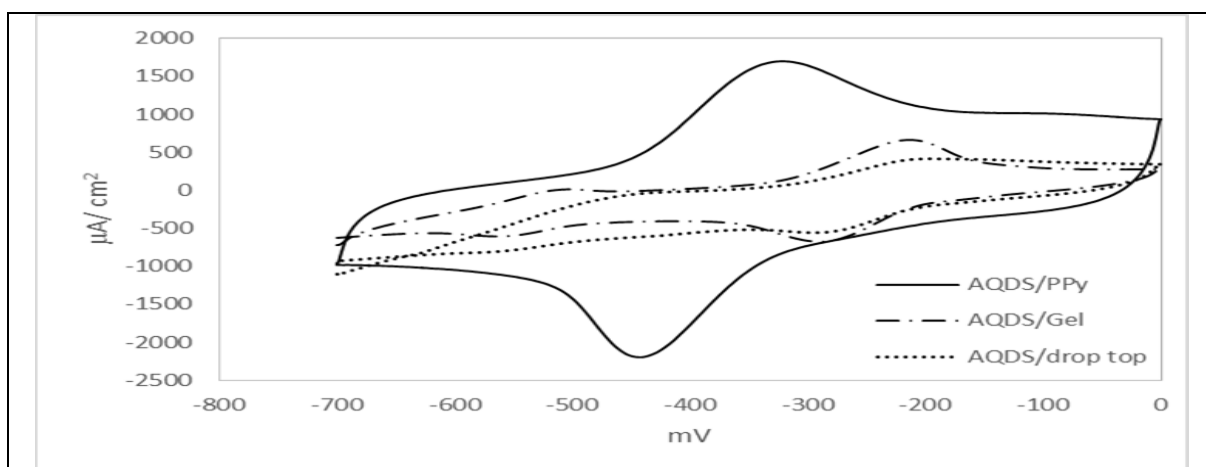


B.4 Cyclic voltammograms (CV) of non-soluble mediators embedded in graphite composite of 730 mg graphite matrix at 20 mV/ s.



(a) and (b) refer to peak waves from active redox couple detected below -400mV (vs. Ag/AgCl) and (c) refers to peak waves from active redox couple detected above -200 mV (vs. Ag/AgCl). Analysed with CV in 0.1 M PB electrolyte at room temperature.

B.5 Cyclic voltammograms (CV) on different method applying 9,10-Anthraquinone-2,6-disulfonic acid disodium salt (AQDS) on surface of MWCNT modified 730 mg graphite composite anodes at scan rate 20 mV/s.



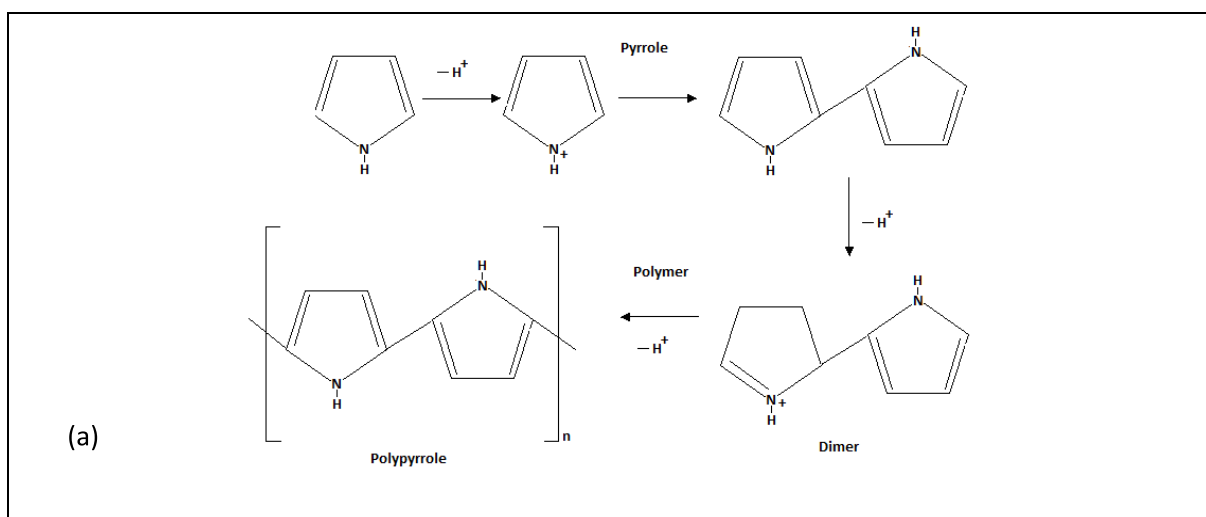
Analysed in 0.1 M PB electrolyte at room temperature.

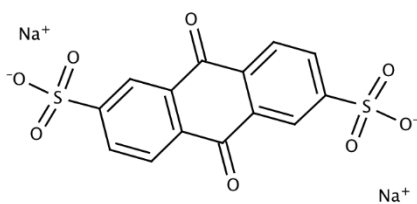
Top: $E_{1/2} = -246$ mV, $\Delta E_p = 97$ mV, ($n=2$)

Gel: $E_{1/2} = -252$ mV, $\Delta E_p = 76$ mV

PPy: $E_{1/2} = -381$ mV, $\Delta E_p = 124$ mV

B.6 Synthesis of polypyrrole (PPy) and molecular structure of 9,10-Anthraquinone-2,6-disulfonic acid disodium salt (AQDS)





(b)

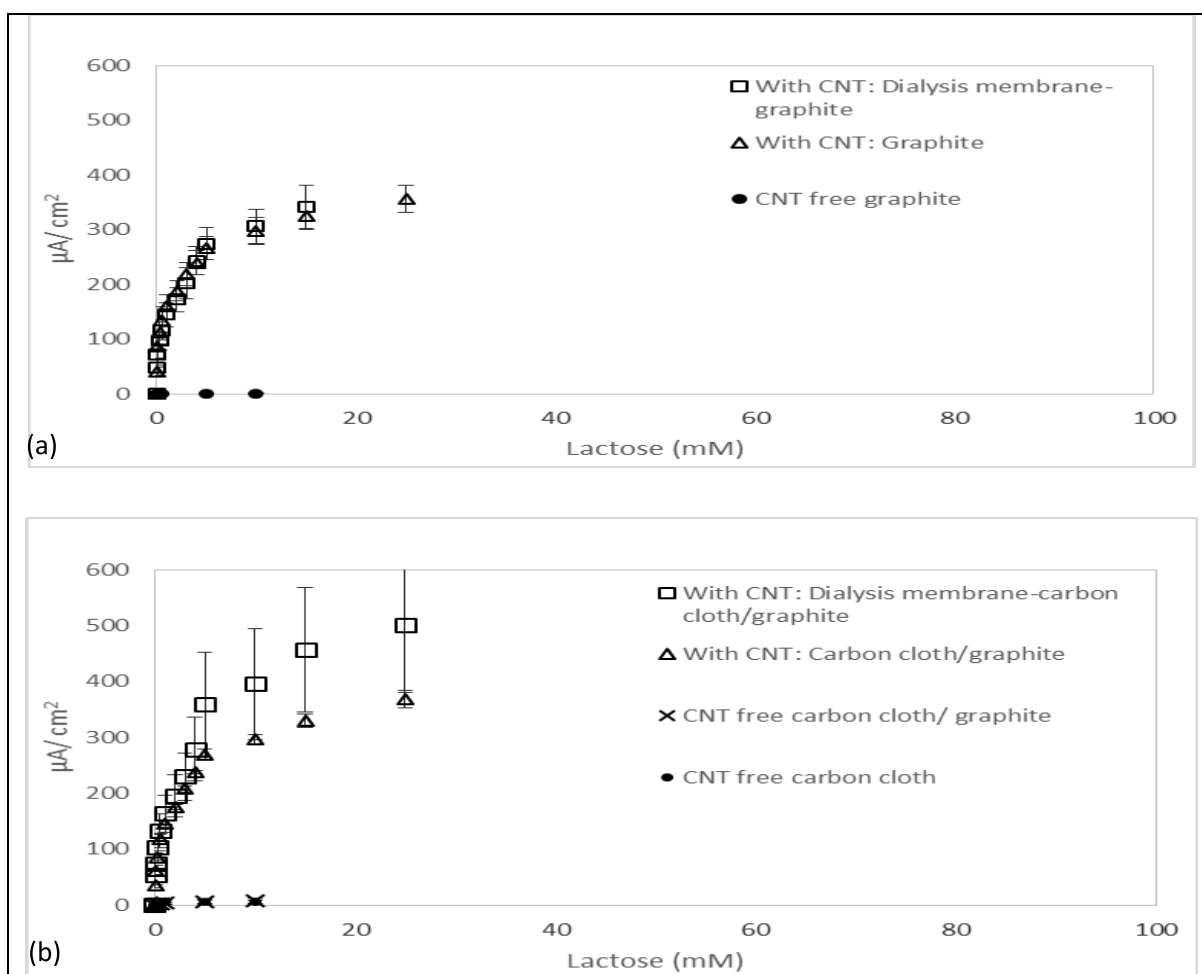
(a) The electropolymerization of pyrrole generally starts with the diffusion of pyrrole monomer to the electrode surface and later with the oxidation reaction of pyrrole at the interface between the electrode and electrolyte solution. Oxidative polymerization of pyrrole proceeds via the formation of dimer molecules during the nucleation process, followed by the oligomerization reaction. Pyrrolium cation radical acts as the main initiator in this process, which leads to the increase of synthesized PPy on the surface of anode. Electrical conductivity of PPy is attributed to the electrons hopping along and across the polymer chains with conjugating bonds (Karami et al. 2013)

(b) 9,10-Anthraquinone-2,6-disulfonic acid disodium salt (AQDS: $C_{14}H_6Na_2O_8S_2$) (Glentham Life Sciences Ltd, 2013)

Appendix C

Cellulose dehydrogenase/ epoxy-graphite composite with aryl diazonium reduction for lactose detection

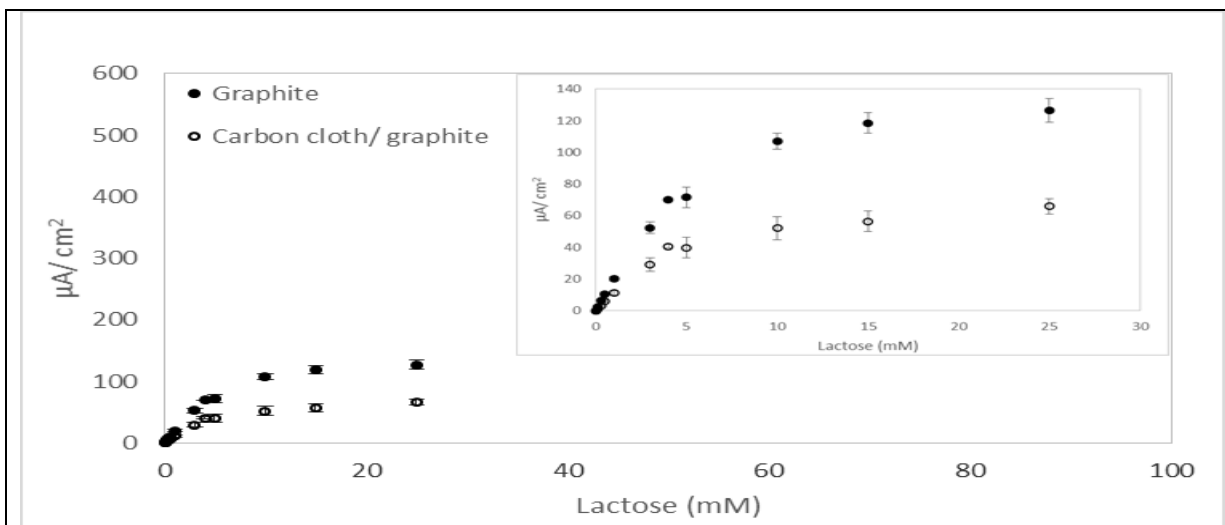
C.1 Lactose detection capability in different lactose concentrations via batch mode for electrodes made from commercial graphite rod materials (a) and combined commercial material electrodes (b).



The anodes were tested using the direct current potential amperometry (DCPA) analysis technique in a three electrode system comprising of the anode as working electrode, a platinum auxiliary for counter electrode and an Ag/AgCl for reference electrode at +100 mV/ s. The electrolyte was 200 mM lactose diluted in 0.1 M citrate buffer to make into different lactose concentrations. Error bars represent standard error of the mean (n=3).

Note: Lactose concentrations analysed were at 0.04 mM, 0.08 mM, 0.3 mM, 0.5 mM, 1 mM, 2 mM, 3 mM, 4 mM, 5 mM, 10 mM, 15 mM and 25 mM.

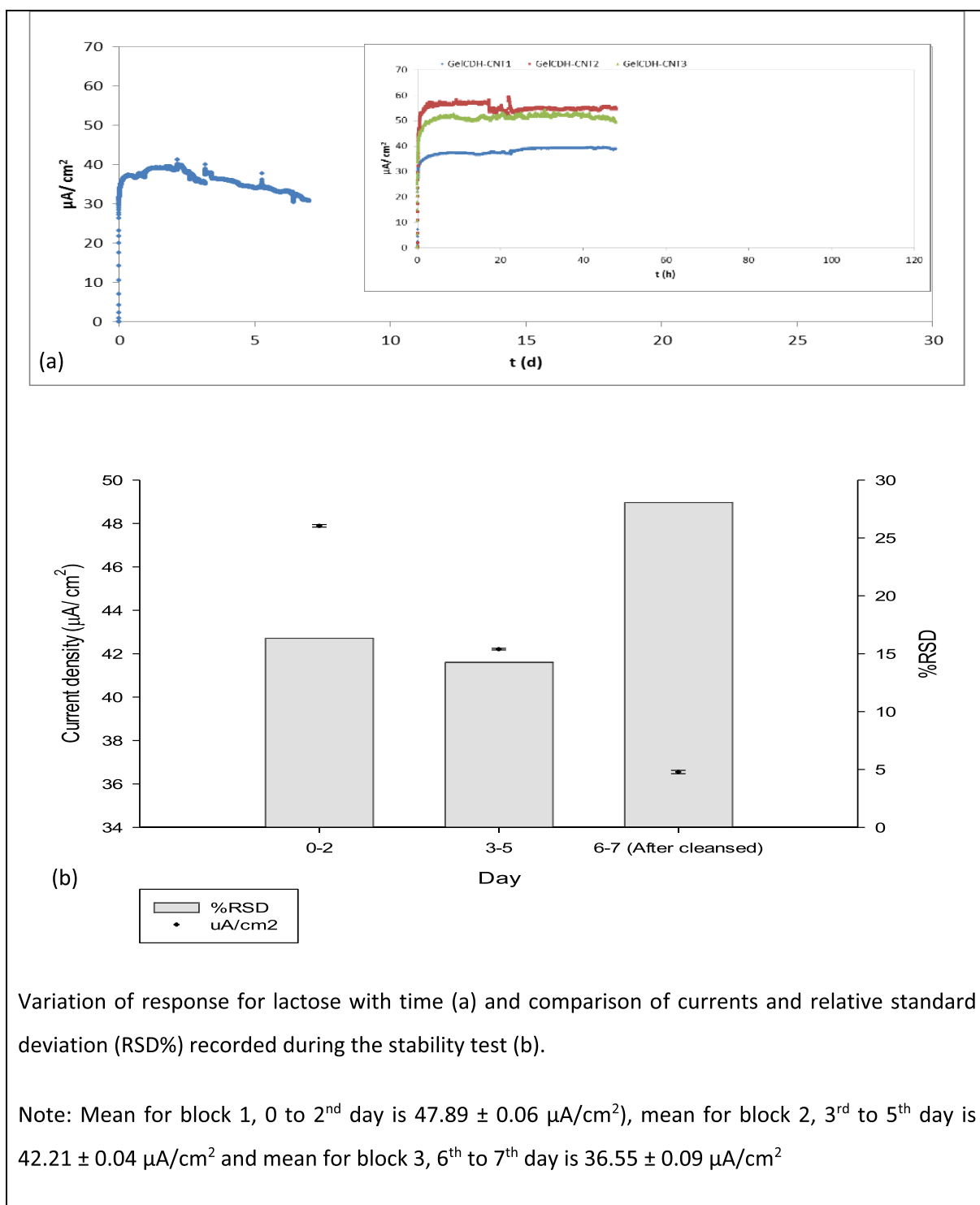
C.2 Lactose detection capability in different lactose concentrations via continuous intermittent flushing for commercial material electrodes with MWCNT added into the system.



The anodes were tested using the direct current potential amperometry (DCPA) analysis technique in drum air-cathode enzymatic fuel cell comprising of the anode as working electrode, air for counter electrode and an Ag/AgCl for reference electrode at +100 mV/ s. The electrolyte was 200 mM lactose diluted in 0.1 citrate buffer to make into different lactose concentrations. Error bars represent standard error of the mean (n=3).

Note: Lactose concentrations analysed were at 0.5 mM, 2 mM, 5 mM, 8 mM, 10 mM, 12 mM and 15 mM.

C.3 Stability test for commercial graphite material anodes modified surface with CDH-gelled at 5 mM lactose.



References

- Abrevaya, X.C., Sacco, N.J., Bonetto, M.C., Hilding-Ohlsson, A., Cortón, E. 2015. Analytical applications of microbial fuel cells. Part I: Biochemical oxygen demand. *Biosensors and Bioelectronics*, **63**, 580-590.
- Aelterman, P., Versichele, M., Boon, N., Verstraete, W. 2008. Loading rate and external resistance control the electricity generation of microbial fuel cells with different three-dimensional anodes. *Bioresource Technology*, **99**, 8895–8902.
- Allaoui, A., Bai, S., Cheng, H.M., Bai, J.B. 2002. Mechanical and electrical properties of a MWNT/epoxy composite. *Composites Science and Technology*, **62**(15), 1993-1998.
- Antonopoulou, G., Stamatelatos, K., Bebelisa, S., Lyberatos, G. 2010. Electricity generation from synthetic substrates and cheese whey using a two chamber microbial fuel cell *Biochemical Engineering Journal* **50**, 10–15
- Atlas, R.M. 2005. *Handbook of microbiological media. Second Edition ed.* Taylor & Francis Group, Florida.
- Balasubramanian, K., Burghard, M. 2006. Biosensors based on carbon nanotubes. *Analytical and Bioanalytical Chemistry*, **385**(3), 452-468.
- Barnett, J.W., Robertson, S.L., Russel, J.M. 1998. Environmental issue in dairy processing. Trans. E. Portfolio. in: *Chemical Processes in New Zealand*, New Zealand Institute of Chemistry. Palmerston North, pp. 1-16.
- BarriÈre, F., Kavanagh, P., Leech, D. 2006. A laccase-glucose oxidase biofuel cell prototype operating in a physiological buffer. *Electrochimica Acta*, **51**(24), 5187-5192.
- Bhatnagar, M.S. 1996. Epoxy resins (Overview). in: *The Polymeric Materials Encyclopedia*, (Ed.) J.C. Salamone, CRC Press. New York, pp. 2233.
- Bitton, G. 2005. Overview of wastewater treatment. 3 ed. in: *Wastewater Microbiology*, Vol. , John Wiley & Sons, Inc. New Jersey, pp. 220 - 222.
- Bond, D.R., Lovley, D.R. 2003. Electricity production by *Geobacter sulfurreducens* attached to electrodes. *Applied and environmental microbiology*, **69**(3), 1584-1555.
- Bond, D.R., Lovley, D.R. 2005. Evidence for involvement of an electron shuttle in electricity generation by *Geothrix fermentans*. *Applied And Environmental Microbiology*, **71**(4), 2186-2189.
- Bullen , R.A., Arnot , T.C., Lakeman, J.B., Walsh, F.C. 2006. Review : Biofuel cells and their development. *Biosensors and Bioelectronics*, **21**, 2015–2045.
- Burkitt, R., Whiffen, T.R., Yu, E.H. 2016. Iron phthalocyanine and MnOx composite catalysts for microbial fuel cell applications. *Applied Catalysis B: Environmental*, **181**, 279-288.
- California Institute of Technology. 2013. Fuel cells for sustainable energy --- science meets social responsibility in: *Solid state ionics and electronics research group*, Vol. 2015, California Institute of Technology. California.
- Canevascini, G., Etienne, K., Meier, H. 1982. A direct enzymatic lactose assay using cellobiose-(lactose-)dehydrogenase from *Sporotrichum thermophile*. *Zeitschrift für Lebensmitteluntersuchung und -Forschung A*, **175**(2), 125-129.
- Chae, K.-J., Choi, M.-J., Lee, J.-W., Kim, K.-Y., Kim, I.S. 2009. Effect of different substrates on the performance, bacterial diversity, and bacterial viability in microbial fuel cells *Bioresource Technology*, **100**, 3518-3525.
- Chan, Y.J., Chong, M.F., Law, C.L., Hassell, D.G. 2009. A review on anaerobic–aerobic treatment of industrial and municipal wastewater *Chemical Engineering Journal*, **155**, 1-18.
- Chang, I.S., Moon, H., Jang, J.K., Kim, B.H. 2005. Improvement of a microbial fuel cell performance as a BOD sensor using respiratory inhibitors. *Biosensors and Bioelectronics*, **20**, 1856-1859.
- Chang, R. 1994. Graphite: Covalent crystals. 5th-International Edition ed. in: *Chemistry*, McGraw-Hill. New York, pp. 447.
- Chaplin, M. 2004. What are biosensors?, Faculty of Engineering, Science and the Build Environment. London.

- Cheng, S., Liu, H., Logan, B.E. 2006. Increased power generation in a continuous flow MFC with advective flow through the porous anode and reduced electrode spacing. *Environmental Science & Technology*, **40**(7), 2426-2432.
- Chollangi, A., Hossain, M.M. 2007. Separation of proteins and lactose from dairy wastewater. *Chemical Engineering and Processing*, **46**(5), 398-404.
- Commault, A.S., Lear, G., Weld, R.J. 2015. Maintenance of Geobacter-dominated biofilms in microbial fuel cells treating synthetic wastewater. *Bioelectrochemistry*, **106**(0), 150-158.
- Compton, R., McAuley, C.B.-., Dickinson, E. 2012. Cyclic voltammetry: Coupled homogenous kinetics and adsorption. in: *Understanding voltammetry: problems and solutions*, Imperial College Press. London, pp. 140-141.
- Conzuelo, F., Gamella, M., Campuzano, S., Ruiz, M.A., Reviejo, A.J., Pingarro, J.M. 2010. An integrated amperometric biosensor for the determination of lactose in milk and dairy products. *Journal of Agricultural and Food Chemistry*, **58**(12), 7141-7148.
- Corb, I., Manea, F., Radovan, C., Pop, A., Burtica, G., Malchev, P., Picken, S., Schoonman, J. 2007. Carbon-based composite electrodes: Preparation, characterization and application in electroanalysis. *Sensors*, **7**, 2626-2635.
- Cunningham, A.B., Lennox, J.E., Ross, R.J. 2001-2008. The Biofilms Hypertextbook: Intermediate level. in: *Chapter 2: Biofilm formation and growth*, Vol. 2014, Montana State University. Montana, pp. Section 3: Biofilm development.
- Cutright, T.J. 2002. Biotechnology principles.
- Daniel, D.K., Mankidy, B.D., Ambarish, K., Manogari, R. 2009. Construction and operation of a microbial fuel cell for electricity generation from wastewater. *International Journal of Hydrogen Energy*, **34**, 7555-7560.
- de Souza, R.R., Bergamasco, R.n., da Costa, S.C.u., Feng, X., Faria, S.H.B., Gimenes, M.L. 2010. Recovery and purification of lactose from whey. *Chemical Engineering and Processing: Process Intensification*, **49**(11), 1137-1143.
- Dirckx, P. 1997. Biofilm structure with labels, (Ed.) Biofilm.jpg, Center for Biofilm Engineering. Montana.
- Du, L., Jana, S.C. 2007. Highly conductive epoxy/graphite composites for bipolar plates in proton exchange membrane fuel cells. *Journal of Power Sources*, **172**(2), 734-741.
- Du, Z., Li, H., Gu, T. 2007. A state of the art review on microbial fuel cells: A promising technology for wastewater treatment and bioenergy. *Biotechnology Advances*, **25**, 464-482.
- Emilygardel. 2010. Tapping into microbially produced electricity. in: *Masticated Science the latest science, in digestible pieces*, Vol. 2015.
- Eriksson, J. 2010. Renewable Energy v.s Fossil Fuel, Vol. 2011, Renewable power news.
- Eshkenazi, I., Maltz, E., Zion, B., Rishpon, J. 2000. A three-cascaded-enzymes biosensor to determine lactose concentration in raw milk. *Journal of Dairy Science*, **83**(9), 1939-1945.
- Farlex, I. 2012. Control Process. in: *The Free Dictionary*, Farlex Incorporated.
- Feng, C., Ma, L., Li, F., Mai, H., Lang, X., Fan, S. 2010a. A polypyrrole/anthraquinone-2,6-disulphonic disodium salt (PPy/AQDS)-modified anode to improve performance of microbial fuel cells *Biosensors and Bioelectronics*, **25**, 1516-1520.
- Feng, C., Wan, Q., Lv, Z., Yue, X., Chen, Y., Wei, C. 2011. One-step fabrication of membraneless microbial fuel cell cathode by electropolymerization of polypyrrole onto stainless steel mesh. *Biosensors and Bioelectronics*, **26**(9), 3953-3957.
- Feng, Y., Yang, Q., Wang, X., Logan, B.E. 2010b. Treatment of carbon fiber brush anodes for improving power generation in air-cathode microbial fuel cells. *Journal of Power Sources*, **195**(7), 1841-1844.
- Ferguson, G., Dakers, A., Gunn, I. 2003. Sustainable wastewater management: A handbook for smaller communities, (Ed.) T.M.f.t. Environment, Ministry for the Environment Wellington, pp. 1-200.
- Fox, P.F. 2009. Lactose: Chemistry and properties. 3rd ed. in: *Advanced Dairy Chemistry Volume 3: Lactose, Water, Salts and Minor Constituents*, (Eds.) P.L.H. McSweeney, P.F. Fox, Springer. Cork.
- Franks, A.E., Nevin, K.P. 2010. Review: Microbial fuel cells, a current review. *Energies*, **3**, 899-919.

- Ghasemi, M., Ismail, M., Kamarudin, S.K., Saeedfar, K., Daud, W.R.W., Hassan, S.H.A., Heng, L.Y., Alam, J., Oh, S.-E. 2013. Carbon nanotube as an alternative cathode support and catalyst for microbial fuel cells. *Applied Energy*, **102**, 1050–1056.
- Glithero, N., Clark, C., Gorton, L., Schuhmann, W., Pasco, N. 2013. At-line measurement of lactose in dairy-processing plants. *Analytical and Bioanalytical Chemistry*, **405**(11), 3791-3799.
- Göktug, T., Sezgintürk, M.K., Dinçkaya, E. 2005. Glucose oxidase-[beta]-galactosidase hybrid biosensor based on glassy carbon electrode modified with mercury for lactose determination. *Analytica Chimica Acta*, **551**(1-2), 51-56.
- Golnik, A. 2003. Energy density of gasoline. in: *The physics factbook*, (Ed.) G. Elert, Vol. 2015. hypertextbook.com.
- Gong, Z.Q., Sujari, A.N.A., Ab Ghani, S. 2012. Electrochemical fabrication, characterization and application of carboxylic multi-walled carbon nanotube modified composite pencil graphite electrodes. *Electrochimica Acta*, **65**(0), 257-265.
- Gooding, J.J. 2005. Nanostructuring electrodes with carbon nanotubes: A review on electrochemistry and applications for sensing. *Electrochimica Acta*, **50**(15), 3049-3060.
- Gülce, H., Gülce, A., Yildiz, A. 2002. A novel two-enzyme amperometric electrode for lactose determination. *Analytical Sciences*, **18**(2), 147.
- Harreither, D.W. 2010. Cellobiose Dehydrogenase – an electrifying enzyme: Biochemical and electrochemical characterisation of cellobiose dehydrogenase for its application in biosensors and biofuel cells. in: *Department for Food Science and Technology, Division of Food Biotechnology*, University of Natural Resources and Applied Life Sciences. Vienna, pp. 269.
- Harreither, W., Coman, V., Ludwig, R., Haltrich, D., Gorton, L. 2007. Investigation of graphite electrodes modified with cellobiose dehydrogenase from the ascomycete *Myriococcum thermophilum*. *Electroanalysis*, **19**(2-3), 172-180.
- Haslett, N.D. 2012. Development of a eukaryotic microbial fuel cell using *Arxula adenivorans*. in: *Department of Agricultural Sciences*, Vol. Doctor of Philosophy, Lincoln University, pp. 245.
- Haslett, N.D., Rawson, F.J., Barri´re, F.d.r., Kunze, G., Pasco, N., Gooneratne, R., Baronian, K.H.R. 2011. Characterisation of yeast microbial fuel cell with the yeast *Arxula adenivorans* as the biocatalyst. *Biosensors and Bioelectronics*, **26**(9), 3742-3747.
- Hassanzadeh, H., Mansouri, S.H. 2005. Efficiency of ideal fuel cell and Carnot cycle from a fundamental perspective. *Proceedings of the Institution of Mechanical Engineers*, **219**(A4), 245.
- Henriksson, G., Johansson, G., Pettersson, G.r. 2000. A critical review of cellobiose dehydrogenases. *Journal of Biotechnology*, **78**(2), 93-113.
- Hong, S.W., Choi, Y.S., Chung, T.H., Song, J.H., Kim, H.S. 2009. Assessment of sediment remediation potential using microbial fuel cell technology. *World Academy of Science, Engineering and Technology*, **54**, 683-689.
- Huang, J., Zhu, N., Yang, T., Zhang, T., Wu, P., Dang, Z. 2015. Nickel oxide and carbon nanotube composite (NiO/CNT) as a novel cathode non-precious metal catalyst in microbial fuel cells. *Biosensors and Bioelectronics*, **72**, 332-339.
- Hutchinson, A.J., Tokash, J.C., Logan, B.E. 2011. Analysis of carbon fiber brush loading in anodes on startup and performance of microbial fuel cells. *Journal of Power Sources*, **196**(22), 9213-9219.
- Ieropoulos, I.A., Greenman, J., Melhuish, C., Hart, J. 2005. Comparative study of three types of microbial fuel cell. *Enzyme and Microbial Technology*, **37**, 238-245.
- Janni, K.A., Schmidt, D.R., Christopherson, S.H. 2007. Milk house wastewater characteristics. in: *Extension*, Vol. 1206, University of Minnesota. Minnesota, pp. 1-4.
- Jenkins, D.M., Delwiche, M.J. 2003. Adaptation of a manometric biosensor to measure glucose and lactose. *Biosensors and Bioelectronics*, **18**(1), 101-107.
- Jiang, L., Liu, H., Liu, J., Yang, Q., Cai, X. 2008. A sensitive biosensor based on Osmium-complex mediator and glucose oxidase for low concentration glucose determination. *Journal of Electroanalytical Chemistry*, **619-620**, 11-16.

- Jung, S., Regan, J.M. 2007. Comparison of anode bacterial communities and performance in microbial fuel cells with different electron donors. *Applied Microbiology and Biotechnology*, **77**, 393-402.
- Karami, H., Nezhad, A.R. 2013. Investigation of pulse-electropolymerization of conductive polypyrrole nanostructures. *International Journal of Electrochemical Science*, **8**, 8905 - 8921.
- Karayannidou, E.G., Achilias, D.S., Sideridou, I.D. 2006. Cure kinetics of epoxy-amine resins used in the restoration of works of art from glass or ceramic. *European Polymer Journal*, 3311-3323.
- Karthikeyan, R., Krishnaraj, N., Selvam, A., Wong, J.W.-C., Lee, P.K.H., Leung, M.K.H., Berchmans, S. 2016. Effect of composites based nickel foam anode in microbial fuel cell using *Acetobacter acetii* and *Gluconobacter roseus* as biocatalysts. *Bioresource Technology*.
- Kellam, S. 1998. The manufacture of lactose. in: *Chemical Processes in New Zealand*, (Ed.) H. Wansbrough, The Lactose Company of New Zealand Ltd. Edendale, Southland.
- Khan, M.R., Chan, K.M., Ong, H.R., Cheng, C.K., Rahman, W. 2015. Nanostructured Pt/MnO₂ catalysts and their performance for oxygen reduction reaction in air cathode microbial fuel cell. *International Journal of Electrical, Computer, Electronics and Communication Engineering*, **9**(3), 295-301.
- Kiely, P.D., Cusick, R., Call, D.F., Selembo, P.A., Regan, J.M., Logan, B.E. 2010. Anode microbial communities produced by changing from microbial fuel cell to microbial electrolysis cell operation using two different wastewaters. *Bioresource Technology*.
- Kim, B., Ikeda, T., Park, H., Kim, H., Hyun, M., Kano, K., Takagi, K., Tatsumi, H. 1999. Electrochemical activity of an Fe(III)-reducing bacterium, *Shewanella putrefaciens* IR-1, in the presence of alternative electron acceptors. *Biotechnology Techniques*, **13**(7), 475-478.
- Kim, B.H., Park, H.S., Kim, H.J., Kim, G.T., Chang, I.S., Lee, J., Phung, N.T. 2004. Enrichment of microbial community generating electricity using a fuel-cell-type electrochemical cell. *Appl Microbiol Biotechnol*, **63**, 672-681.
- Kim, H.J., Park, H.S., Hyun, M.S., Chang, I.S., Kim, M., Kim, B.H. 2002. A mediator-less microbial fuel cell using a metal reducing bacterium, *Shewanella putrefaciens*. *Enzyme and Microbial Technology*, **30**, 145-152.
- Kim, J.R., Min, B., Logan, B.E. 2005. Evaluation of procedures to acclimate a microbial fuel cell for electricity production. *Applied Microbial Biotechnology*, **68**, 23-30.
- Kirgoz, U.A., Odaci, D., Timur, S., Merkoci, A., Pazarlioglu, N., Telefoncu, A., Alegret, S. 2006. Graphite epoxy composite electrodes modified with bacterial cells. *Bioelectrochemistry*, **69**(1), 128-131.
- Kumar, A.S., Swetha, P. 2011. Simple adsorption of anthraquinone on carbon nanotube modified electrode and its efficient electrochemical behaviors. *Colloids and Surfaces A: Physicochemical and Engineering Aspects*, **384**(1-3), 597-604.
- Kumar, G.G., Sarathi, V.G.S., Nahm, K.S. 2013. Recent advances and challenges in the anode architecture and their modifications for the applications of microbial fuel cells. *Biosensors and Bioelectronics*, **43**(0), 461-475.
- Lanas, V., Logan, B.E. 2013. Evaluation of multi-brush anode systems in microbial fuel cells. *Bioresource Technology*, **148**(0), 379-385.
- Lanthier, M., Gregory, K.B., Lovley, D.R. 2008. Growth with high planktonic biomass in *Shewanella oneidensis* fuel cells. *FEMS Microbiol Lett*, **278**, 29-35.
- Larsson, T., Elmgren, M., Lindquist, S.-E., Tessema, M., Gorton, L., Henriksson, G. 1996. Electron transfer between cellobiose dehydrogenase and graphite electrodes. *Analytica Chimica Acta*, **331**(3), 207-215.
- Larsson, T., Lindgren, A., Ruzgas, T., Lindquist, S.E., Gorton, L. 2000. Bioelectrochemical characterisation of cellobiose dehydrogenase modified graphite electrodes: ionic strength and pH dependences. *Journal of Electroanalytical Chemistry*, **482**(1), 1-10.
- Lewis, R. 2008. Fuel cell or not fuel cell? That is the question., Vol. 2011, H₂O Energy Technologies, Inc.

- Li, B., Zhou, J., Zhou, X., Wang, X., Li, B., Santoro, C., Grattieri, M., Babanova, S., Artyushkova, K., Atanassov, P., Schuler, A.J. 2014. Surface Modification of Microbial Fuel Cells Anodes: Approaches to Practical Design. *Electrochimica Acta*, **134**(0), 116-126.
- Li, S.-L., Freguia, S., Liu, S.-M., Cheng, S.-S., Tsujimura, S., Shiraib, O., Kanob, K. 2010. Effects of oxygen on *Shewanella decolorationis* NTOU1 electron transfer to carbon-felt electrodes. *Biosensors and Bioelectronics*, **25**, 2651–2656
- Li, X.M., Cheng, K.Y., Selvam, A., Wong, J.W.C. 2013. Bioelectricity production from acidic food waste leachate using microbial fuel cells: Effect of microbial inocula. *Process Biochemistry*, **48**(2), 283-288.
- Liu, H., Cheng, S., Logan, B.E. 2005. Production of electricity from acetate or butyrate using a single-chamber microbial fuel cell. *Environmental Science & Technology*, **39**(2), 658-662.
- Liu, Y., Jin, X.-J., Dionysiou, D.D., Liu, H., Huang, Y.-M. 2015. Homogeneous deposition-assisted synthesis of iron, nitrogen composites on graphene as highly efficient non-precious metal electrocatalysts for microbial fuel cell power generation. *Journal of Power Sources*, **278**, 773-781.
- Llopis, X., Merkoci, A., del Valle, M., Alegret, S. 2005. Integration of a glucose biosensor based on an epoxy-graphite-TTF.TCNQ-GOD biocomposite into a FIA system. *Sensors and Actuators B: Chemical*, **107**(2), 742-748.
- Logan, B.E. 2004. Extracting hydrogen and electricity from renewable resources. *Environmental Science & Technology*, 161-167.
- Logan, B.E. 2008. Mechanism of electron transfer. in: *Microbial Fuel Cell*, John Wiley & Sons, Inc. New Jersey, pp. 13.
- Logan, B.E., Hamelers, B., Rozendal, R., Schroder, U., Keller, J., Freguia, S., Aelterman, P., Verstraete, W., Rabaey, K. 2006. Microbial fuel cells: Methodology and technology. *Environmental Science & Technology*, **40**(17), 5181-5192.
- Logan, B.E., Regan, J.M. 2006. Electricity-producing bacterial communities in microbial fuel cells. *TRENDS in Microbiology*, **14**(12), 512-518.
- Logoglu, E., Sungur, S., Yildiz, Y. 2006. Development of lactose biosensor based on beta-galactosidase and glucose oxidase immobilized into gelatin. *Journal of Macromolecular Science-Pure and Applied Chemistry*, **A43**(3), 525-533.
- Lorenzo, D.M., Curtisa, P.T., Heada, M.I., Scott, K. 2009. A single-chamber microbial fuel cell as a biosensor for wastewaters. *Water Research*, **43**, 3145–3154.
- Lu, N., Zhou, S.-g., Zhuang, L., Zhang, J.-t., Ni, J.-r. 2009. Electricity generation from starch processing wastewater using microbial fuel cell technology. *Biochemical Engineering Journal*, **43**, 246-251.
- Ludwig, R., Harreither, W., Tasca, F., Gorton, L. 2010. Cellobiose dehydrogenase: A versatile catalyst for electrochemical applications. *Chemphyschem*, **11**(13), 2674-2697.
- Luo, Y., Zhang, F., Wei, B., Liu, G., Zhang, R., Logan, B.E. 2011. Power generation using carbon mesh cathodes with different diffusion layers in microbial fuel cells. *Journal of Power Sources*, **196**(22), 9317-9321.
- Ma, M., You, S., Gong, X., Dai, Y., Zou, J., Fu, H. 2015. Silver/iron oxide/graphitic carbon composites as bacteriostatic catalysts for enhancing oxygen reduction in microbial fuel cells. *Journal of Power Sources*, **283**, 74-83.
- Ma, P.-C., Siddiqui, N.A., Marom, G., Kim, J.-K. 2010. Dispersion and functionalization of carbon nanotubes for polymer-based nanocomposites: A review. *Composites Part A: Applied Science and Manufacturing*, **41**(10), 1345-1367.
- Mahouche-Chergui, S., Gam-Derouich, S., Mangeney, C., Chehimi, M.M. 2011. Aryl diazonium salts: a new class of coupling agents for bonding polymers, biomacromolecules and nanoparticles to surfaces. *Chemical Society Reviews*, **40**(7), 4143-4166.
- Mailley, P., Cummings, E.A., Mailley, S.C., Eggins, B.R., McAdams, E., Cosnier, S. 2003. Composite carbon paste biosensor for phenolic derivatives based on in situ electrogenerated polypyrrole binder. *Analytical Chemistry*, **75**(20), 5422-5428.
- Markillie, R. 2010. High power density fuel cells. in: *News*, Vol. 2015, ITM Power. ITM Power.

- Martin, C.A., Sandler, J.K.W., Shaffer, M.S.P., Schwarz, M.K., Bauhofer, W., Schulte, K., Windle, A.H. 2004. Formation of percolating networks in multi-wall carbon-nanotube-epoxy composites. *Composites Science and Technology*, **64**(15), 2309-2316.
- Martin, C.A., Sandler, J.K.W., Windle, A.H., Schwarz, M.K., Bauhofer, W., Schulte, K., Shaffer, M.S.P. 2005. Electric field-induced aligned multi-wall carbon nanotube networks in epoxy composites. *Polymer*, **46**(3), 877-886.
- Midlands Technical College. 2012. Microbial metabolism, (Ed.) C. catabolism, Midlands Technical College. Columbia.
- Min, B., Kim, J., Oh, S., Regan, J.M., Logan, B.E. 2005. Electricity generation from swine wastewater using microbial fuel cells. *Water Research*, **39**, 4961-4968.
- Moon, H., Chang, I.S., Kim, B.H. 2006. Continuous electricity production from artificial wastewater using a mediator-less microbial fuel cell. *Bioresource Technology*, **97**, 621-627.
- Muti, M., Kuralay, F., Erdem, A. 2012. Single-walled carbon nanotubes-polymer modified graphite electrodes for DNA hybridization. *Colloids and Surfaces B: Biointerfaces*, **91**(0), 77-83.
- Nag, A. 2008. *Biofuels refining and performance*. McGrawHill, New York.
- Najafpour, G.D., Hashemiyeh, B.A., Asadi, M., Ghasemi, M.B. 2008. Biological treatment of dairy wastewater in an upflow anaerobic sludge-fixed film bioreactor. *American-Eurasian J. Agric. & Environ. Sci*, **4**(2), 251-257.
- Nandy, A., Kumar, V., Mondal, S., Dutta, K., Salah, M., Kundu, P.P. 2015. Performance evaluation of microbial fuel cells: effect of varying electrode configuration and presence of a membrane electrode assembly. *New Biotechnology*, **32**(2), 272-281.
- O'Hare, D., Macpherson, J.V., Willows, A. 2002. On the microelectrode behaviour of graphite, epoxy composite electrodes. *Electrochemistry Communications*, **4**(3), 245-250.
- Ocaña, C., Arcay, E., del Valle, M. 2014. Label-free impedimetric aptasensor based on epoxy-graphite electrode for the recognition of cytochrome c. *Sensors and Actuators B: Chemical*, **191**(0), 860-865.
- Osman, M.H., Shah, A.A., Walsh, F.C. 2011. Recent progress and continuing challenges in bio-fuel cells. Part I: Enzymatic cells. *Biosensors and Bioelectronics*, **26**(7), 3087-3102.
- Osman, M.H., Shah, A.A., Walsh, F.C. 2010. Recent progress and continuing challenges in bio-fuel cells. Part II: Microbial. *Biosensors and Bioelectronics*, **26**(3), 953-963.
- Park, D.H., Zeikus, J.G. 2002. Improved fuel cell and electrode designs for producing electricity from microbial degradation. *Biotechnology and Bioengineering*, **81**(3), 348-355.
- Pastorella, G., Gazzola, G., Guadarrama, S., Marsili, E. 2012. Biofilms: Applications in bioremediation. in: *Microbial Biofilms: Current research and applications*, (Eds.) G. Lear, G.D. Lewis, Horizon Scientific Press. UK, pp. 73-98.
- Peng, L., You, S.-J., Wang, J.-Y. 2010. Carbon nanotubes as electrode modifier promoting direct electron transfer from *Shewanella oneidensis*. *Biosensors and Bioelectronics*, **25**, 1248-1251.
- Picot, M., Lapinonniere, L., Rothballer, M., Barriere, F. 2011. Graphite anode surface modification with controlled reduction of specific aryl diazonium salts for improved microbial fuel cells power output. *Biosens Bioelectron*, **28**(1), 181-8.
- Portland Community College. 2000. Lecture 3: Microbial metabolism. in: *Portland Community College*, (Ed.) T.e.t. chain, Portland Community College. Portland.
- Prasad, D., Arun, S., Murugesan, M., Padmanaban, S., Satyanarayanan, R.S., Berchmans, S., Yegnaraman, V. 2007. Direct electron transfer with yeast cells and construction of a mediatorless microbial fuel cell. *Biosensors and Bioelectronics*, **22**.
- Pumera, M., Merkoci, A., Alegret, S. 2006. Carbon nanotube-epoxy composites for electrochemical sensing. *Sensors and Actuators B: Chemical*, **113**(2), 617-622.
- Rabaey, K., Boon, N., Siciliano, S.D., Verhaege, M., Verstraete, W. 2004. Biofuel cells select for microbial consortia that self-mediate electron transfer. *Applied and environmental microbiology*, **70**(9), 5373-5382.
- Rader, G.K., Logan, B.E. 2010. Multi-electrode continuous flow microbial electrolysis cell for biogas production from acetate. *International Journal of Hydrogen Energy*, **35**(17), 8848-8854.

- Rahimnejad, M., Ghoreyshi, A.A., Najafpour, G., Jafary, T. 2011a. Power generation from organic substrate in batch and continuous flow microbial fuel cell operations. *Applied Energy*, **88**(11), 3999-4004.
- Rahimnejad, M., Najafpour, G.D., Ghoreyshi, A.A., Shakeri, M., Zare, H. 2011b. Methylene blue as electron promoters in microbial fuel cell. *International Journal of Hydrogen Energy*, **36**(20), 13335-13341.
- Rajendran, V., Irudayaraj, J. 2002. Detection of glucose, galactose, and lactose in milk with a microdialysis-coupled flow injection amperometric sensor. *Journal of Dairy Science*, **85**(6), 1357-1361.
- Ramakrishnappa, T., Pandurangappa, M., Nagaraju, D.H. 2011. Anthraquinone functionalized carbon composite electrode: Application to ammonia sensing. *Sensors and Actuators B: Chemical*, **155**(2), 626-631.
- Rawson, F.J., Gross, A.J., Garrett, D.J., Downard, A.J., Baronian, K.H.R. 2012. Mediated electrochemical detection of electron transfer from the outer surface of the cell wall of *Saccharomyces cerevisiae*. *Electrochemistry Communications*, **15**(1), 85-87.
- Reiter, S., Habermuller, K., Schuhmann, W. 2001. A reagentless glucose biosensor based on glucose oxidase entrapped into osmium-complex modified polypyrrole films. *Sensors and Actuators B*, **79**, 150-156.
- Rich, L.G. 2003. Effluent BOD5, a misleading parameter for the performance of aerated lagoons treating municipal wastewaters. in: *Aerated lagoon technology*, Vol. 2011, Lagoon systems in maine. South Carolina.
- Ringeisen, B.R., Ray, R., Little, B. 2007. A miniature microbial fuel cell operating with an aerobic anode chamber. *Journal of Power Sources*, **165**, 591-597.
- Rittmann, B.E. 2006. Microbial ecology to manage processes in environmental biotechnology. *Trends in Biotechnology*, **24**(6), 261-266.
- Rosenbaum, M., Zhao, F., Quaas, M., Wulff, H., Schroder, U., Scholz, F. 2007. Evaluation of catalytic properties of tungsten carbide for the anode of microbial fuel cells. *Applied Catalysis B: Environmental*, **74**, 261-269.
- Safina, G., Ludwig, R., Gorton, L. 2010. A simple and sensitive method for lactose detection based on direct electron transfer between immobilised cellobiose dehydrogenase and screen-printed carbon electrodes. *Electrochimica Acta*, **55**(26), 7690-7695.
- Sandler, J., Shaffer, M.S.P., Prasse, T., Bauhofer, W., Schulte, K., Windle, A.H. 1999. Development of a dispersion process for carbon nanotubes in an epoxy matrix and the resulting electrical properties. *Polymer*, **40**(21), 5967-5971.
- Santoro, C., Lei, Y., Li, B., Cristiani, P. 2012. Power generation from wastewater using single chamber microbial fuel cells (MFCs) with platinum-free cathodes and pre-colonized anodes. *Biochemical Engineering Journal*, **62**(0), 8-16.
- Schaetzle, O., Barrière, F.d.r., Baronian, K. 2008. Review: Bacteria and yeasts as catalysts in microbial fuel cells: electron transfer from micro-organisms to electrodes for green electricity *Energy & Environmental Science*, **1**, 607-620
- Schulz, C., Ludwig, R., Micheelsen, P.O., Silow, M., Toscano, M.D., Gorton, L. 2012. Enhancement of enzymatic activity and catalytic current of cellobiose dehydrogenase by calcium ions. *Electrochemistry Communications*, **17**(0), 71-74.
- Scott, K., Rimbu, G.A., Katuri, K.P., Prasad, K.K., Head, I.M. 2007. Application of modified carbon anodes in microbial fuel cells. in: *Trans IChemE*, Vol. 85, pp. 481-488.
- Spitalsky, Z., Tasis, D., Papagelis, K., Galiotis, C. 2010. Carbon nanotube-polymer composites: Chemistry, processing, mechanical and electrical properties. *Progress in Polymer Science*, **35**(3), 357-401.
- Stoica, L., Dimcheva, N., Ackermann, Y., Karnicka, K., Guschin, D.A., Kulesza, P.J., Rogalski, J., Haltrich, D., Ludwig, R., Gorton, L., Schuhmann, W. 2009. Membrane-less biofuel cell based on cellobiose dehydrogenase (anode)/laccase (cathode) wired via specific os-redox polymers. *Fuel Cells*, **9**(1), 53-62.
- Tanaka, K., Vega, C.A., Tamamushi, R. 1983. Thionine and ferric chelate compounds as coupled mediators in microbial fuel cells. *Bioelectrochemistry and Bioenergetics*, **11**(4-6), 289-297.

- Tasca, F., Gorton, L., Harreither, W., Haltrich, D., Ludwig, R., Noll, G. 2009. Comparison of direct and mediated electron transfer for cellobiose dehydrogenase from *Phanerochaete sordida*. *Anal. chem*, **81**, 2791–2798.
- Tasca, F., Gorton, L., Harreither, W., Haltrich, D., Ludwig, R., Noll, G. 2008. Direct electron transfer at cellobiose dehydrogenase modified anodes for biofuel cells. *Journal of Physical Chemistry B*, **112**(26), 9956-9961.
- Tasca, F., Harreither, W., Ludwig, R., Gooding, J.J., Gorton, L. 2011a. Cellobiose dehydrogenase aryl diazonium modified single walled carbon nanotubes: Enhanced direct electron transfer through a positively charged surface. *Analytical Chemistry*, **83**(8), 3042-3049.
- Tasca, F., Zafar, M.N., Harreither, W., Noll, G., Ludwig, R., Gorton, L. 2011b. A third generation glucose biosensor based on cellobiose dehydrogenase from *Corynascus thermophilus* and single-walled carbon nanotubes. *Analyst*, **136**(10), 2033-2036.
- Tayhas, G., Palmore, R., Whitesides, G., M. 1994. Chapter 14: Microbial and enzymatic biofuel cells. in: *Enzymatic conversion of biomass for fuels production*, Vol. 271-290, American Chemical Society. Massachusetts.
- The Japan Institute of Energy. 2008. The asian biomass handbook: A guide for biomass production and utilization, (Eds.) S. Yokoyama, Y. Matsumura, S. Ando, K. Sakanishi, H. Sano, T. Minowa, H. Yamamoto, T. Yoshioka, The Japan Institute of Energy.
- Topcagic, S., Minteer, S.D. 2006. Development of a membraneless ethanol/oxygen biofuel cell *Electrochimica Acta*, **51**, 2168-2172.
- Trashin, S.A., Haltrich, D., Ludwig, R., Gorton, L., Karyakin, A.A. 2009. Improvement of direct bioelectrocatalysis by cellobiose dehydrogenase on screen printed graphite electrodes using polyaniline modification. *Bioelectrochemistry*, **76**(1-2), 87-92.
- U.S Geological Survey. 1997. Bioremediation: Nature's way to a cleaner environment, Vol. 2011, USGS.
- Vahedi, F., Shahverdi, H.R., Shokrieh, M.M., Esmkhani, M. 2014. Effects of carbon nanotube content on the mechanical and electrical properties of epoxy-based composites. *New Carbon Materials*, **29**(6), 419-425.
- Vega, C.A., Fernandez, I. 1987. Mediating effect of ferric chelate compounds in microbial fuel cells with *Lactobacillus plantarum*, *Streptococcus lactis*, and *Erwinia dissolvens*. *Bioelectrochemistry and Bioenergetics*, **17**(2), 217-222.
- Venkata Mohan, S., Velvizhi, G., Annie Modestra, J., Srikanth, S. 2014. Microbial fuel cell: Critical factors regulating bio-catalyzed electrochemical process and recent advancements. *Renewable and Sustainable Energy Reviews*, **40**(0), 779-797.
- Vidali, M. 2001. Bioremediation. An overview. *Pure Appl. Chem.*, **73**(7), 1163-1172.
- Walstra, P. 2003. *Dairy processing : Maximising quality*. Woodhead Publishing, Limited, Cambridge, GBR.
- Wang, H., Wu, Z., Plaseied, A., Jenkins, P., Simpson, L., Engtrakul, C., Ren, Z. 2011. Carbon nanotube modified air-cathodes for electricity production in microbial fuel cells. *Journal of Power Sources*, **196**(18), 7465-7469.
- Wang, X., Falk, M., Ortiz, R., Matsumura, H., Bobacka, J., Ludwig, R., Bergelin, M., Gorton, L., Shleev, S. 2012. Mediatorless sugar/oxygen enzymatic fuel cells based on gold nanoparticle-modified electrodes. *Biosensors and Bioelectronics*, **31**(1), 219-225.
- Wang, Y.-F., Cheng, S.-S., Tsujimura, S., Ikeda, T., Kano, K. 2006. *E. coli*-catalyzed bioelectrochemical oxidation of acetate in the presence of mediators *Bioelectrochemistry*, **69**, 74-81.
- Watson, V.J., Logan, B.E. 2011. Analysis of polarization methods for elimination of power overshoot in microbial fuel cells. *Electrochemistry Communications*, **13**(1), 54-56.
- Weaver, J. 2010. Power from glucose: An implanted biofuel cell may someday power medical devices. in: *Technology Review: Biomedicine*, Massachusetts Institute of Technology (MIT). Cambridge.
- Weld, R.J., Singh, R. 2011. Functional stability of a hybrid anaerobic digester/microbial fuel cell system treating municipal wastewater. *Bioresource Technology*, **102**(2), 842-847.

- Xu, F., Duan, J., Hou, B. 2009. Electron transfer process from marine biofilms to graphite electrodes in seawater. *Bioelectrochemistry*.
- Yakovleva, M., Buzas, O., Matsumura, H., Samejima, M., Igarashi, K., Larsson, P.-O., Gorton, L., Danielsson, B. 2012. A novel combined thermometric and amperometric biosensor for lactose determination based on immobilised cellobiose dehydrogenase. *Biosensors & Bioelectronics*, **31**(1), 251-256.
- Yu, H.N., Lim, J.W., Suh, J.D., Lee, D.G. 2011. A graphite-coated carbon fiber epoxy composite bipolar plate for polymer electrolyte membrane fuel cell. *Journal of Power Sources*, **196**(23), 9868-9875.
- Zebda, A., Gondran, C., Le Goff, A., Holzinger, M., Cinquin, P., Cosnier, S. 2011. Mediatorless high-power glucose biofuel cells based on compressed carbon nanotube-enzyme electrodes. *Nat Commun*, **2**, 370.
- Zhu, H.Q., Zhang, Y.M., Yue, L., Li, W.S., Li, G.L., Shu, D., Chen, H.Y. 2008. Graphite-carbon nanotube composite electrodes for all vanadium redox flow battery. *Journal of Power Sources*, **184**(2), 637-640.
- Zou, Y., Xiang, C., Yang, L., Sun, L.-X., Xu, F., Cao, Z. 2008. A mediatorless microbial fuel cell using polypyrrole coated carbon nanotubes composite as anode material. *International Journal of Hydrogen Energy*, **33**, 4856-4862.